Zeitschrift: IABSE congress report = Rapport du congrès AIPC = IVBH Kongressbericht

Band: 13 (1988)

Rubrik: A. Applications of advanced materials

DAILY THEME A

Applications of Advanced Materials

Utilisation de matériaux d'avant-garde

Anwendungen neuartiger Baustoffe

Chairmen:	A. Sarja, Finland L. Finzi, Italy
Technical Adviser:	D. J. Lee, UK
Keynote Lecturers:	S.W. Tsai, USA K. Okada, Japan

The theme will be introduced by two Keynote Lecturers and printed in the Post-Congress Report, which will be mailed to the participants after the Congress.

Le thème sera introduit par deux orateurs invités, dont les exposés magistraux seront publiés dans le Rapport Post-Congrès; celui-ci sera envoyé aux participants après le Congrès.

Das Thema wird von zwei eingeladenen Referenten eingeführt, deren Referate im Schlussbericht des Kongresses veröffentlicht werden. Dieser Schlussbericht wird den Teilnehmern nach dem Kongress zugestellt.

Leere Seite
Blank page
Page vide

Concrete-Filled High Tensile Steel Tubular Structures

Structures en tubes d'acier à haute résistance remplis de béton

Konstruktionen aus betongefüllten, hochfesten Stahlrohren

Toshiro SUZUKI
Professor. Dr.
Tokyo Inst. of Technology
Tokyo, Japan

Toshiyuki OGAWA
Assoc.Prof. Dr.
Tokyo Inst. of Technology
Tokyo, Japan

Shojiro MOTOYUI
Struct.Eng. Dr.
Tokyu Construction
Tokyo, Japan

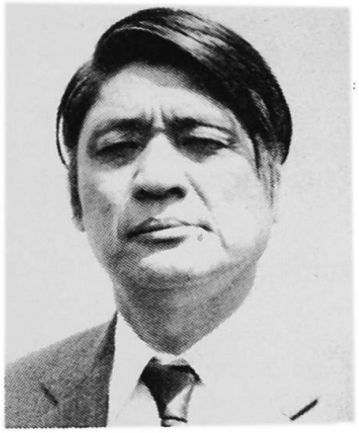

Toshiro Suzuki, born 1936, received his doctor of engineering degree at the University of Tokyo. His major research activities include strength of steel structures and application of new concrete. He was awarded the Prize from Architectural Institute of Japan for his study in 1981.

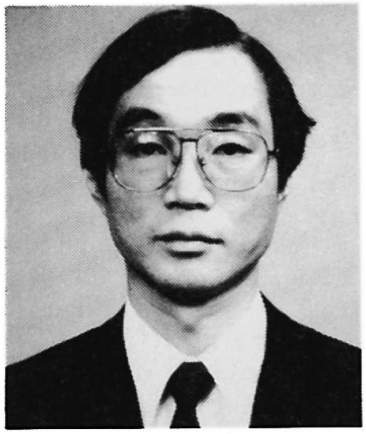

Toshiyuki Ogawa, born 1951, received his doctor of engineering degree at Tokyo Institute of Technology. His special research interests are stability problems, computational mechanics and wind engineering.

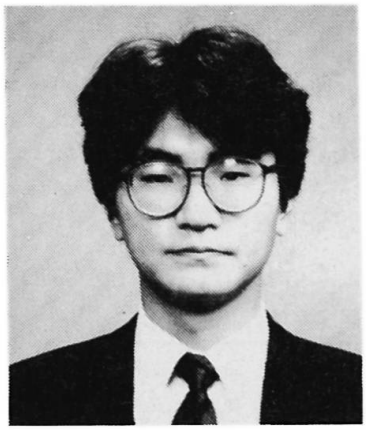

Shojiro Motoyui, born 1958, received his doctor of engineering degree at Tokyo Institute of Technology. His research is mainly concerned with buckling and ultimate strength of shell structures. He is at present structural engineer at Tokyu Construction.

SUMMARY
This paper describes the analytical method for examining the mechanical properties of concrete-filled high tensile steel tubes with emphasis on their buckling and post-buckling behaviors. Special attention is paid to the role and the modeling of the filled concrete which prevents the growth of the buckling waves in steel walls. The general features of this material are discussed from the obtained results.

RÉSUMÉ
Cette contribution décrit une méthode analytique pour l'examen des caractéristiques mécaniques de tubes d'acier à haute résistance remplis de béton, en considérant leur comportement de flambage et de post-flambage. Une attention particulière est portée sur le rôle et la modélisation du béton de remplissage qui empêche l'apparition des ondes de flambage des parois d'acier. Les caractéristiques générales de ce matériau sont discutées sur la base des résultats obtenus.

ZUSAMMENFASSUNG
Dieser Beitrag beschreibt ein analytisches Verfahren zur Untersuchung der mechanischen Eigenschaften von betongefüllten, hochfesten Stahlrohren, unter Berücksichtigung des Beul- und Nachbeulstadiums. Besondere Aufmerksamkeit gilt dabei dem Verhalten und der Modellisierung des Füllbetons, der die Entstehung von Beulwellen der Stahlwände verhindert. Aus den gewonnenen Erkenntnissen werden allgemein gültige Materialeigenschaften erörtert.

1. INTRODUCTION

For the last decades, high strength structural steel tubes are frequently used for structural members in large structures such as tall buildings. In these structures, members can be thinner than ordinary mild steel members by the use of high tensile steel. As a result, high tensile steel tubes are designed efficiently and the radius (diameter) to thickness ratio of steel tubes is larger. Therefore, the mechanical properties of high tensile steel tubes, particularly the local buckling strength of tubes must be fully investigated. The study has been carried out also in our laboratory[2,3].
However, there is not enough of the necessary basic data on the local buckling behavior of high tensile steel tubes, especially on the buckling behavior of concrete-filled high tensile steel tubes. It is generally thought that the local buckling behavior of composite members (concrete encased steel members) is controlled with the concrete. It is not clear whether the similar constraint effect of concrete for concrete-filled high tensile steel tubes can be expected or not. The reason is that the outward deflection of the steel wall may grow under pure compression by the effect of hoop tension.
In this paper, the nonlinear analysis is carried out to study the constraint effect of the concrete on the local buckling behavior of high tensile steel tubular structures under axial compression. The buckling strength and deformation capacity are discussed.

2. MODELING OF CONCRETE-FILLED HIGH TENSILE STEEL TUBULAR STRUCTURES

2.1 Main assumptions

In this section, we describe the modeling of concrete-filled high tensile steel tubular structures under axial compression (see Fig.1). At first we make the following assumptions for the local buckling problem of concrete-filled high tensile steel tubes.

1. The effect of concrete on the local buckling will be estimated at unilateral boundary conditions. Figure 2 shows the method how we determine such a unilateral boundary surface when analyzing the buckling behavior by the step-by-step method.
2. The relationship between stresses and strains follows the Hooke's law to the elastic region and the Prandtl-Ruess stress-strain relation to the plastic region; the stress-strain relation is assumed to be the round-house type for the purpose of considering the influence of residual stresses in steel tubes because of the plastic forming and welding[1].
3. Buckling modes of steel tubes are axi-symmetric. In this paper, we do not consider asymmetric buckling modes.

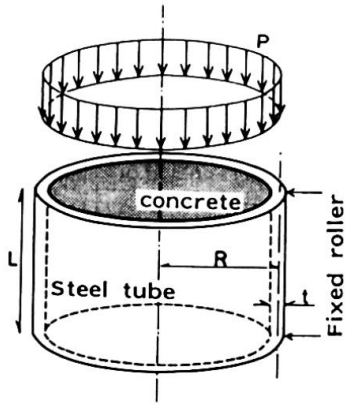

Fig. 1 Geometry

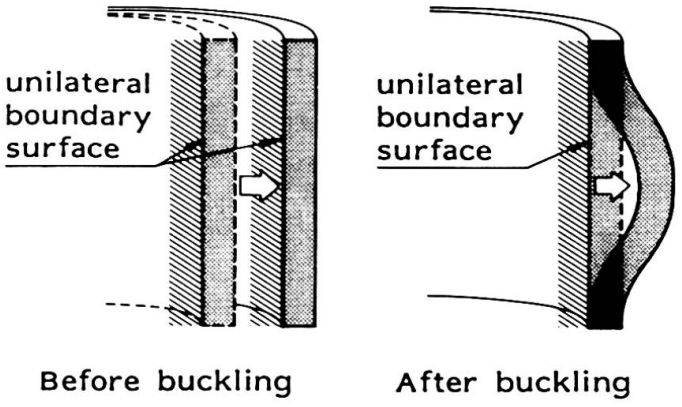

Fig. 2 Determination of concrete surface

4. Friction on the surface between the steel tube and the concrete in tubes (boundary surface) is ignored.

The above assumptions enable us to consider that the concrete in tubes will simply control the local plastic buckling behavior of high tensile steel tubes.

2.2 Analytical method

Here, we briefly describe the analytical method. The characteristics of the analytical method used in this paper are the followings[2,3].

- The present analytical method considers both the geometrical and material nonlinearity.
- The mode superposition method is implemented as numerical techniques.
- The effect of concrete in tubes on contact constraints or unilateral boundary conditions is estimated by the penalty formulation.
- The arc-length-control procedure is adopted to overcome such numerical difficulty that the tangent stiffness becomes indefinite near the buckling load.
- The tube wall is divided into some layers through the thickness, and whether the layer is elastic or plastic state is decided according to the von Mises yield criterion.

3. LOCAL BUCKLING OF HIGH TENSILE STEEL TUBES

3.1 Geometrical and material properties of analytical models

In this section, we actually discuss the local buckling behavior of high tensile steel tubes with unilateral boundary condition.

As to the material parameter, the two types of HT55 series and HT80 series are examined where HT55 series and HT80 series represent steel tubes with the minimum tensile strength of 540 MPa (55kgf/mm^2) and 785 MPa (80kgf/cm^2), respectively. The material properties are the followings[3].

- The value of proportional limit stress: σp is 231 MPa for HT55 series and 476 MPa for HT80 series.
- The value of yield stress: σy (0.2% offset yield stress) is 518 MPa for HT55 series and 760 MPa for HT80 series.

As to the geometric parameter, the radius to wall thickness ratio (R/t) of steel tubes is adopted. As the value of the ratio, we examined the four types for HT55 series and the two types for HT80 series. The behaviors of high tensile steel tubes without concrete were also examined in comparison with that of the concrete-filled tubes

Table 1. Geometrical and material properties of high tensile steel tubes

	HT55 series								HT80 series			
R/t, αc	50, 4.0		35, 5.6		22, 9.0		20,10.0		22, 6.2		15, 9.0	
filled or empty	f.	e.	f.	e.	f.	e.	f.	e.	f.	e.	f.	e.
yield stress(σy)	518 MPa								760 MPa			
Length to radius(L/R)	2.0											

where αc is the nondimensional parameter[2].

3.2 Results and discussions

At first, we discuss the characteristics of each compressive stress (σ) - compressive strain (ε) relation curves for concrete-filled high tensile steel tubes. Here, the compressive stress is given by the axial load divided by the cross sectional area, and the compressive strain by the axial displacement

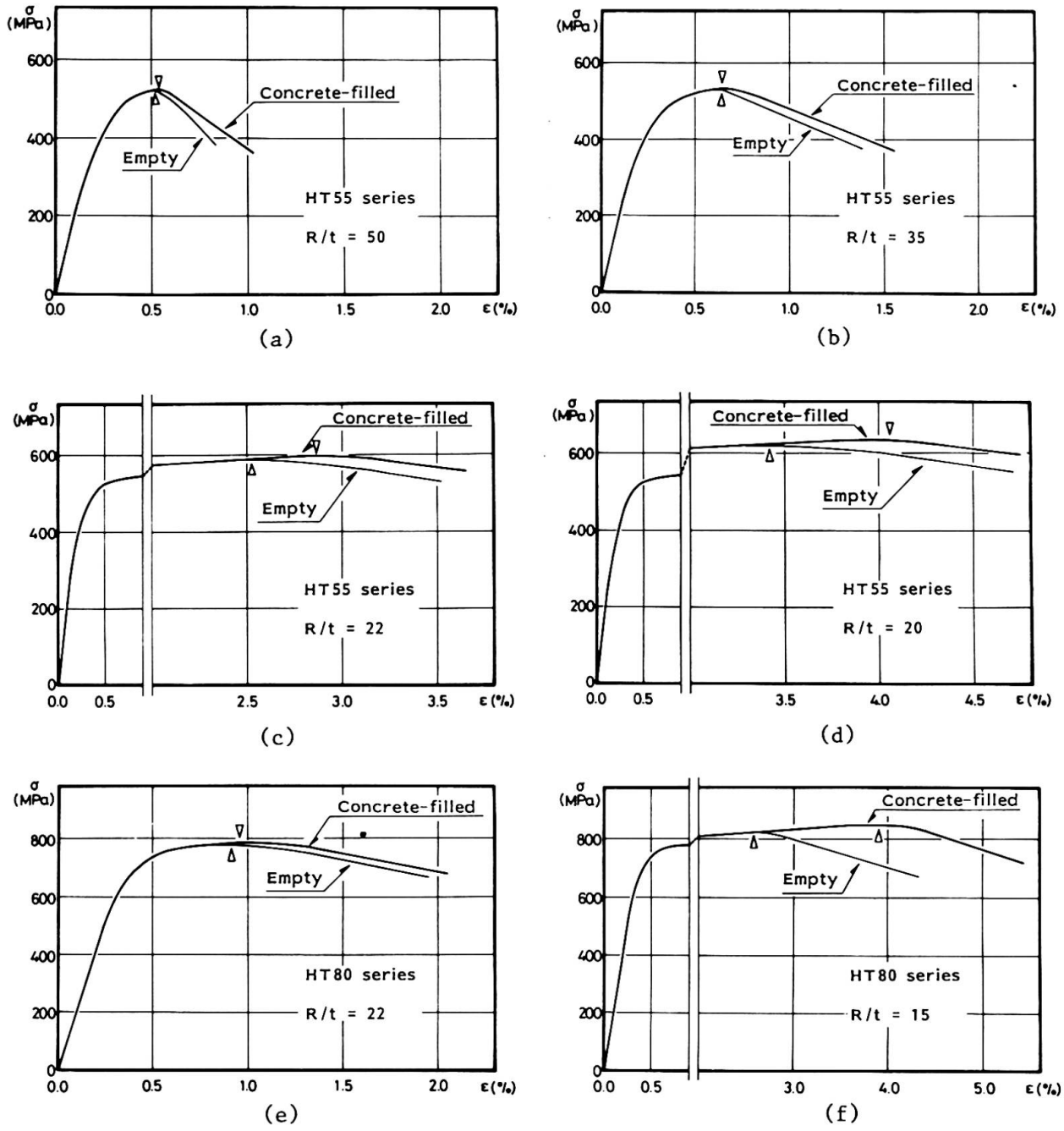

Fig. 3 Compressive stress-strain relation curves

divided by the tube length. Figures 3(a)-3(f) show compressive stress-compressive strain relation curves for high tensile concrete-filled or empty steel tubes with the radius to thickness ratio R/t=50, 35, 22 and 20 for the HT55 series and R/t=22 and 15 for the HT80 series.

In case of HT55 series, the maximum compressive stress (σm) and the strain (εm) at the maximum load level of the concrete-filled steel tubes with R/t=50 and R/t=35 is nearly equal to that of the empty steel tubes, though the results for each condition in tubes somewhat differ in the behavior after the buckling (see Fig.3(a) and (b)). In the results of steel tubes with R/t=22 and R/t=20, the effect of concrete in tubes on the plastic local buckling behavior appears contrastively (see Fig.3(c) and (d)). Particularly the strain at the maximum stress of the concrete-filled steel tube with R/t=20 is quite large compared

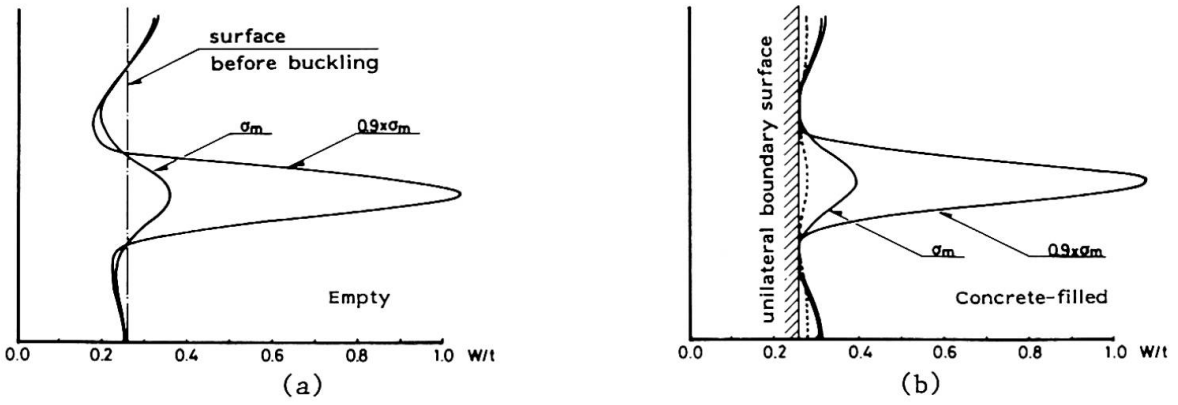

Fig. 4 Distribution of lateral displacement of tubes

with that of the empty steel tube.
In case of HT80 series, the results of concrete-filled steel tubes with R/t=22 is nearly equal to the results of empty ones, and this tendency is similar to ones with R/t=35 for HT55 series (see Fig.3(e)). The results of concrete-filled and empty steel tubes with R/t=15 is considerably different on the strain at the maximum compressive stress in the same manner as the results of steel tubes with R/t=20 for HT55 series (see Fig.3(f)).
Thus, the constraint effect of the concrete on the control with the plastic local buckling behavior becomes even stronger when the radius to thickness ratio of steel tubes is smaller.
Figure 4 shows the distribution of lateral displacement of concrete-filled and empty tubes with R/t=22 for HT55 series at the point of the maximum stress and at the point of 0.9 x σm after buckling. In the empty tube, the deflection of clear cosine wave grows near the point of the maximum stress(see Fig.4(a)). As to the tube with concrete, the constraint effect of the concrete controls the sudden growth of inward lateral displacement of the steel tube. The dotted line in Fig.4(b) shows the deflection line of the concrete-filled steel tube at the buckling load of the empty tube. As shown in this figure, the concrete-filled tube does not buckle at the buckling load of the empty tube. The maximum stress of the concrete-filled tube, therefore, rises more than the maximum stress of the empty tube.

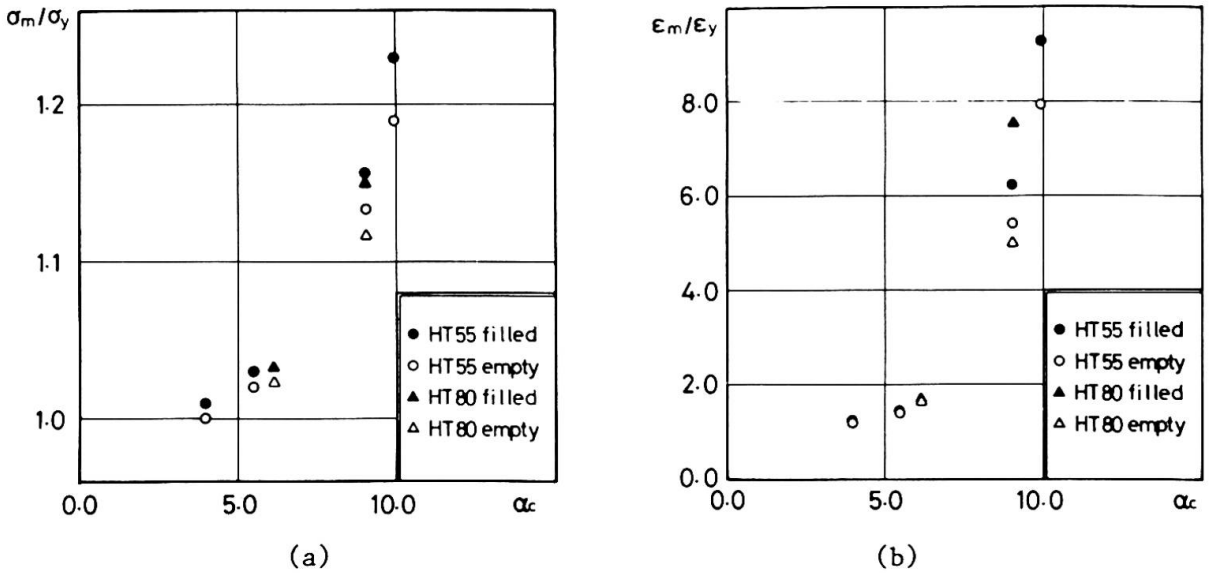

Fig. 5 Relation between αc and σm/σy, εm/εy

Next, by the nondimensional parameter (αc), three factors of the strength increase ratio and the plastic deformation capacity are discussed to clarify the mechanical properties of concrete-filled high tensile steel tubes. The strength increase ratio is the maximum compressive stress (σm) divided by the compressive yield stress (σy). The deformation capacity is the strain (εm) at the maximum compressive stress divided by the strain (εy) at the compressive yield stress. The parameter αc is written as

$$\alpha c = E/\sigma y \times t/D, \quad \text{where } E: \text{Young's modulus}, D: \text{diameter of tubes}, \sigma y: \text{yield stress}, t: \text{thickness of tubes} \qquad (1)$$

Figures 5(a) and (b) show the relationship between αc and $\sigma m/\sigma y$, $\varepsilon m/\varepsilon y$ of concrete-filled and empty tubes respectively. The constraint effect of concrete in tubes on the plastic local buckling of tubes considerably appears when αc becomes greater than 9. This matter means that when the value of the radius to thickness ratio is less than about $11500/\sigma y$, the concrete in tubes is efficient to prevent the plastic local buckling of tubes.
In comparison with the results of tubes with $\alpha c=9.0$ for HT55 series and HT80 series, the degree of the constraint effect of the concrete on the plastic deformation capacity fairly depends on the material property, though the effect is almost the same on the stress increase ratio.
Thus, the constraint effect of concrete on the buckling of tubes is more efficient when the radius to thickness ratio of steel tubes is smaller, or the yield stress of steel tubes is higher.

4. CONCLUSION

The properties of concrete-filled high tensile steel tubes under pure compression, has discussed by the nonlinear analysis with considering unilateral boundary condition of concrete in tubes. The analytical research seems to be very useful to discuss the mechanical properties in paying attention to the pure constraint effect of the concrete on the buckling behavior of the steel tube. The results obtained may be summarized as follows.

- In thick wall steel tubes, the effect of concrete in tubes on the properties of the strength increase ratio and the plastic deformation capacity is efficient compared with thin wall steel tubes in both HT55 series and HT80 series, where the thick wall steel tubes mean ones with the diameter to thickness ratio less than $23000/\sigma y$(MPa) or $3500/\sigma y$(psi).
- As to the comparison of the HT55 series with the HT80 series, the effect of concrete in tubes for the HT80 series is more remarkable than that for the HT55 series.
- As to the slope of strength inferiority, the values for the two types of concrete-filled and empty high tensile steel tubes make little difference.

REFERENCES

1. B.KATO, Local Buckling of Steel Circular Tubes in Plastic Region. Proc. of Int. Colloquium on Stability of Structures under Static and Dynamic Loads. ASCE. 1977.
2. T.SUZUKI and others, Plastic Local Buckling Strength of High Strength Structural Steel Tubes. Proc. of 2nd Int. Conference of IIW, held at Boston. U.S.A., Welding of Tubular Structures, July, 1984.
3. T.SUZUKI and others, A Study of Inelastic Buckling of High Strength Steel Pipes under Axial Compression. Transaction of Architectural Institute of Japan, November, 1982.

Universal Composite Construction, a New Successful Technology

Construction mixte universelle, nouvelle technologie performante

Die universale Verbundbauweise, eine neue erfolgreiche Technologie

J.B. SCHLEICH
Department Manager
ARBED-Research Centre
Luxembourg

J.B. Schleich, born 1942, obtained his civil engineering degree at Liège-University where he was involved for two years in teaching and research. He was active for eleven years in the construction steelwork industry. Since 1984 he is responsible for research on steel construction at ARBED-Research Centre. He has served as President of ECCS and is now Chairman of TC5 on CAD/CAM of the same European Association.

SUMMARY
The paper deals with a new and powerful approach to fire resistance engineering, which allows full advantage to taken of composite construction based on rolled H-sections mainly concreted between the flanges. This leads to a new functional and aesthetic architecture, reinstating the use of visible steel.

RÉSUMÉ
Cette contribution donne un aperçu sur une nouvelle approche puissante de détermination de la résistance au feu, permettant de profiter pleinement des avantages de la construction mixte à base de profils laminés H bétonnés entre les ailes. Ceci conduit à une nouvelle architecture fonctionnelle et esthétique réhabilitant l'acier visible.

ZUSAMMENFASSUNG
Dieser Text gibt eine Uebersicht über eine neue Methode der Feuerwiderstandsbemessung, welche es gestattet, die Vorteile der auf I-Walzträgern basierenden und zwischen den Flanschen ausbetonierten Verbundkonstruktion voll auszunutzen. Dies wiederum erlaubt eine neue funktionelle und aesthetische Architektur, mit der erneuten Verwendung von sichtbarem Stahl.

1. INTRODUCTION

At the Department Bridges and Structural Engineering of the University of LIEGE (Belgium) new developments have been done on steel and composite structures within a C.E.C. research, under the leadership of ARBED-LUXEMBOURG [1,2]. The first aim of this research was to establish a computer program for the analysis of steel and composite structures under fire conditions. This numerical code is based on the finite element method using beam elements with subdivision of the cross section in a rectangular mesh. The thermal problem is solved by a finite difference method based on the heat balance between adjacent mesh-elements of the cross section.

This programm CEFICOSS-which means "Computer Engineering of the FIre resistance for COmposite and Steel Structures"-has to be considered as a general thermo-mechanical numerical computer code allowing to predict the behaviour under fire conditions of structural building parts such as columns, beams or frames. These structural elements could be composed either of bare steel profiles or of steel sections protected by any insulation, either of any composite cross-section type. In order to verify the simulation results given by CEFICOSS and to estimate with greater accuracy the fundamental physical parameters, it was decided to perform a new series of full scale fire tests based on the ISO-834 heating curve. Thus a better comparison was guaranteed between test and simulation results and most interesting informations got available on a new type of composite structure developed by ARBED.

2. FIRE RESISTANCE ENGINEERING

2.1. Theoretical background

As explained in detail by [2], this numerical code is based first on the finite element method using beam elements. Therefore any frame structure composed of interconnected columns and beams could be discretized as shown in Fig. 1. The chosen beam element has 2 nodes and 3 degrees of freedom at each node. The cross-section itself of this beam element is divided into a rectangular mesh, which allows to know exactly in function of time the stress and strain history of each mesh-element. Furthermore this cross-section subdivision allows to analyse finally any type of column or beam. The same rectangular mesh is directly used when calculating the evolution in function of time of the differential cross-section temperature field. Temperatures are obtained by a finite difference method, the second main numerical procedure used in this computer code.

2.2. Thermo-mechanical analysis

CEFICOSS is a new tool, which at last makes feasible a lot of new investigations, seriously improving our knowledge on the fire safety level of real structures. First of all as internal temperature and stress fields can be established for any cross section, the optimum fire design is provided without paying for excessive fire protection. Steel reinforcements could be foreseen at more convenient places as temperature fields would be known. Internal stress fields could give us the correct physical explanation for certain failure behaviours. Moreover the global deformation of structures can be calculated in order to show either its evolution in function of elapsed time, either the situation just before failure [3].

Most important is of course the prediction of the real failure time. In this respect it is worthwile to underline the perfect duality existing in CEFICOSS

between the mathematical failure expression and its physical meaning. Indeed failure is mathematically reached when the value of the Determinant related to the Structure Stiffness Matrix (DSSM) falls zo zero. Physically this means that a static equilibrium can no more be obtained because either the buckling of a column is occuring, either a plastic hinge has formed in a statically determinate beam. In both situations we assist to rapidly growing deformations leading to the collapse of the structural element.

In real structures the failure understanding becomes of course more difficult but failure is still obtained when the value of DSSM falls to zero. Physically the failure of a global frame corresponds to the successive formation of plastic hinges leading with or without a column buckling to a so-called structural mechanism [4].

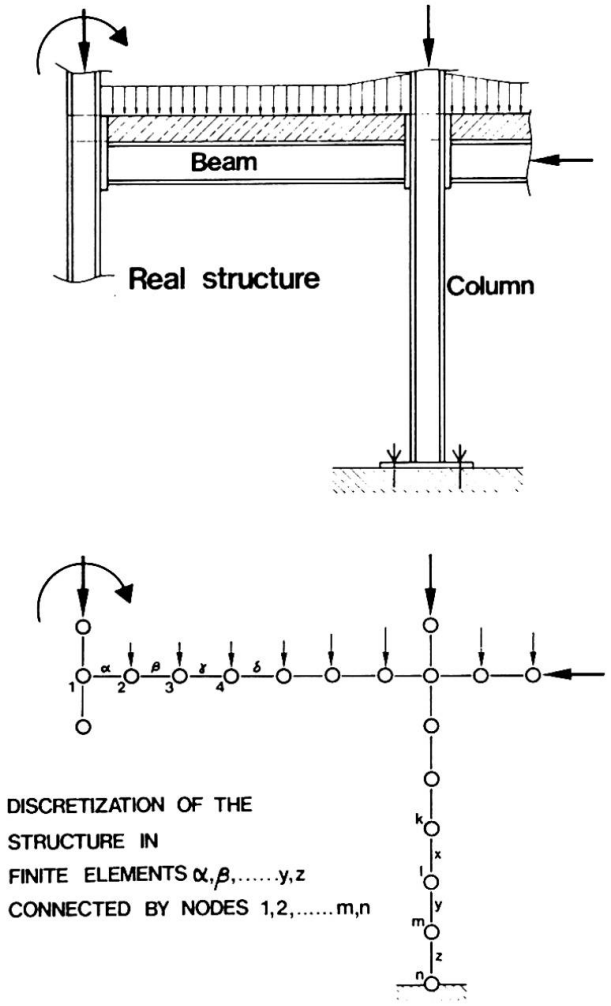

Fig.1 Real structure with finite element division

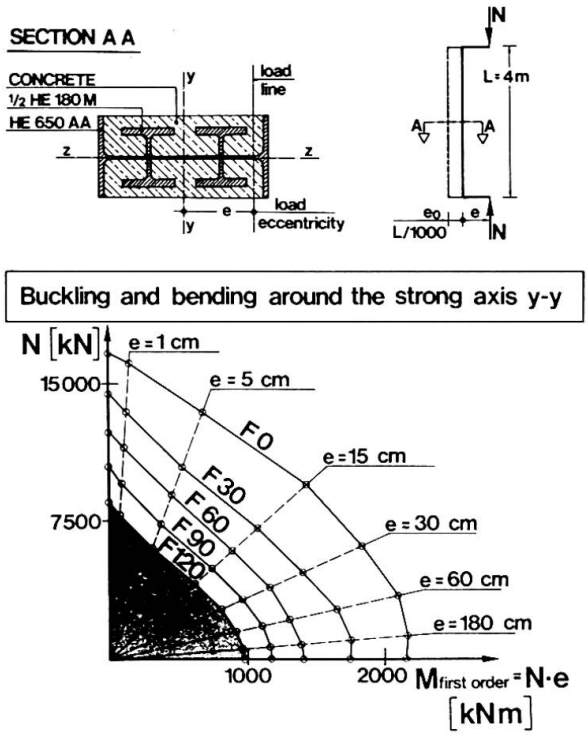

Fig.2 Example of N-M Interaction Failure Diagram for service condition (Fo) and the ISO-fire classes (F30 to F120)

2.3. N-M Interaction Diagrams

For direct use by engineers and architects, practical design tools are being established in case of four different composite column cross-section types [5]. Vertical loads and bending moments are considered simultaneously, allowing to elaborate N-M Interaction Failure Diagrams covering the whole static field from pure axial loads to pure bending moments. It is for the first time that such N-M Interaction Failure Diagrams are elaborated for fire conditions (F30 to F120) while considering the buckling effect (see Fig. 2). Because of the perfectly working failure duality, CEFICOSS gives for the whole N-M field a clear mathematical failure, corresponding either to a Column Buckling in the area of axial loads and up to higher eccentricities (60 to 180 cm), either to a Plastic Hinge Failure in the area of highest eccentricities and pure moments.

2.4. Collapse of Real Structures

Thanks to the powerful numerical tool CEFICOSS, we can at last study the global behaviour of complete structures under local fires. This could be of the highest interest as on one side fires should remain localized through building compartments and as on the other side separately heated structural elements, as parts of a global frame, will probably not induce global collapse at an early fire stage.

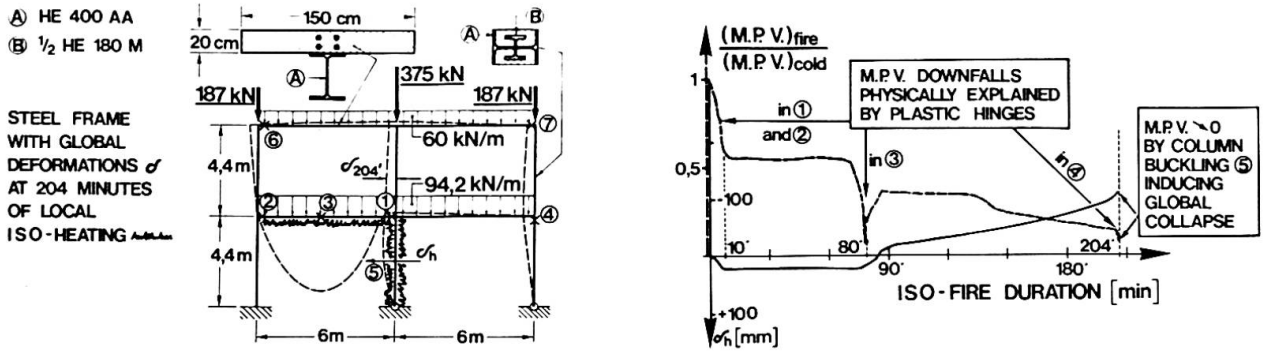

Fig.3 Collapse study of a real structure under a local ISO-influence.

It is for the first time that the effect of a local ISO-fire on a global steel structure has been analysed in a credible and reproducible way. This study shows that even naked, not protected steel beams could have a rather high fire resistance [6]. The analysed frame shown in Fig. 3, designed for cold service conditions with wind and snow loads, is slightly overdesigned as concrete slabs have a thickness of 20 cm. Nevertheless, provided the HE 400 AA not protected steel beams are connected to the concrete slabs by correctly designed shear studs, provided the beams have conveniant connections to the composite columns and provided wind and snow loads are supposed not to act simultaneously during the fire, the heated beam is able to transmit loads to the neighbouring columns up to 204 minutes of fire rage. The physical failure history is doubled up by the mathematical Minimum Proper Value (M.P.V.) evolution, which clearly shows critical downfalls at every physical structural stiffness weakening due to local plastic hinges. As long as these plastic hinges allow equilibrium with a new internal load redistribution, the M.P.V. value remains positive; it falls to zero when equilibrium definitively becomes impossible.

3. ARCHITECTURAL POINT OF VIEW.

Now last but not least this computer code will contribute to improve undoubtedly the image of steel construction. Indeed architects will have the free choice for composite structural sections of any shapes. However above all, construction elements with visible steel surfaces will become available for any fire safety levels. This important aspect is illustrated by Figures 4 to 7 showing some of the possible composite column cross-sections, based on rolled H profiles and normally presenting a systematical alternation from steel to concrete surfaces. This so-called Universal Composite Construction undoubtedly allows the creation of most aesthetic building elements and offers vast architectural possibilities [7,8].
Moreover the following caracteristics make this composite construction system most competitive:

- a very high flexibility is guaranteed as a great number of constructional connection types are available, offering always a feasible practical solution (see Fig. 8),

- an extremely high construction speed can be achieved as complete prefabrication is really possible, thus allowing a by far earlier construction finishing than with pure concrete,

- the smallest possible building element cross-sections are conceivable, thus leading to more slender constructions and offering more space for the practical use of the building.

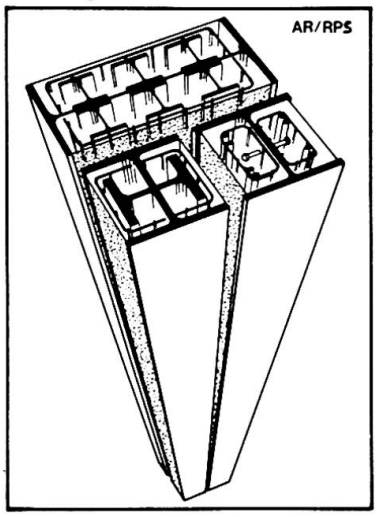

Fig.4

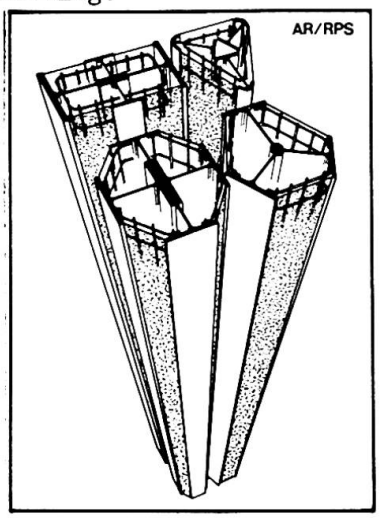

Fig.5

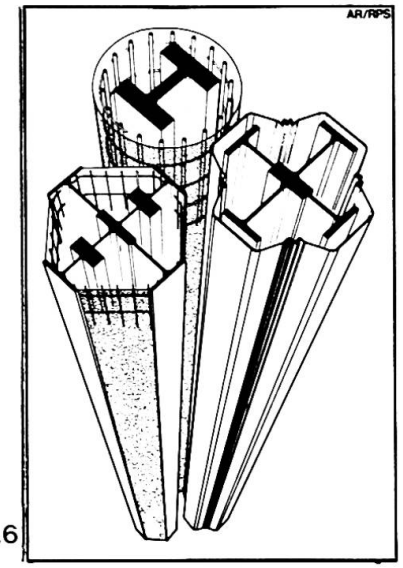

Fig.6

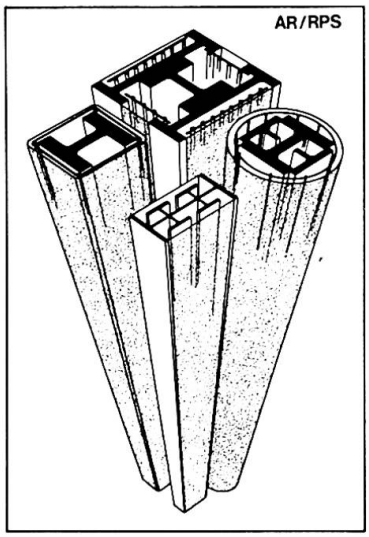

Fig.7

Fig.4,5,6,7 Possible column cross-sections considered by the Universal Composite Construction

Fig.8 Composite beams connected to a composite column

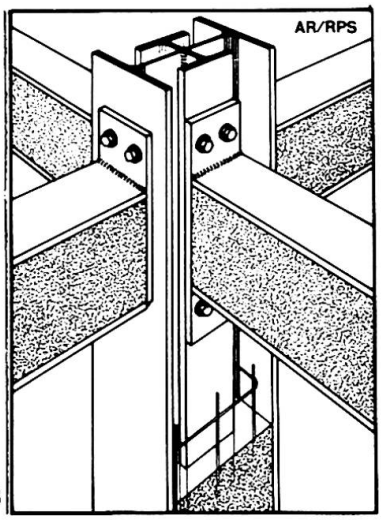

Fig.8

4. FUTURE DEVELOPMENTS AND CONCLUDING REMARKS

Various studies have been undertaken in order to increase the application field of this Universal Composite Construction. So it could be concluded from first calculations, that composite structures have a very promising behaviour in face of Natural Fires [3]. Indeed it could be demonstrated that the inner part of composite cross-sections is heated up to a rather low maximum temperature and that a Critical Load Level exists below which the structural composite element will not fail any more.

Furthermore a first successful attempt was done to establish for a given structure the equivalent time of ISO-fire exposure, t_{eq}^{ISO}, for which the load bearing capacity under ISO-fire is identical to the minimum load bearing capacity under a given natural fire [3]. This Load Bearing Equivalence is of course by far more accurate and useful than the Temperature Equivalence proposed up to now but which is completely inadequate for composite construction.

Finally credible studies will allow to find out the conditions under which even Unprotected Steel Sections are fire resistant. On one side indeed heavy steel profiles could be classified in the Fire Class F 60 [9], whereas light steel sections as a part of complete structures could even have by far Higher Fire Resistances (see chapter 2.4 and Fig. 9).

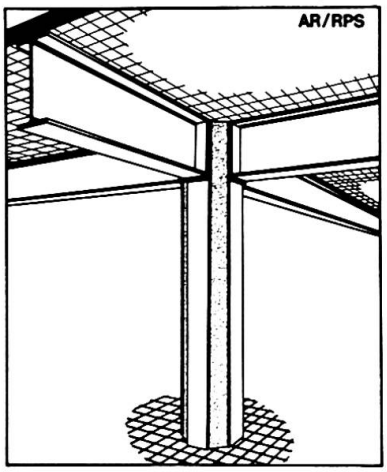

Fig.9 Composite space frame with naked steel beams, fire resistant up to F120 under localized fire.

At last a C.E.C. Research has been started, in order to adapt this Universal Composite Construction to Earthquake Conditions [10]. The idea is to combine the good ductility of rolled sections with the damping qualities of concrete, and to take advantage of the concrete filling between the profile-flanges in order to improve local steel buckling. It will be a challenge to develop beam-column connections with a high Cyclic Bending Moment Capacity and a simultaneous Prefabrication Ability.

5. ACKNOWLEDGEMENTS

Several of the before mentioned studies are based on the four C.E.C. Researches 7210-SA/502, 504, 505 and 506 which, finished or still under way, could profit of an important financial support from the COMMISSION OF THE EUROPEAN COMMUNITY

BIBLIOGRAPHY

1. SCHLEICH J.B., REFAO-CAFIR, Computer Assisted Analysis of the Fire Resistance of Steel and Composite Concrete-Steel Structures, C.E.C. Research 7210-SA/502. Final Report EUR 10828 EN, Luxembourg 1987.
2. FRANSSEN J.M., Etude du comportement au feu des structures mixtes acier-béton, Thèse de Doctorat. Université de Liège, Février 1987.
3. SCHLEICH J.B., Numerische Simulation-zukunftsorientierte Vorgehensweise zur Feuersicherheitsbeurteilung von Stahlbauten. Allianz Versicherungs-AG, Der Maschinenschaden 60, Heft 4, 1987.
4. SCHLEICH J.B., CEFICOSS, a Computer program for the fire engineering of steel structures; International Conference on Mathematical Models for Metals and Materials Applications. THE INSTITUTE OF METALS, London, October 1987.
5. SCHLEICH J.B., Practical design tools for composite steel-concrete construction elements, submitted to ISO-fire, considering the interaction between axial load N and bending moment M; Intermediate Reports RT3 and RT4 of C.E.C. Research 7210-SA/504. ARBED-Research Centre, Luxembourg, 1987.
6. SCHLEICH J.B., Global Behaviour of Steel Structures under Local Fires; R.P.S. Working Documents. ARBED Research Centre, Luxembourg, 1987-88.
7. SCHLEICH J.B., L'acier face aux incendies. Congrès National du Syndicat National des Architectes Agréés et des Maîtres d'Oeuvre en Bâtiment, Angers, Mai 1987.
8. BAUS R., SCHLEICH J.B., Prédétermination de la résistance au feu des Constructions mixtes. Annales de l'Institut Technique du Bâtiment et des Travaux Publics, N°457, Septembre 1987.
9. SCHLEICH J.B., Practical design tools for unprotected steel columns, submitted to ISO-fire, considering the interaction between axial load N and bending moment M; Intermediate Reports RT1 and RT2 of C.E.C. Research 7210-SA/505. ARBED Research Centre, Luxembourg, 1987.
10. ARBED Research Centre, Seismic Resistance of Composite Structures. C.E.C. Research 7210-SA/506, B-G-I-L, 1987-90.

Study of Braided Aramid Fiber Rods for Reinforcing Concrete

Renforcement du béton par des tiges en fibres Aramid tressées

Bewehrung von Beton mit Stäben aus Aramidfaser-Geflecht

Masaharu TANIGAKI
Research Engineer
Mitsui Constr. Co., Ltd.
Tokyo, Japan

Tadashi OKAMOTO
Senior Res. Engineer
Mitsui Constr. Co., Ltd.
Tokyo, Japan

Tomio TAMURA
Senior Res. Engineer
Mitsui Constr. Co., Ltd.
Tokyo, Japan

Sumiyuki MATSUBARA
Chief Res. Engineer
Mitsui Constr. Co., Ltd.
Tokyo, Japan

Setsuro NOMURA
Prof. Dr. Eng.
Science Univ. of Tokyo
Tokyo, Japan

SUMMARY
This paper describes the concrete reinforcing capability of fiber reinforced plastics' rods, FiBRA, which are made by weaving Aramid fibers in braided form. The tensile characteristics and durability of FiBRA were tested. Flexural tests were also performed on concrete beams using FiBRA as the flexural reinforcement, with prestressing tendons. As a result, it was confirmed that FiBRA can be easily put to practical use for reinforcing concrete.

RÉSUMÉ
Cette contribution décrit les possibilités de renforcement du béton par des tiges FiBRA, réalisées en tissant des fibres d'Aramid sous forme de tresses. Les caractéristiques de résistance à la rupture et la durabilité des tiges FiBRA ont été testées. Des essais de flexion ont également été exécutés sur des poutres en béton armées et précontraintes, par des tiges FiBRA. En conclusion il a été confirmé que les tiges FiBRA présentent de nombreuses applications pratiques pour le renforcement du béton.

ZUSAMMENFASSUNG
Dieser Beitrag zeigt die Möglichkeiten, Beton mit FiBRA-Stäben, einem Geflecht aus Aramidfasern, zu bewehren. Die FiBRA -Stäbe wurden auf Zugfestigkeit und auf Dauerhaftigkeit geprüft. Daneben wurden auch Biegeversuche an mit FiBRA-Stäben bewehrten und vorgespannten Betonträgern durchgeführt. Diese Untersuchungen bestätigten, dass FiBRA-Stäbe in grossem Umfang zur Bewehrung von Beton eingesetzt werden können.

1. INTRODUCTION

Recently, research has been going on for utilization of high-performance fibers as concrete reinforcing material with the purpose of improving the durability of reinforced concrete or prestressed concrete. The authors developed rod materials (FiBRA) of continuous fibers woven in braid form as substitutes for reinforcing bars and prestressing tendons, and the performances as structural materials were tested. This report is on tension tests, tensile fatigue tests, relaxation tests, heat resistance tests, and alkali resistance tests performed in particular on a rod material using Aramid fibers to confirm its basic performance, and flexural tests of concrete beams using this rod material as a substitute for reinforcing bars and prestressing tendons to grasp its concrete reinforcing effect.

2. OUTLINE OF FiBRA

The manufacturing process of FiBRA is shown in Fig. 1, while the characteristics of the Aramid fibers (Kevlar® 49) and epoxy resin used are given in Table 1. The manufacturing method consisted of using 6000-denier continuous fibers and weaving them into braids which were impregnated with epoxy resin and hardened. As shown in Photo. 1, a regular pattern of protrusions and depressions unique to the braid is formed on the rod. Weaving in braid form imparts the following two important properties to the FiBRA:

- Tensile force applied to the rod is uniformly transmitted to the entire cross section.
- The bond force to concrete is increased through the protrusions and depressions formed at the surface.

Furthermore, to increase the bond force even more, a FiBRA with a granular material such as sand adhered to the surface was developed.

Table 2 shows the fundamental physical properties of the rods used in the various tests.

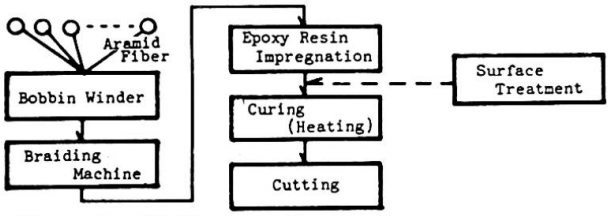

Fig. 1 FiBRA manufacturing process

Photo. 1 Configuration of FiBRA

Table 1 Characteristics of Aramid fiber and epoxy resin

Material \ Characteristic	Tensile strength (MPa)	Young's modulus (GPa)	Elongation (%)	Remarks
Aramid fiber	2745	130	2.4	Kevlar® 49.
Epoxy resin	78	1.42	5.5	Epicote 827 + TETA

Table 2 Basic physical properties of FiBRA

Braided material	Av. dia. (mm)	Typical strength (KN)	Typical strength (t)	Typical tensile strength (MPa) Full cross section	Typical tensile strength (MPa) Aramid fiber	Sp. gr. (g/cm³)
KS16	4.0	15.7	1.6	1255	2089	1.29
KS64	8.0	62.8	6.4			
KS96	10.0	94.6	9.6			
KS128	12.0	125.5	12.8			
KS192	14.0	188.3	19.2			

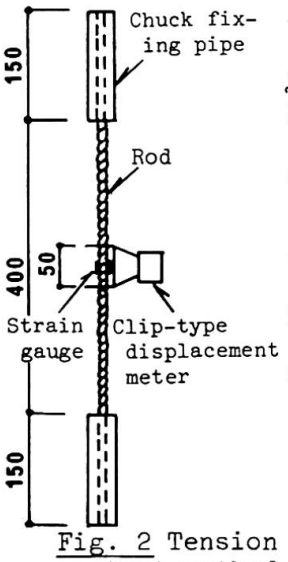

Fig. 2 Tension test method

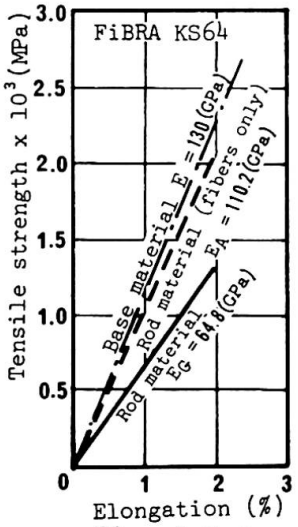

Fig. 3 σ-ε relationship

3. TENSILE CHARACTERISTICS

3.1 Tension Tests

Tension tests were performed on the rods listed in Table 2. The testing method is shown in Fig. 2.

Fig. 3 is an example of the relationship between tensile strength and elongation of KS64. An example of tensile strength distributions of KS64 is shown in Fig. 4. The overall average was 70.1 KN, 85 percent of the theoretical strength calculated from the amount of fibers used, with no case less than the typical tensile strength. The Young's modulus when calculated for the total cross-sectional area (E_G) including epoxy resin was 64.8 GPa, and for cross-sectional area of fibers only 110.2 GPa. Compared based on fibers only, it was 84.5 percent of the Young's modulus of 130.4 GPa of Kevlar® 49.

3.2 Tensile Fatigue Test

Partial pulsating tensile fatigue tests were performed on FiBRA of KS64. The tests were carried out at room temperature varying the stress range with the lower limit load constant at 50 percent of actual rupture and the fatigue limit where rupture would not occur even at 2 million cycles was determined. The results of the tests are shown in Table 3. With stress ranges under 374.6 MPa, rupture did not occur even at 2 million cycles, but in case of 443.3 MPa, rupture occurred at approximately 305,000 cycles.

3.3 Relaxation Test

Relaxation tests were performed under room temperature on KS64 FiBRA. The initial loads were the three levels of 0.7, 0.6, and 0.5 times the tensile strength P_u of KS64. The results of the tests are shown in Fig. 5. The relaxation values of the specimens were 3 to 4 times that of the prestressing steel at 10 hours, and 2 to 2.5 times at 100 hours. With prestressing steel, relaxation value is higher the greater the initial load, but with FiBRA, although there was some amount of scatter, differences depending on initial load were not recognized.

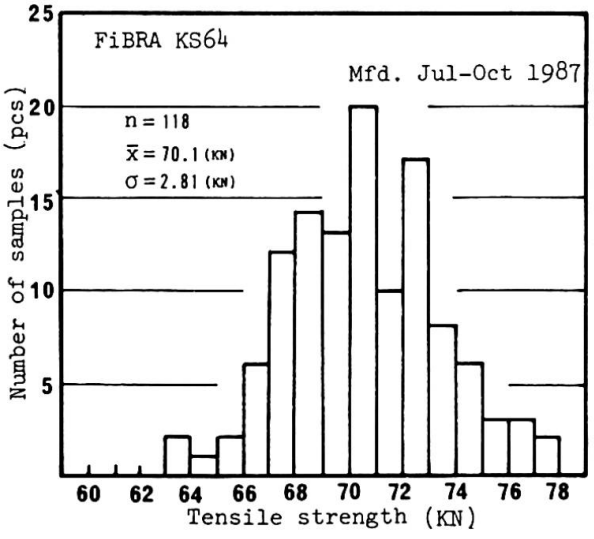

Fig. 4 Tensile strength distribution

Table 3 Tensile fatigue strength test results

Test	Lower limit		Upper limit		Stress range (MPa)	Cycles to rupture x 10^3
	Load (KN)	Stress (MPa)	Load (KN)	Stress (MPa)		
1	32.26	645.3	46.97	939.5	294.2	>2090
2	32.26	645.3	42.52	990.5	345.2	>3577
3	32.26	645.3	50.99	1019.9	374.6	>2063
4	32.26	645.3	54.43	1088.5	443.3	305

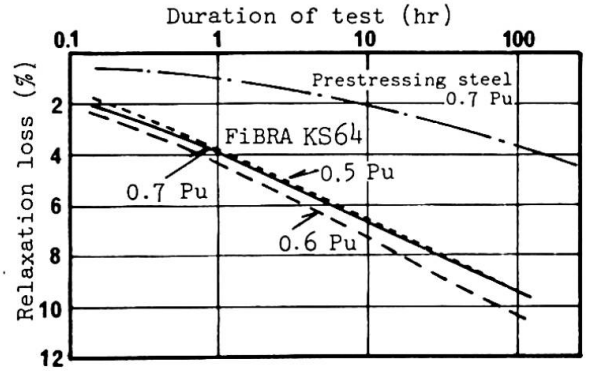

Fig. 5 Relaxation curve

4. DURABILITY

4.1 Heat Resistance Tests

Tests were of the two kinds of dry heat and moist heat tests using small-diameter FiBRA of KS16. Tension tests of the rods were performed for evaluation of heat resistance expressed in terms of ratios of strengths maintained with the strengths for no treatment as 100.

The results of the tests are shown in Fig. 6. In both kinds of testing the ratios of tensile strengths maintained up to treatment temperature of 220°C were high at around 95 percent to indicate very great heat resistance for an organic fiber.

4.2 Alkali Resistance Tests

The tests consisted of immersing KS16 FiBRA in a solution of pH = 13, with temperatures during immersion at the four levels of room temperature, 40, 60, and 80°C. Evaluation of alkali resistance was expressed by ratio of tensile strength maintained with the strength for no treatment as 100.

The results of the tests are shown in Fig. 7. Up to immersion temperature of 40°C strengths were maintained more or less at the values of untreated up to 2000 hours after immersion. For 60°C and 80°C, a tendency for strengths to decline slightly was seen when more than 1400 hours had elapsed, but ratios of strengths maintained were high exceeding 95 percent.

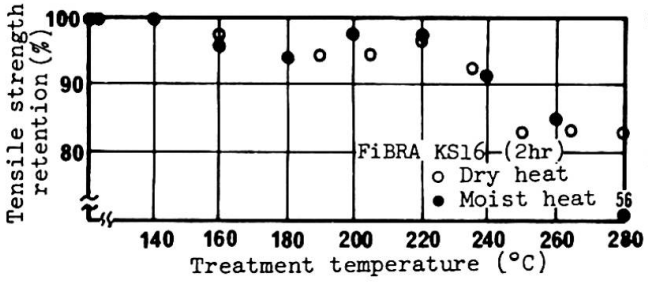

Fig. 6 Heat resistance test results

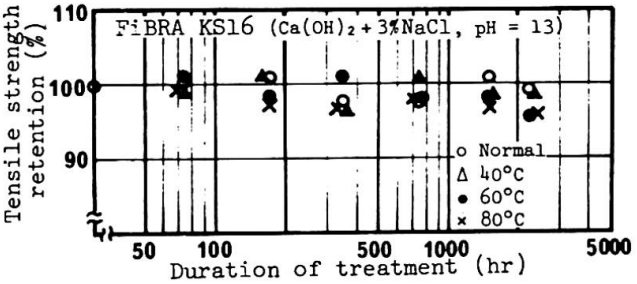

Fig. 7 Alkali resistance test results

5. FLEXURAL TESTS OF PRC (PARTIALLY PRESTRESSED CONCRETE) BEAMS

5.1 Specimens

Flexural tests were performed on PRC beams using FiBRA as main reinforcement and as prestressing tendons in pretensioning. The configuration of specimens was that of a T-beam of beam width 22.5 cm, beam depth 30 cm, and total length 360 cm as shown in Fig. 8. As indicated in Table 4, a total of five specimens were tested with FiBRA used as reinforcing bars the four kinds from KS64 to KS192 listed in Table 2, quartz sand being adhered to the FiBRA surfaces to enhance bonding properties. The parameters of the specimens were the three levels of tensile reinforcement ratio of main reinforcement of 0.13, 0.26, and 0.39 percent, and the three levels of prestress in terms of bottom fiber stress of concrete of 0, 1.47, and 2.94 MPa (0, 15, and 30 kg/cm^2).

5.2 Testing Method

Application of load was by two-point loading with bearing span of 300 cm and loading span of 75 cm, one-way monotonic loading used for the specimen F-26-0, and repeating loadings once at each stage of deformation for other specimens. A view of the testing is given in Photo. 2.

5.3 Test Results

Envelopes of the load-deformation curves of the specimens are shown in Fig. 9. After occurrence of initial cracking, loads and deformations increased in approximately straight lines for all specimens with the gradients dependent on flexural reinforcement quantities. All of the specimens showed adequate deformabilities with ultimate states reached on rupturing of FiBRA. The load-deformation curves of the specimens are shown in Fig. 10. Strength reductions due to repetitive loading were small, while residual deformation was smaller with increased level of prestress. Cracking patterns at 1/100 (D = 3 cm) deformations are shown in Fig. 11. Flexural cracks occurred well-scattered to show that bonding property of FiBRA is good. The test results are given in Table 6. The experimental values of first crack load and calculated values by Eq. (1) agreed well with each other. Consequently, it was thought that the required prestressing force had been adequately transferred. As for ultimate bending load obtained from rupture strength of FiBRA using Eq. (2), it coincided with the experimental value, showing that flexural strength can be estimated with fairly good accuracy.

$$P_{crt} = 2\{Z(0.564\sqrt{F_c} + \sigma_p) - M_o\}/\ell \quad \ldots\ldots\ldots\ldots\ldots (1)$$

$$P_{ut} = 2\{0.875 d f_R + (d_p - d/8) f_p\}/\ell \quad \ldots\ldots\ldots\ldots\ldots (2)$$

where, Z: section modulus, F_c: concrete strength, σ_p: bottom fiber stress due to prestress, M_o: bending moment due to dead weight, ℓ = 112.5 cm, d = 26 cm, d_p = 20 cm, f_R: rupture strength of main reinforcement, f_p: rupture strength of prestressing tendon.

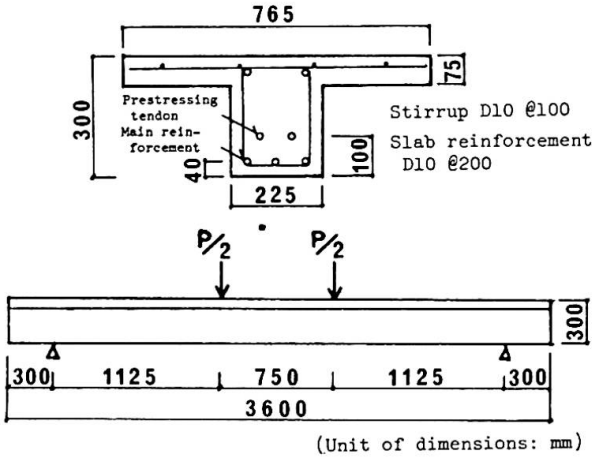

Fig. 8 Specimen configuration

Table 4 Types of flexural specimens

Specimen	Main reinforcement		Prestressing tendon		
	Type	Tensile reinforcement ratio (%)	Type	Tensioning force KN/pc	Bottom fiber prestressing stress MPa
F-13-15	3-KS64	0.13	2-KS96	30.7	1.47 [15.0 kg/cm²]
F-26-15	3-KS128	0.26			
F-39-15	3-KS192	0.39			
F-26-0	3-KS128	0.26		0.0	0.00 (0.0)
F-26-30			2-KS192	61.3	2.94 (30.0)

Table 5 Material characteristics

a) Concrete

	Comp. strength F_c (MPa)	Young's modulus ×10⁴(MPa)
At prestressing	28.5	2.53
At flexural testing	35.4	2.70

b) FiBRA strength

	Theoretical KN	Typical KN	Test value KN
KS64	86.2	62.7	69.1
KS96	123.5	94.1	101.3
KS128	164.6	125.4	132.2
KS192	247.9	188.2	191.6

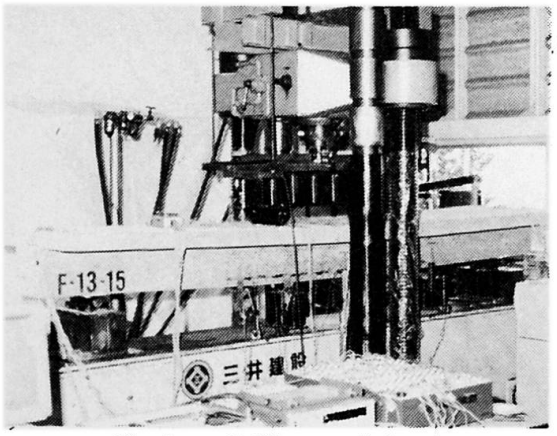

Photo. 2 View of test

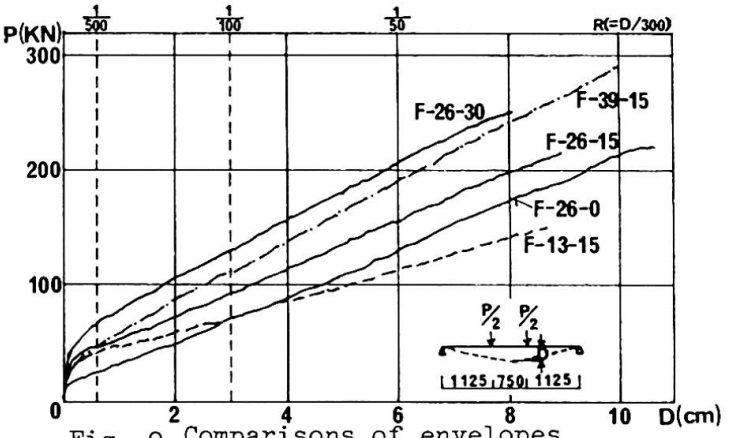

Fig. 9 Comparisons of envelopes of load-deformation curves

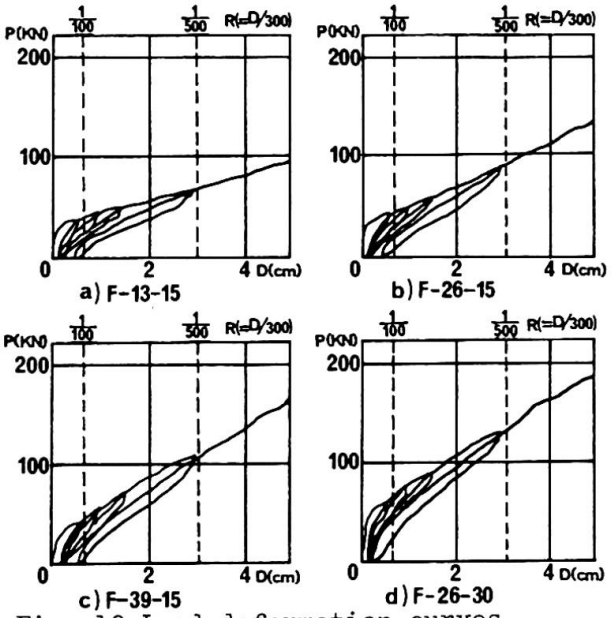

Fig. 10 Load-deformation curves of specimens

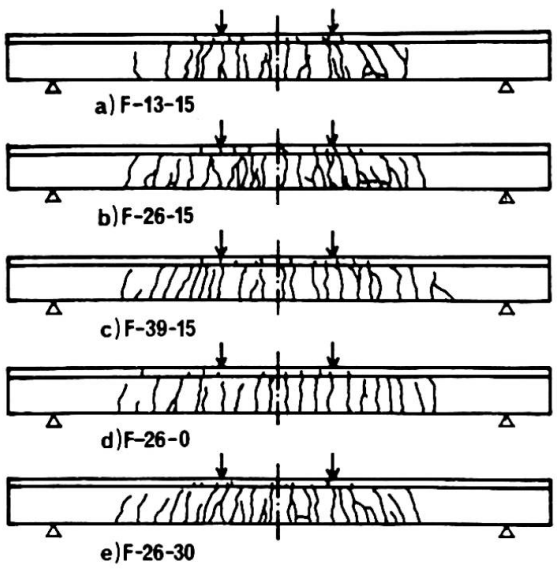

Fig. 11 Cracking patterns at 1/100 (D = 3 cm) deformations

Table 6 Test results

Specimen	At first crack				At ultimate state				
	Test value		Theoretical	Pcr/Pcrt	Test value			Theoretical	Pu/Put
	Bending moment Mcr(KN·m)	Load Pcr(KN)	Load Pcrt(KN)		Deflection Du (cm)	Bending moment Mu(KN·m)	Load Pu (KN)	Load Put(KN)	
F-13-15	16.4	29.1	27.9	1.04	8.68	85.5	152	144	1.05
F-26-15	19.7	35.1	27.9	1.25	8.93	121.3	216	221	0.98
F-39-15	16.4	29.1	27.9	1.04	10.1	165.4	294	293	1.00
F-26-0	8.38	14.9	21.3	0.70	10.1	121.3	216	221	0.98
F-26-30	26.4	46.8	44.8	1.05	8.02	140.5	250	274	0.91

6. CONCLUSION

The following were disclosed through the tests carried out:

- According to the results of tension tests, and heat resistance and alkali resistance tests, FiBRA possesses ample practicality as a concrete reinforcing material capable of withstanding long-term use.
- Relaxation loss and tensile fatigue properties of FiBRA are within ranges making possible use as prestressing tendons.
- In concrete beams using FiBRA as flexural reinforcement (main reinforcement and prestressing tendons) the characteristics of FiBRA were amply demonstrated and high strengths and ductilities were indicated.

It is thought concrete members reinforced with FiBRA can be used extensively for durable structures in marine environments and other severe environments requiring chemical resistance.

REFERENCES

1. OKAMOTO, T., and MATSUBARA, S., Fundamental Property of Aramid Fiber Reinforced Concrete, Architectural Institute of Japan Convention, 1985.

2. OKAMOTO, T., MATSUBARA, S., and TANIGAKI, M., Study on Braided Aramid Fiber Rods (Part 1, Tensile Characteristics and Durability), (Part 2, Effectiveness for Reinforcing Concrete), Architectural Institute of Japan Convention, 1987.

Concrete with Glass Metal Reinforcement

Béton renforcé par des fibres en verre-métal

Bewehrung von Beton mit Metall-Glas-Fasern

Béla MAGYARI
Dr.techn.
State Building Company
Kecskemét, Hungary

Béla Magyari born in 1942, received his civil engineering degree at the Technical University of Budapest. Between 1976 and 1982 he carried out detailed experiments on sleeve splicing of reinforcing bars. Presently Béla Magyari is working at a Building Company and is in charge of concrete composites.

SUMMARY
This paper describes the fibre-reinforcement of concrete. The fibres used were glass-metal fibres. Special composition of concretes, as well as grading of aggregates were determined experimentally. In addition to strength tests, concretes with glass-metal reinforcement were tested under repeated loading. The main aim of the experiments was to promote the material for industrial use.

RÉSUMÉ
Des fibres de verre-métal ont été utilisées pour le renforcement du béton. Les compositions spéciales du béton et la granulométrie des agrégats ont été déterminées expérimentalement. Des essais de résistance ont permis de contrôler les bétons renforcés par des fibres en verre-métal également à la fatique, par des charges alternées. L'objectif principal des expériences était la promotion à l'échelle industrielle.

ZUSAMMENFASSUNG
Zur Bewehrung von Beton wurden Metall-Glas-Fasern verwendet. Die spezielle Zusammensetzung des Betons sowie die Abstufung der Zuschlagstoffe wurden durch Versuche bestimmt. Neben Festigkeitsuntersuchungen wurden die mit Metall-Glas-Fasern verstärkten Betonsorten auch auf Ermüdung geprüft. Das Ziel der Untersuchungen war eine industrielle Anwendung in der Baupraxis.

1. INTRODUCTION

Recently application of new fibre reinforcements for concretes arouse wide interest, so their behaviour differing from that of traditional concretes. In addition to investigations of synthetic fibre reinforcements and the composites reinforced therewith, mortars having been reinforced with glass metal fibres stood in the centre of interest at the end of the seventies [1-3] . The tests showed advantageous mechanic behaviour, simultaneously theoretical suppositions relating to the reinforcement of mortars having been reinforced with discontinuous glass metal fibres became verified. The aim of the present study is to extend the investigations to concretes, as well as to promote industrial introduction.

2. COMPOSITION OF THE COMPOSITE

2.1 Concrete

Concrete having been used in course of said tests were not of standarized composition, optimal composition was determined experimentally. Composition of the concrete expressed in weight: 64 % graded sand and gravel with a maximal grain size of 8 and 16 mm, 28,5 % C 550 Portland Cement, 7,2 % water and 0,3 % plasticizer Mighty 100.

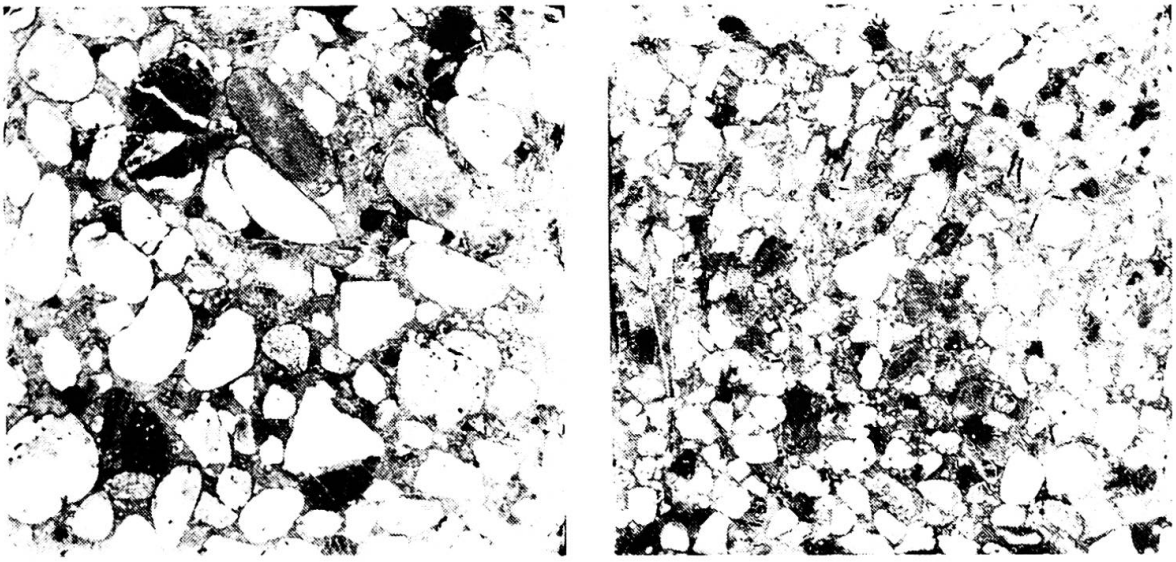

Fig.1 Fibre-reinforced concretes, of 8 mm and 16 mm grain size

Glass metal fibres were added to the mixture in course of dry-mixing. After having finished mixing, fibre-reinforced concrete was poured into the moulds and compacted by a table-vibrator. From the composite with the maximal grain size of 8 mm prisms 40x40x160 mm, from the composite with the maximal grain size of 16 mm prisms 70,7x70,7x250 mm were prepared. Curing under water was continued maximally for 28 days.
Characteristic sections of concretes tested are illustrated in Fig.1.

2.2 Glass metal fibre

The applied glass-metal fibre was prepared in the Iron and Metal Works Csepel with a composition of $Fe_{74}Cr_6B_{14}Si_6$. The length of the glass metal fibre amounted to 40 mm, average thickness to 0,036 mm and width to 1,65 mm.

One side of the glass metal band was smooth, the other one rough. According to the examinations having been performed on individual fibres Young-modulus of the applied glass metal fibre was 153 GPa while it's tensile strength was 1,3 GPa.

3. TESTING OF FIBRE-REINFORCED CONCRETES

3.1 Mechanical tests

Specimens having been cured in water were subjected to strength tests at the age of 7, 28 and 90 days. In course of the tests ductility being proportional with fibrebatches and considerable energy absorbing ability could be observed.

Based on the results of strength tests, as well as on basis of the analysis of the concrete structure we propose to use glass metal reinforced concretes with a grain size of D_{max} = 8 mm instead of the maximal grain size of D_{max} = 16 mm. Characteristic results of strength tests are summarized in Table 1-2.

Batch of fibres vol.%	Strength measured at the age of					
	7 days MPa		28 days MPa		90 days MPa	
	bending	compr.	bending	compr.	bending	compr.
0	10,5	70,9	12,4	87,0	12,7	89,5
0,25	11,3	79,3	13,4	86,5	13,3	85,9
0,50	12,5	76,1	14,2	73,5	14,6	87,3
1,00	17,4	72,8	18,8	72,4	19,6	81,0

Table 1 Strength data of concretes with D_{max} = 8 mm

Batch of fibres vol.%	Strength measured at the age of					
	7 days MPa		28 days MPa		90 days MPa	
	bending	compr.	bending	compr.	bending	compr.
0	8,5	51,4	8,7	59,0	9,2	81,2
0,12	8,6	57,3	9,8	55,6	9,9	85,1
0,25	9,4	54,3	10,0	64,2	10,3	75,0
0,50	10,7	55,5	10,8	60,0	11,4	72,2

Table 2 Strength data of concretes with D_{max} = 16 mm.

3.2 Repeated loads

We tested the effect of frequently repeated pulsating pressing loads on fibre-reinforced specimens and specimens without fibre reinforcement of the size 40x40x160 with D_{max} = 8 mm. Lowest stress level amounted uniformly to 5 MPa, at a frequency of 250 Hz. Compressive load was applied onto the 40x40 mm surface of the specimens. Limit value of fatigue belonging to 2 millions repetitions for the specimen without fibre reinforcement amounted to 35 MPa, while for the specimen containing 0,5 vol.% glass metal fibre the value amounted to 50 MPa. Tests were begun with the specimens at the age of 90 days, with 6 specimens each.

The effect of few repetitions was measured for compressive loads on specimens 70,7x70,7x250 mm, with D_{max} = 16 mm, containing 0,25 vol.% glass metal fibre. As loading stages 10 loadings downwards and 10 loadings upwards were performed and we measured the stress-strain datas. Characteristic curve of deformation is shown in Fig.2.

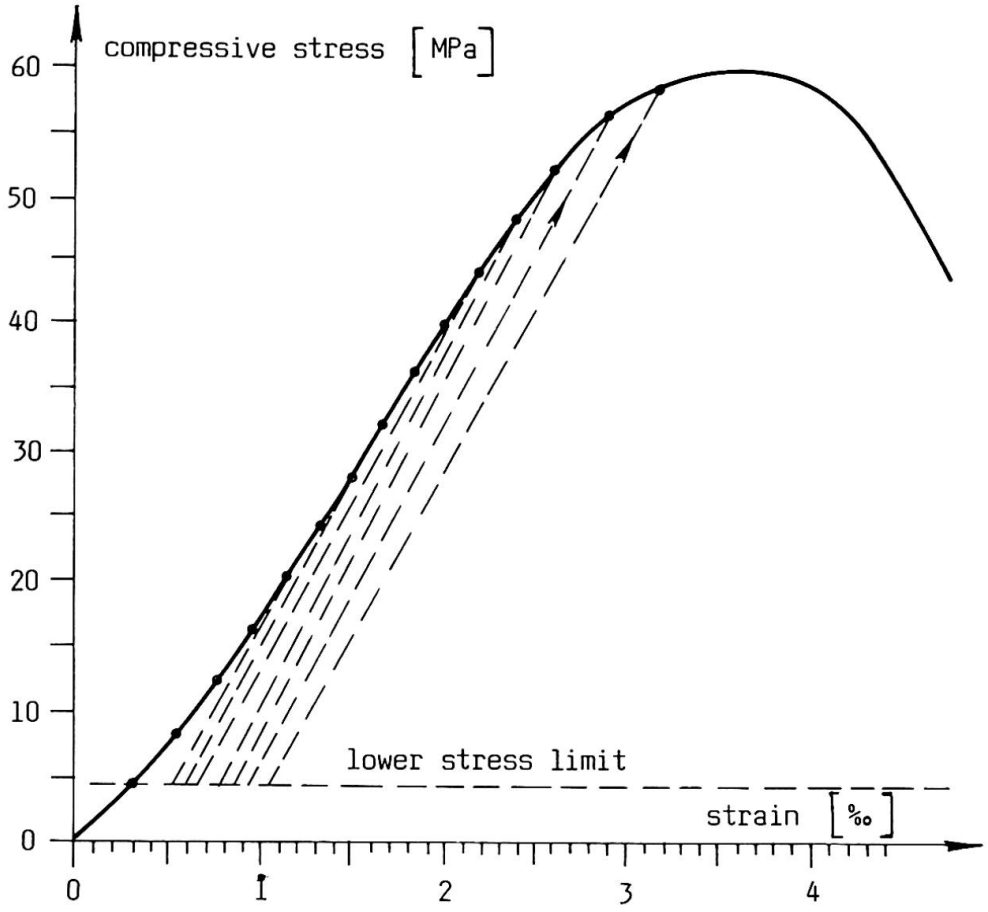

Fig.2 Curve of deformation of concretes with glass metal fibre content

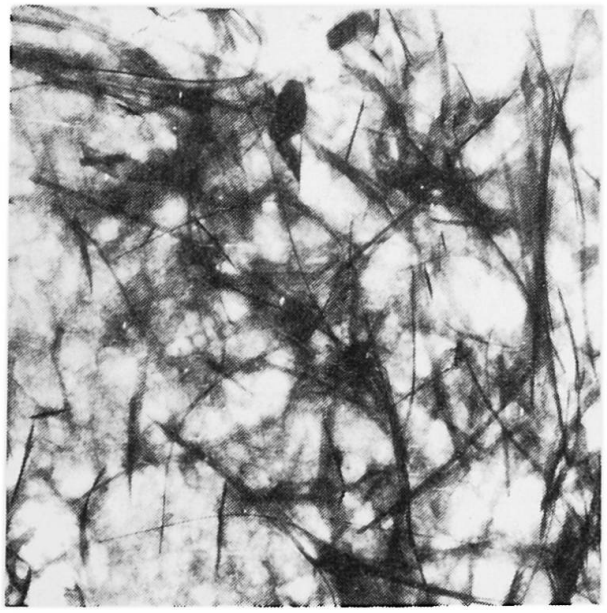

3.3 Structure tests

Parallel with mechanic tests slices were cut from every specimen for macroscopic and microscopic analysis of the structure and the radiograph. Fig.3 shows a characteristic radiograph.

Experiences having been gained in course of structure analyses were fed back to the planning of the composition. In such a manner it succeeded that glass metal fibres should be embedded into the cement paste with their entire surface.

Fig.3 Radiograph of concrete, of 8 mm grain size

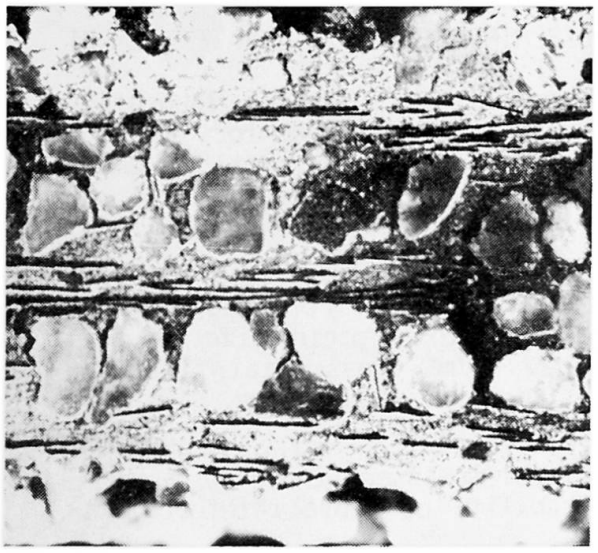

4. MODEL TESTS

In order to study the phenomens taking place in the reinforced fine mortar part of concretes, special plates with lamination of the size 70x250x10 mm were prepared, tested as two-support beams with concentraded force, with a span of 80 mm. In the slabs fibre reinforcement was arranged irregularly in the plane Fig.4 . Tests were performed at the age of 7, 28 and 90 days, in addition to glass metal fibre (b) - polypropylene fibre (c), glass - (d), steel fibre (e) and reference specimens (a) were also used. Stress-deflection diagrams are shown in Fig.5 - fibre length amounted uniformly to 40 mm. Batch of fibres 1 vol.%

Fig.4 Section of fibre-reinforced slab

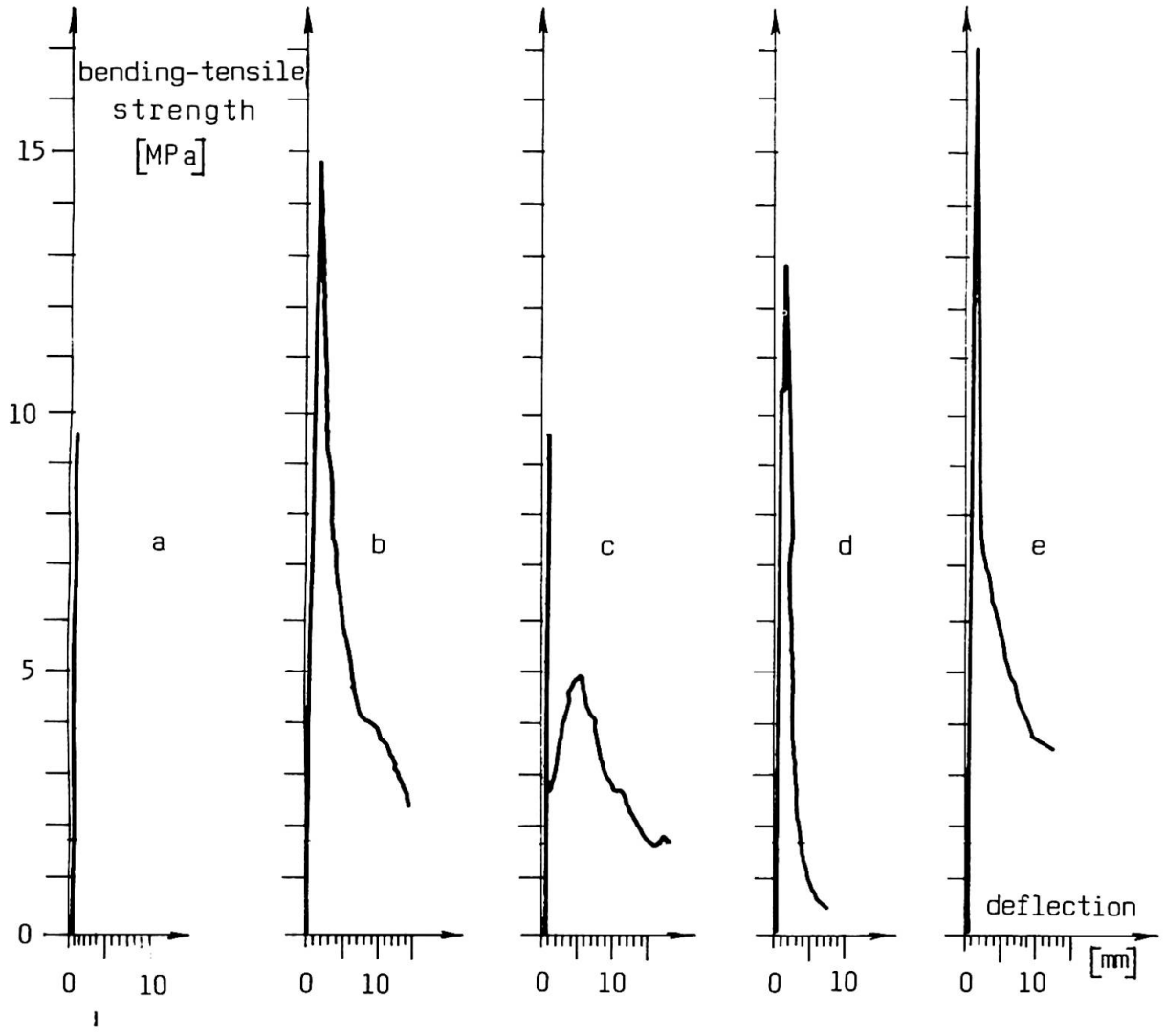

Fig.5 Bending test of fibre-reinforced slabs at the age of 28 days

5. EXPERIMENTAL PRODUCTION OF ELEMENT

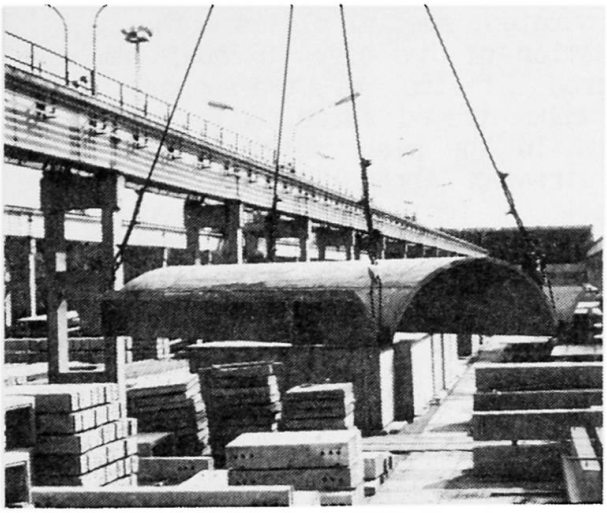

As a result of intensive laboratory work the time has come for applying glass metal fibre in pactice, among others for a 30 mm thick shell structure, as it is to be seen in Fig.6.

Composition of the concrete applied: 600 kg/m^3 C 450 Portland Cement, aggregate with a grain size of max. 8 mm, 22 kg/m^3 glass metal fibre and 3 kg/m^3 polipropylene fibre.

Water/cement ratio equalled to 0,35. Structural tests confirmed applicability of fibre reinforcement.

Fig.6 30 mm thick shell unit with glass metal fibre reinforcement

6. CONCLUSION

Composition of the mixture represents the fundamental matter in case of glass metal fibre reinforced concretes, where aggregate frame, cement quality and quantity, size of the glass metal fibre and the batch added play a special role. Model tests define well the effect of reinforcement, they refer also to the phenomene occuring in the reinforced concrete. In addition to favourable mechanic behaviour excellent resistance of the reinforced concrete to frequently repeated loading should be specially emphasized. In fibre-reinforcing microscopic shots and radiographs play an important role. After having finished the tests concerning glass metal, experimental production of elements was put in action.

REFERENCES

1. ARGON A.S., HAWKINS, KUO, Reinforcement of Mortar with Metglas Fibres. J.of mat.Sci.July 1979.
2. ARGON A.S., Old Materials - New Materials, Proc. 3rd Int. Conf. on Mechanical Behaviour of Materials, Cambridge, 1979.
3. ACKERMANN L., FOURNIER, Reinforcement of Concrete with Metallic Glass Ribbons.
Fourth Int. Conf. on Rapidly Quenched Metals, Sendai 1981.

New Materials for Tunnel Supports

Nouveaux matériaux pour le soutènement de tunnels

Neue Materialien im Tunnelausbau

Kentaro IKEDA
Research Engineer
Shimizu Corporation
Tokyo, Japan

Kenzo SEKIJIMA
Research Engineer
Shimizu Corporation
Tokyo, Japan

Hajime OKAMURA
Professor
Univ. of Tokyo
Tokyo, Japan

Kentaro Ikeda, born in 1958, received his M. Eng. degree from Nihon University in 1982. He has been engaged in research and design of concrete structures with new materials in the Shimizu Corporation.

Kenzo Sekijima, born in 1951, received his M. Eng. degree from the University of Tokyo in 1976. He has been engaged in research and design of concrete structures with new materials in the Shimizu Corporation.

Hajime Okamura, born in 1938, received his Dr. Eng. degree from the University of Tokyo in 1966. He is a professor of the civil engineering department at the University of Tokyo.

SUMMARY
For the purpose of improving the durability and work productivity of tunnel supports, the non-corrosive, light-weight new material fiber reinforced plastics formed in grid shapes to replace steel bars has been applied for shotcrete and concrete lining. Furthermore fiber reinforced plastics rock bolt has been resently developed.

RÉSUMÉ
Le matériau plastique armé de fibres -un nouveau matériau non corrosif et léger fabriqué en treillis et destiné à remplacer les barres d'aciers -a été développé dans le but d'améliorer la durabilité et la productivité dans les soutènements de tunnel. Ce matériau est mis en application dans les soutènements en béton projeté et en béton de revêtement. On a aussi développé des aucrages dans la roche en matériau plastique armé de fibres.

ZUSAMMENFASSUNG
Zur Verbesserung und Gleitschalungen von Lebensdauer und Arbeitsproduktivität im Tunnelausbau wurde für Spritzbeton das nichtrostende, leichte, Material FRP in Gitterform als Ersatz für Stahlbewehrung verwendet. Außerdem wurden Felsanker aus FRP entwickelt.

1. INTRODUCTION

Recently in Japan, the New Austrian Tunnelling Method (NATM) has rapidly become popular according as the progress of rock mechanics. The tunnel supports in NATM are mainly composed of shotcrete, rock bolts and concrete lining. Welded wire fabrics or steel bars are often used for reinforcing shotcrete or concrete lining. However, these materials including rock bolts are made of steel, therefore the durability of the tunnel supports attacked by ground water or flowing water is not reliable, and the work productivity is low due to their heavy weight.

On the other hand, the newly developed New Fiber Composite Material for Reinforcing Concrete (NEFMAC) to replace steel bars, which is made of fiber reinforced plastics (FRP), is non-corrosive and light in weight, therefore it is well suited for the reinforcing materials for shotcrete or concrete lining. Another newly developed FRP rock bolt has enough tensile and bond strength, and it is easy for handling. The characteristics and applications of these materials for tunnel supports are described in this paper.

2. CHARACTERISTICS OF NEFMAC

Table 1 Characteristics of NEFMAC

• Non-corrosive	• Improving the durability of concrete structure under severe condition
• Using continuous fibers	• Effective use of fibers
• Enough strength at the cross points	• Sufficient anchorage to concrete • Lapped splice joint
• Light in weight (specific gravity ≒ 2)	• Improving work productivity in the field
• Forming in complicated shapes	

NEFMAC is a new composite material for reinforcing concrete, which is made of high strength continuous glass and/or carbon fibers impregnated with resin and formed in grid shapes by the filament winding method [1]. Its characteristics are shown in Table 1. Fig. 1 shows the load - strain relationships of deformed steel bar ϕ10mm (Grade 50), NEFMAC G10 (glass fiber) and H10 (glass and carbon fiber).

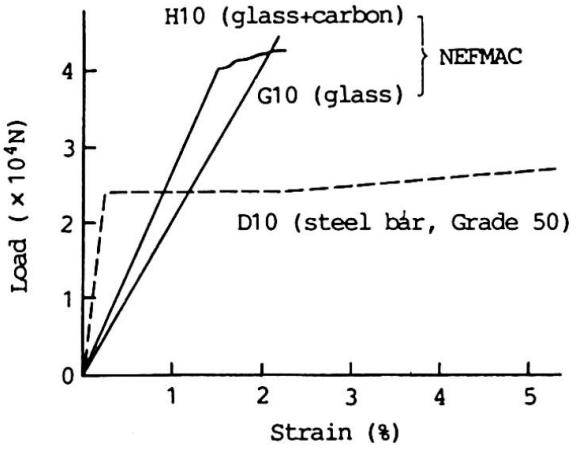

Fig. 1 Load-strain relationship of NEFMAC and deformed steel bar

3. APPLICATION FOR REINFORCING GRIDS FOR SHOTCRETE

3.1 Function and Setting Method of Reinforcing Grids

The purpose of reinforcing grids is to improve the rebound ratio and ductility of shotcrete and to prevent it from falling off. Generally they are set between the primary and secondary layers of shotcrete to exhibit their function. The easy, speedy and continuous setting method of NEFMAC on the surface of the primary shotcrete with quenched staples using compressed-air gun has newly been developed. This new setting method of NEFMAC is shown in Fig. 2.

Fig. 2 Setting method of reinforcing grids for shotcrete

3.2 Clearance between Reinforcing Grids and Surface of Primary Shotcrete

Fig. 3 shows the average clearance between each reinforcing grids and the surface of the primary shotcrete. The averages and deviations of the clearance become smaller as the stiffness of reinforcing grids becomes lower. From this result, NEFMAC can curtail the amount of the secondary shotcrete as much as the difference of the clearance between NEFMAC and welded wire fabrics when they secure the same cover from the surface of the secondary shotcrete.

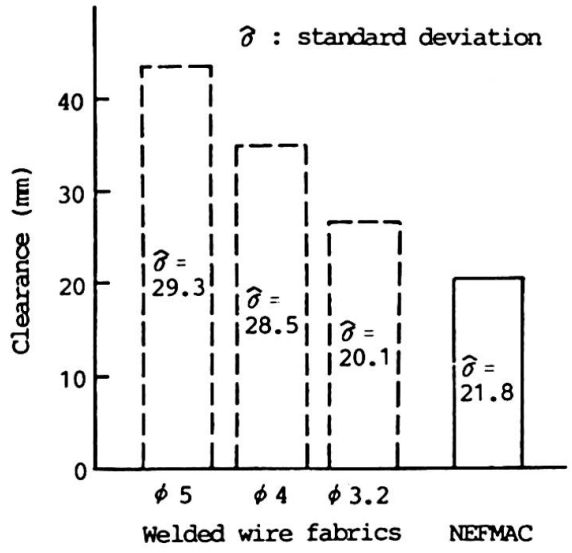

Fig. 3 Clearance between reinforcing grids and surface of primary shotcrete

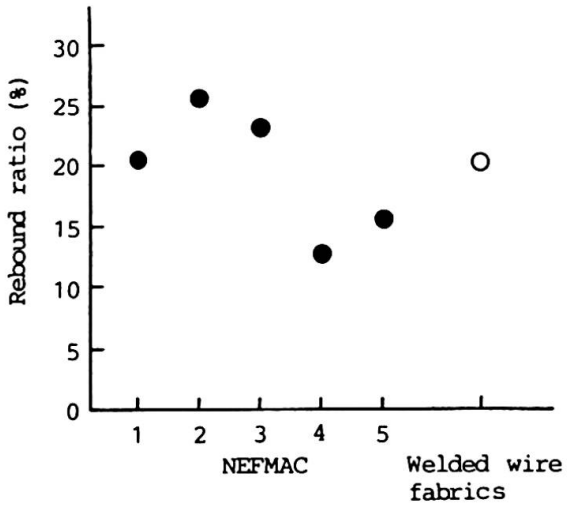

Fig. 4 Rebound ratio of shotcrete

3.3 Rebound Ratio of Shotcrete

The rebound ratio of the secondary shotcrete with NEFMAC is almost the same as that with welded wire fabrics (See Fig. 4).

3.4 Work Productivity and Economy

The new setting method of NEFMAC with staples is more efficient than the ordinary ones of welded wire fabrics, so the setting rate became 1.7 to 5 times higher. Furthermore, the amount and time of the secondary shotcrete decreased. Then the cycle time decreased. For the above reasons, this method has also a merit in economy.

4. APPLICATION FOR REINFORCEMENTS FOR CONCRETE LINING

4.1 Reinforcements for Invert and Arch

Since NEFMAC can be formed in curved shape as well as flat one, and is light in weight, it was adopted as reinforcements for concrete lining of a water-conveyance tunnel in order to greatly improve work productivity. The reinforcements for invert and arch were formed separately in longitudinal and circumferential directions for the sake of transportation and setting in the tunnel. Since NEFMAC has enough strength at the cross points, it was set with lapped splice joints. The reinforcements for invert and arch are shown in Fig. 5 and Fig. 6 respectively.

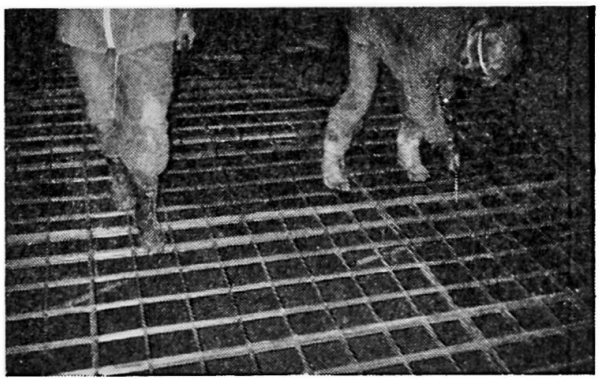

Fig. 5 Reinforcements for invert of concrete lining

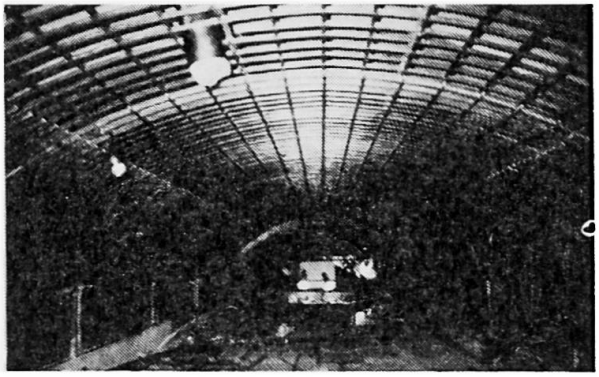

Fig. 6 Reinforcements for arch of concrete lining

4.2 Work Productivity

NEFMAC was transported into the tunnel in pre-assembled form, therefore the assembling time became about one third shorter than that of steel bars. Furthermore, NEFMAC is light in weight and easy to be set without expert workers.

5. FRP ROCK BOLT

5.1 Characteristics

In general, FRP rock bolt has enough durability and it is much lighter in weight than steel one, furthermore it is easy to be cut and removed when the surrounding rock is excavated. However, ordinary FRP rock bolt is only effective as temporary support but not as permanent one because of its small head strength. Therefore, the new FRP rock bolt which has a special type of head has been developed, so its tensile strength is equal to or greater than that of steel one. And on its surface, continuous fibers impregnated with resin are wound spirally to improve bond property.

5.2 Head Displacement and Bond Property

Fig. 7 shows the pull load-head displacement relationship of the steel rock bolt (ϕ25mm, L=2.5m) and the equivalent FRP one at the pull test in a tunnel. FRP rock bolt has large displacement but enough tensile strength, so it can be used as permanent support. Fig. 8 shows the distribution of longitudinal and bond forces of two kinds of rock bolts. Most of bond force on the steel rock bolt occurs near the rock surface, but that on FRP rock bolt becomes larger inside in accordance with the increase in the pull load. From these results, FRP rock bolt has small stiffness, it will be more effective for soft or swelling rock than hard one.

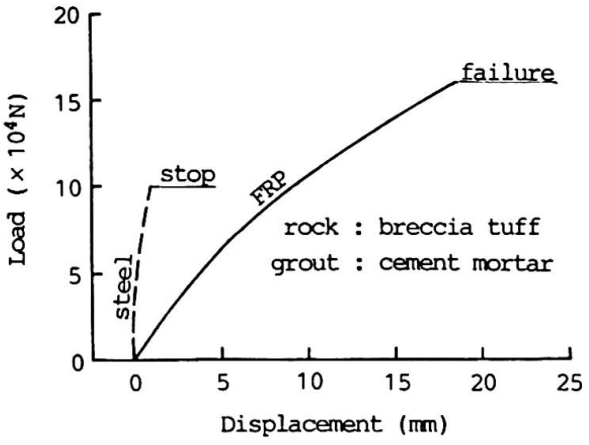

Fig. 7 Pull load-head displacement relationship of rock bolt

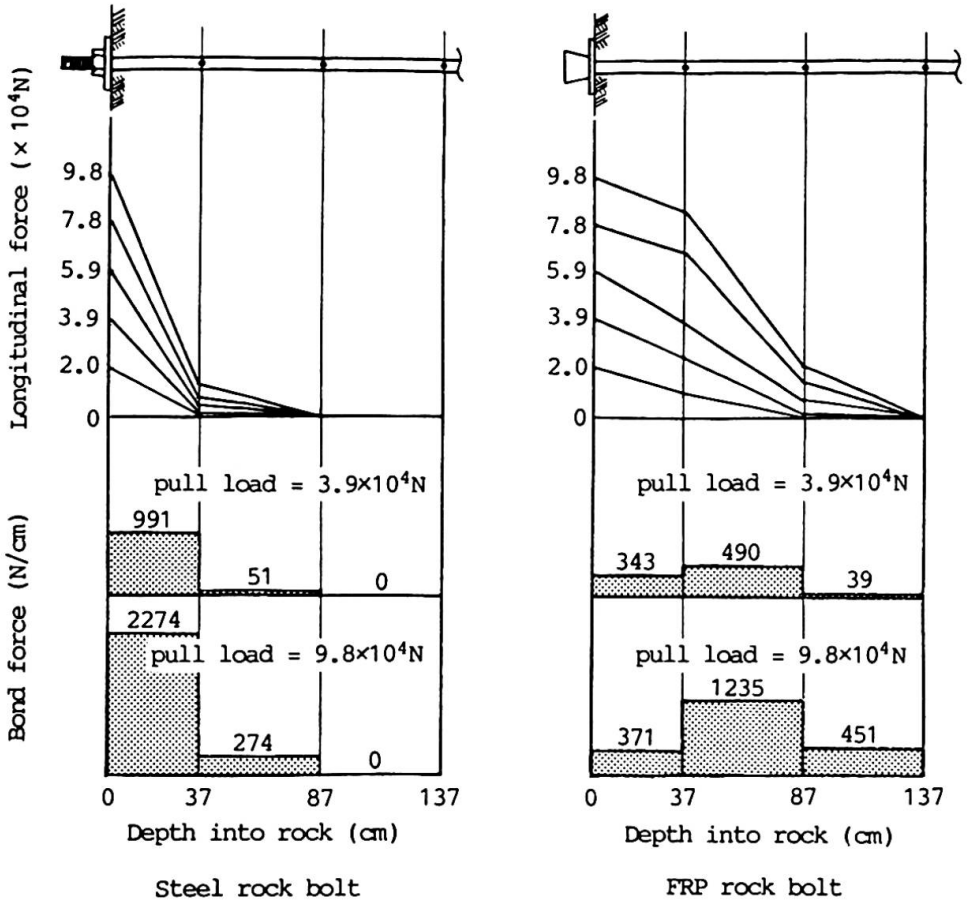

Fig. 8 Distribution of longitudinal and bond force of rock bolt

6. CONCLUDING REMARKS

NEFMAC has already been used as reinforcing grids for shotcrete at several tunnels in Japan. It was also used at an advancing drift because it is easy to be excavated after setting. In the near future, it will be used at large underground rock caverns such as electric power plants or petroleum storage. On the other hand, there are only a few application cases of NEFMAC as reinforcements for concrete lining, but it is best suited for repairing tunnels under severe conditions and reducing the term of works. FRP rock bolt can be used as permanent support and it will be effective for soft or swelling rock.

ACKNOWLEDGEMENT

The authors wish to show their profound appreciation to President Hideo FUTAGAWA of Dai Nihon Glass Industry Co., Ltd., Minoru SUGITA and Teruyuki NAKATSUJI of Shimizu Corporation, and the other project members.

REFERENCE

1. FUJISAKI T., SEKIJIMA K., MATSUZAKI Y. and OKAMURA H., New Material for Reinforced Concrete in place of Reinforcing Steel Bar, IABSE Symposium in Paris-Versailles, September 1987.

Test Methods and Applications of Steel Fibre Reinforced Concrete

Méthodes d'essai et applications du béton armé de fibres d'acier

Prüfmethoden und Anwendung von Stahlfaserbeton

Guofan ZHAO
Professor
Dalian Inst. of Technol.
Dalian, China

Guofan Zhao, born in 1925, obtained his Civil Engineening degree from the Jiao-Tong University, Shanghai, China, in 1949. Since 1950 he has been actively engaged in teaching and research in reinforced and prestressed concrete and structural safety. Currenty, he is a member of the IABSE, RILEM.

Chengkui HUANG
Senior Engineer
Dalian Inst. of Technol.
Dalian, China

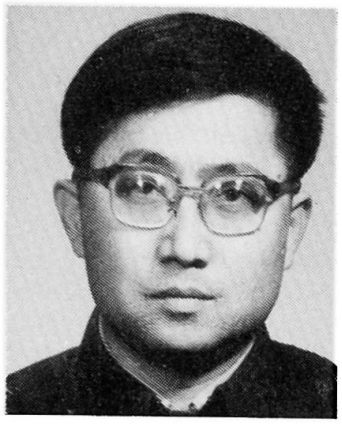

Chengkui Huang, born in 1941, obtained his BS degree from Qing Hua University, Beijing and MS degree from Dalian Institute of Technology. Prior to joining the faculty at Dalian Institute of Technology he was engaged in concrete dam practice, since 1978 he has been engaged in research and teaching in reinforced concrete structures.

SUMMARY
This paper reports the findings of a series of research projects carried out on steel fibre reinforced concrete (SFRC) which had the following objectives: to elucidate the special procedures required for the testing of SFRC; to investigate the mechanical properties and the cost of SFRC with three types of fibres; the behaviour of composite beams with a view to concrete pavements; the effect of steel fibres on the properties of lightweight concrete with respect to multistory buildings.

RÉSUMÉ
Cette contribution donne un aperçu sur les résultats d'une série de recherches effectuées sur le béton armé de fibres d'acier, en ce qui concerne les aspects suivants: les caractéristiques des méthodes d'essai, l'estimation du coût et les propriétés mécaniques de bétons renforcés de 3 types de fibres; les propriétés de poutres composites en béton de fibres; l'effet des fibres d'acier sur les propriétés du béton à agrégats légers, pour des applications dans la réparation de chaussées et dans le bâtiment.

ZUSAMMENFASSUNG
Dieser Beitrag beschreibt die Resultate von Forschungsprojekten über Beton mit Stahlfaserbewehrung. Die Ziele waren die folgenden: die Eigenarten der verschiedenen Prüfmethoden, die Untersuchung der mechanischen Eigenschaften und der Kosten von 3 verschiedenen Faserarten, das statische Verhalten von Betonbalken mit Stahlfasern und die Auswirkung von Stahlfasern auf die Eigenschaften von Leichtbeton, wie er im Strassenbau und im Hochbau angewendet wird.

1. INTRODUCTION

Considerable research efforts have been made on steel fibre reinforced concrete with the growth of its application in the last decade in China. In order to provide useful data for design and standardized testing to allow meaningful comparison of reported test results in the literature, the proposals for the trial edition of "Method of Test for SFRC" have been prepared. In this course a series of mechanical tests on SFRC has been carried out and it is found that most test methods for plain concrete are suitable for SFRC and some test procedures for SFRC are different from that for plain concrete.

An obstacle to use the SFRC is its cost higher than plain concrete, therefore to find the SFRC in high quality and low cost is very important. For this purpose, three types of steel fibres have been used in the tests to investigate and compare their influence on the mechanical properties and the cost of SFRC.

In order to develop more applications of SFRC to pavement and high-rise building, the flexural properties of the composite beams with SFRC and plain concrete layers and the mechanical properties of SFRC with lightweight aggregate made from expanded shale have been stadied experimentally.

2. TEST METHOD

Following suitable existing test methods, the authors have carried out many tests on mechanical properities of SFRC in recent years in the structural laboratory of Dalian Institute of Technology. It is recognized that most of test methods for plain concrete can be used in SFRC tests, such as compresive strength, splitting tensile strength, modulus of elasticity, shrinkage, creep and some other tests.

Some specialities of test motheds for SFRC have been found as follows: In specimen preparation external vibration should be used, rodding is not accepted, internal vibration may be used in some cases where the effect of fibre orientation and distribution caused by internal vibration on the test result is not important. Slump is not a good indicator of workability and the Vebe procedure is a good way to get it. In compressive strenth tests the standard specimens (150x150x150 mm cube or 150x150x300 mm prism) used coventionally in China are appropriate for SFRC ,sometimes smaller specimens (100x100x100mm, 100x 100x300mm) may be used, but the effect of size of SFRC specimens on test results is more severe than that of plain concrete. According to the statistics of 120 specimens, the ratio of the compressive strenth of 150x150x150 mm cube to that of 100x100x100 mm cube is 0.91 for SFRC , but it is 0.95 for plain concrete [2]. For evaluating the engineering property of SFRC, the stress-strain curve in tension and compression and the load-deflection curve in flexure should be obtained. It is well known that testing equipment may be a problem for obtaning the above curves, so the testing machine with closed loop and high rigidity shold be used in those tests. In China, conventional testing machines have been widely used in most laboratories, for avoiding abrupt failure and obtaining the descending portion of the curves, the testing machine should be stiffened by loading the specimens in parallel with two steel rods for tension and with four stiff springs for compression. In this manner, most tests might be successful. Potentionmeters or LVDT displacement transducers are prefered to dail gages or strain gages as transducers for measuring the deflection, elongation or strain and automatic dynamic data acquisition system with computer or X-Y recorder should be used to get data fast.

One of the properties of concrete which is improved by the addition of fibres is energy absorption, it can be represented by the toughness index. The toughness index is calculated as the area under the normalized load-deflection curve out to the reference deflecion Dr, Ti=(L/Lp)x(D/Dr)x100, were Dr=span/150, Lp=the peak of load.

3. THE MECHANICAL PROPERTIES OF SFRC

Three types of fibres have been used in the tests: (1) Hooked fibres made from sheared thin steel sheets in rectangulor cross section (H-fibre), (2) Melt extract fibres made from waste steel and iron in kidney shaped cross section (M-fibre), (3) Straight fibres produced by cutting the unraveled wire from scrap or wornout steel cables and wire ropes (S-fibre),which are much cheaper than the other two, the cost of S-fibres is approximately 50% of that of M-fibres or 30% of that of H-fibres. The aspect ratio (length to equivalent diameter) is about 50 for H-fibre and M-fibre,75 for S-fibre. To allow comparison the properties of SFRC with deffrent types and contents of steel fibres, the matrix of all specimens are the same for each group of tests.

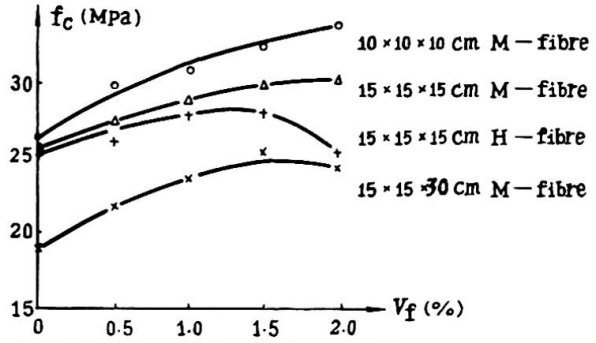

Fig.1 Relationship Between Compresive Strength of SFRC and Fibre Content

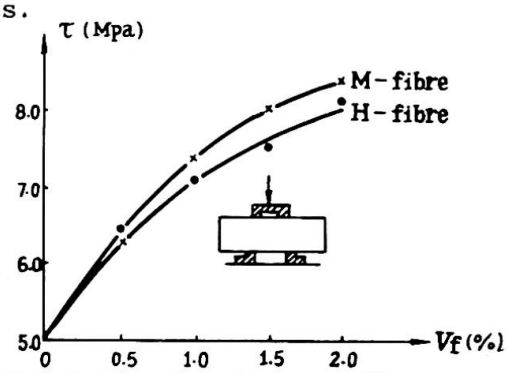

Fig.2 Relationship Between Shear Strength of SFRC and Fibre Content

Typical results of tests are shown in Fig. 1 to 7, which indicate that all mechanical strengths except compressive strength increase singnificantly with the increasing of steel fibre content. Refer to Fig.1, the compressive strength is likely maximum at Vf=1.5% and the improvement ranges from 0 to 21 percent, if the content of steel fibre by volume is more than 1.5%, the compressive strength decreases with the content increasing because the workability and density of SFRC is deteriorated.

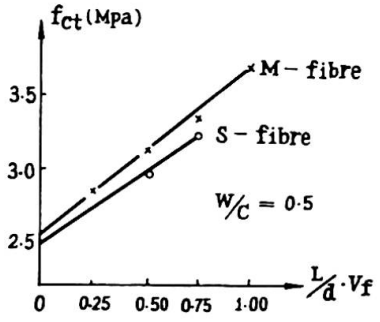

Fig.3 Typical Results of Splitting Tensile Test on SFRC

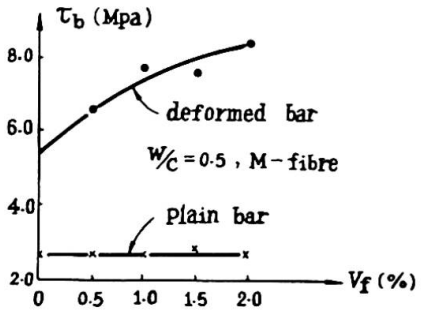

Fig.4 Ultimate Bond Strength of Reinforcing Bars in SFRC

The shear strength, splitting tensile strength and rupture modulus (Fig.2,3 and

6) are improved by addition of 2% fibres by 35 percent, 44 percent and 55 percent, respectively.

Referring to the property of beam-column joint, the bond strength around reinforcing bar should be examined, test data indicate that the improvements are more significant for deformed bars and negligible for plain bars.

The improvement for the thoughness and post-elasticity property of SFRC is more and more evident with the content of fibres increasing (Fig.5 and 6), the thoughness index of SFRC with 2% fibres is 41 times more than that of plath concrete.

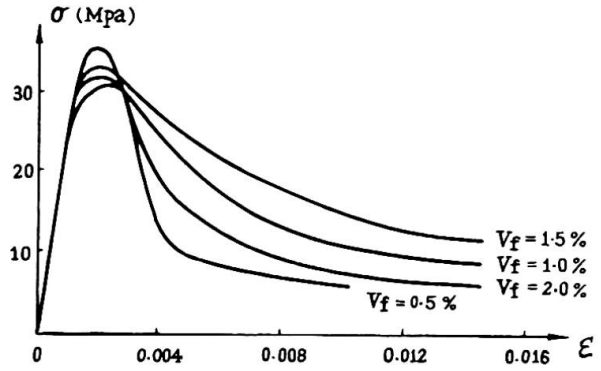

Fig.5 Stress-Strain Curves in Compresion for SFRC

On the basis of above mentioned properties, the melt extract fibres are prefered because of their high surface area/volume ratio, irregular contour and rough surface which improve the adhesive and frictional bonds, and the optimal content is about 1.5 percent by volume (1/d Vf=.75). But considering the cost, the cut wires made from waste steel wire rope are also accessible, and the economic content of fibres may be 1 to 1.5 percent by volume (1/d Vf=.75--1.00).

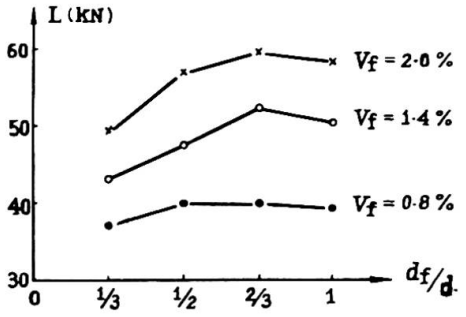

Fig.6 Modulus of rupture of SFRC as a Function of Fibre Content

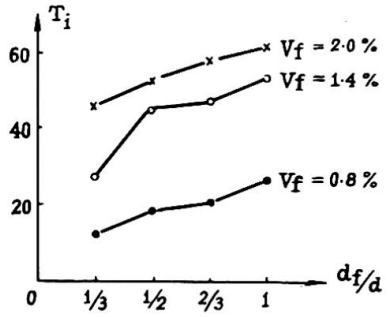

Fig.7 Tougthness Index of SFRC as a Function of Fibre Content

4. THE PROPERTIES OF COMPOSITE BEAMS

For simulating the pavement composed of two layers of concrete and SFRC, the authors have carried out the tests of composite beams on their flexural and shear properties. All the beams are 550mm long(span=450mm) in 150 150mm section. Two layers are adhered to each other and composed in three cases: ratios of depth of SFRC layer to the total depth of beam are 1/3, 1/2, 2/3, respectively.

The rupture modulus and toughness of composite beams varing with ratio of layer

depths are illustrated in Fig.8. At the ratio of depths =1/2 and 2/3, the rupture moduli of composite beams are almost same as that of SFRC beams, and the toughness indexes of composite beam are lower slightly than that of SFRC beams . Therefore it implies that composite pavement with SFRC and plain concrete layers is applicable in repairing old pavement and constructing road and some engineering properties should be studied further.

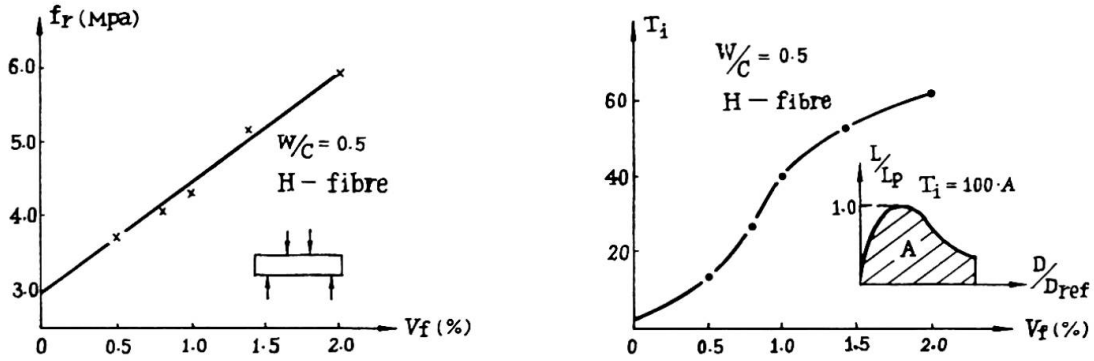

(a) Modulus of rupture (b) Toughness Index

Fig.8 Test results for Composite Beams in Flexure as a Function of Ratio of Layer depths

5. SFRC WITH LIGHTWEIGHT AGGREGATE

In the tests, lightweight concrete (density 1.95)contains river sand and aggregate made from expanded shale of ball shaped in diameter smaller than 10mm. The formula of matrix are the same for each series of steel fibre reinforced lightweight concrete specimens

It has a strong appeal to the authors that the improvement in both compresive strength and other properties of lightweight concrete by addition of steel fibres is more significant than that of plain concrete. On the following data the emphasis should be puted: By addition of steel fibres of 2.0% the improvements are 40–50 percent in compressive strength, 65 percent in splipping tensile strength,95 percent in shiear strength and 90 percent in rupture modulus,respectively. On other hand, the failure behaviour of lightweight concrete is also improved by addition of steel fibres and appear in a more ductile manner.

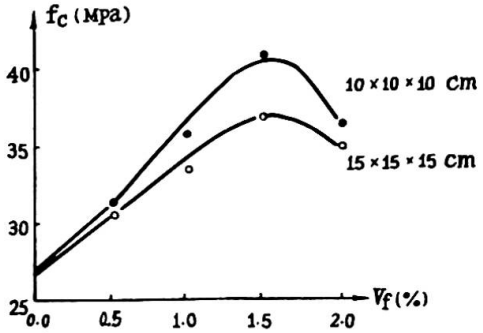

Fig.9 Compresive Strength of Lightweight Concrete Improved by Addition of Steel Fibres

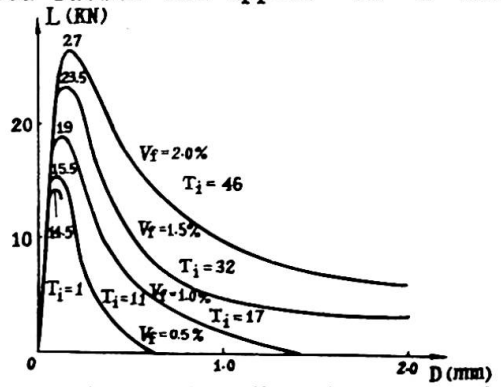

Fig.10 Load-Deflection Cuves in Flexure for SFRC with Lightweight Aggregate

The lightweight aggregate concrete reinforced by steel fibres will be beneficial to its uses in frames and shear walls in multistory buildings especially in

beam-column joints and beams of coupled shear walls. In those cases, the shear strength, flexural strength and ductility of structures will be improved in a singnificant manner.

6. CONCLUSIONS

1). Most test methods for plain concrete are suitable for SFRC but some special procedures required by the nature of SFRC should be provided.
2). The melt extract steel fibres are in higher quality and lower cost.Using drawn wire fibres made from waste steel rope is also a good way to lower the cost of SFRC.
3). The test results of composite beams imply that combining the SFRC layer with plain concrete layer in pavement may be a ecnomic means.
4). The improvements in mechanical strength and failure behavior of lightweight concrete by the addition of steel fibres are in a more singnificant manner, which indicates potential extensive applications in multistory buildings.

7. ACKNOWLEDGEMENT

The authors would like to thank Mr. Zhao Yibing, Mr. Gao Danying, Mr. Zhang Zhonggang and Miss Qiu Xiuhua, Department of Civil Engineering, Dalian Institute of Technology for their asistance in many tests. The financial support of this investigation by the Chinese Technical committee on Design and Construction Standards for Concrete Structures is gratefully acknowlodged.

REFERENCE

1. Guan Liqiu and Zhao Guofan, A Study on the Mechanism of Fibre Reinforcement in Short Steel Fibre Concrete,RILEM Symposium FRC86.
2. China Academy of Building Research,The Standard of Test Method for Plain Concrete, 1986,Beijing.
3. China Academy of Water Conservancy and hydraulic Engineering Research,The Standard of Test Method for Concrete in Water Conservancy and Hydraulic Engineering, 1982, Beijing.
4. E. K. Schrader: Formulating Guidance for Testing of Fibre Concrete in ACI Committee 544, RILEM Symposium 1978.
5. JSCE FRCD Research Subcommittee, Recommendation for Design and Construction of Steel Fibre Reinforced Concrete, 1983, Japan.
6. Cheng Longbao, The Production Technique of Melt Extract Steel Fibres, Qing An Steel Factory, Heilong Jiang Province, China, 1986.

Properties of Fibre Glass Reinforced Cement Composites

Caractéristiques du béton renforcé de fibres de verre

Eigenschaften von mit Glasfasern bewehrtem Beton

Karol KOMLOŠ
Chief scientist
Inst. of Constr.
Bratislava, Czechoslovakia

Bohumil BABÁL
Scientist
Inst. of Constr. and Archit.
Bratislava, Czechoslovakia

Matej VANIŠ
Assoc. Prof.
Slovak Techn. Univ.
Bratislava, Czechoslovakia

Jana KOZÁNKOVÁ
Research worker
Slovak Techn. Univ.
Bratislava, Czechoslovakia

SUMMARY
The paper deals with the testing of long term resistance of fibre glass in the alkaline medium of Portland cement. The applied Czechoslovak alkali resistant fibre glasses were incorporated into the Portland cement matrix. The long term ageing process was studied. Some of the specimens were stored in water, and the rest were dry cured. The modulus of rupture was determined at the age of 28, 90, 180, and 360 days. The composite texture was studied by the SEM method.

RÉSUMÉ
L'étude examine la résistance à longue durée des fibres de verre dans le milieu alkalin du ciment Portland. Les fibres de verre tchécoslovaques ont été utilisées pour renforcer la matrice de ciment Portland. La résistance à longue durée a été examinée sur des éprouvettes. Une partie de celles-ci était stockées dans l'eau, une autre partie dans un environnement sec. La résistance à la flexion a été déterminée aprés 28, 90, 180, 360 jours. La microstructure des ciments à fibres de verre a été étudiée par la méthode SEM.

ZUSAMMENFASSUNG
Dieser Beitrag befasst sich mit der Untersuchung der Langzeitbeständigkeit von Glasfasern in der alkalischen Portlandzement-Matrix. Verwendet wurden tschechoslowakische, alkalibeständige Glasfasern, die in die Zementmatrix eingebettet wurden. Die Langzeitbeständigkeit wurde an Prüfkörpern untersucht. Ein Teil dieser Prüfkörper wurde im Wasser, ein anderer Teil wurde trocken gelagert. Die Biegezugfestigkeit wurde im Alter von 28, 90, 180, 360 Tagen ermittelt. Das Verbundwerkstoffgeffgefüge wurde mittels der SEM Methode untersucht.

1. INTRODUCTION

The extension of fibre reinforced cement composites /FRC/ to the field of building materials plays a peculiar role of its own in the already wide and wellestablished area of application for composite materials. Glass fibre reinforced cement and concrete GRC/, with its rapidly increasing applications in construction /e.g.clading panels, permanent formwork, small components, hydraulics and marine applications/, is a composite material consisting of a cement or concrete matrix reinforced by a small proportion of glass fibres.

The function of the fibres in the relatively brittle cement matrix is to delay and control the tensile cracking of the material so that an unstable and uncontrolled tensile crack growth is transformed into a slow controlled crack growth. It is this unique characteristic of fibre reinforcement that gives the composite properties of post-cracking tensile resistance, increased tensile strain capability and enhanced energy absorption.

The basic problem of GRC application is the attack by the alkalies associated with hydrating cements. This problem is being solved either by applying alkali resistant glass fibres provided with effective coating materials, e.g. Cem-FIL 1 and Cem-FIL 2 fibres of following composition: SiO_2= 62.5%; ZrO_2= 16.3%; NaO_2 = 14.8%; Al_2O_3= 0.85%; CaO = 5.05%; K_2O = 0.3%, produced by Pilkington Brothers Ltd in Great Britain, or by decreasing the alkalinity of the cement matrix, e.g. the procedure developed by l´Industrielle de Préfabrication in France, which enables the application of E-glass fibres.

In Czechoslovakia much attention has been paid to the problem of alkali resistance of glass fibres, and the result of these studies was the development of two types of alkali resistant glass fibres. Glass fibres REZAL and ESAP are of low zirkonium dioxyd content, SVÚS 16 belongs to the high zirkonium dioxyd content.

In our previous work [1] we studied the suitability of several methods of determining the chemical resistance of glass fibres in alkaline media. These investigations have shown that the autoclave test method has a more severe effect on the glass fibres than the standard method. The most deterious effects were obtained with a NaOH and Na_2CO_3 mix as the reacting solution. The submitted paper, which is a continuation of the above study, deals with the long-term alkali resistance of Czechoslovak glass fibres incorporated in the cement matrix.

2. EXPERIMENTAL PROGRAMME

2.1. Materials and mixes

A Portland cement type 400 was used to manufacture the cement paste. The physico-mechanical properties of the applied cement fulfilled the requirements of the Czechoslovak Standard ČSN 722121. As fibre reinforcement REZAL, ESAP, and SVÚS 16 alkaliresistant glass fibres were applied. Their chamical composition is given in Table 1. The fibre length was 36 mm. The water/cement ratio of the cement paste was 0.370. The following fibre weight fractions of glass fibres were incorporated into the cement paste: 0.4; 1.0; 1.6; 2.2; 3.3; and 4.4 per cent. The batches were mixed in

Components in weight% / Fibre Type	SiO_2	ZrO_2	BaO	Na_2O	Al_2O_3	CaO	Fe_2O_3	TiO_2
REZAL	59,29	4,97	9,94	10,4	5,10	10,3	—	—
ESAP	65,70	4,95	6,80	10,5	4,60	7,3	0,15	—
SVUS16	58,30	11,40	—	14,3	—	8,6	—	7,4

Table 1 Glass fibre chemical composition

laboratory pan mixer, and the fibres were incorporated into the cement paste in such a way to ensure an uniform and random distribution in the cement matrix.

2.2. Casting, curing and testing

The mixes were compacted in steel moulds on a vibrating table /50 Hz; 0.35 mm/. Three specimens 40x40x160 mm could be manufactured simultaneously in these moulds. Together with the fibre reinforced specimens, plain specimens were cast. For each investigated parameter six specimens were manufactured. The obtained values are the mean strength values determined on these specimens.

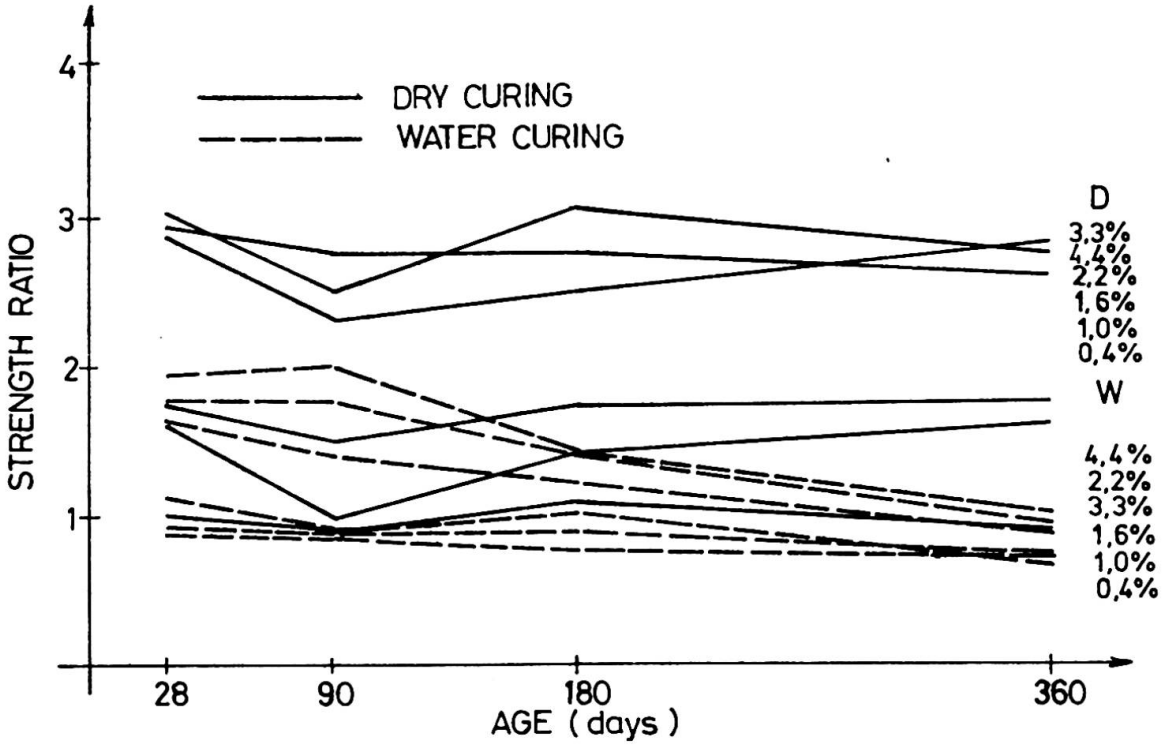

Fig. 1 Strength ratio varsus composite age relationship - fibre typ: REZAL

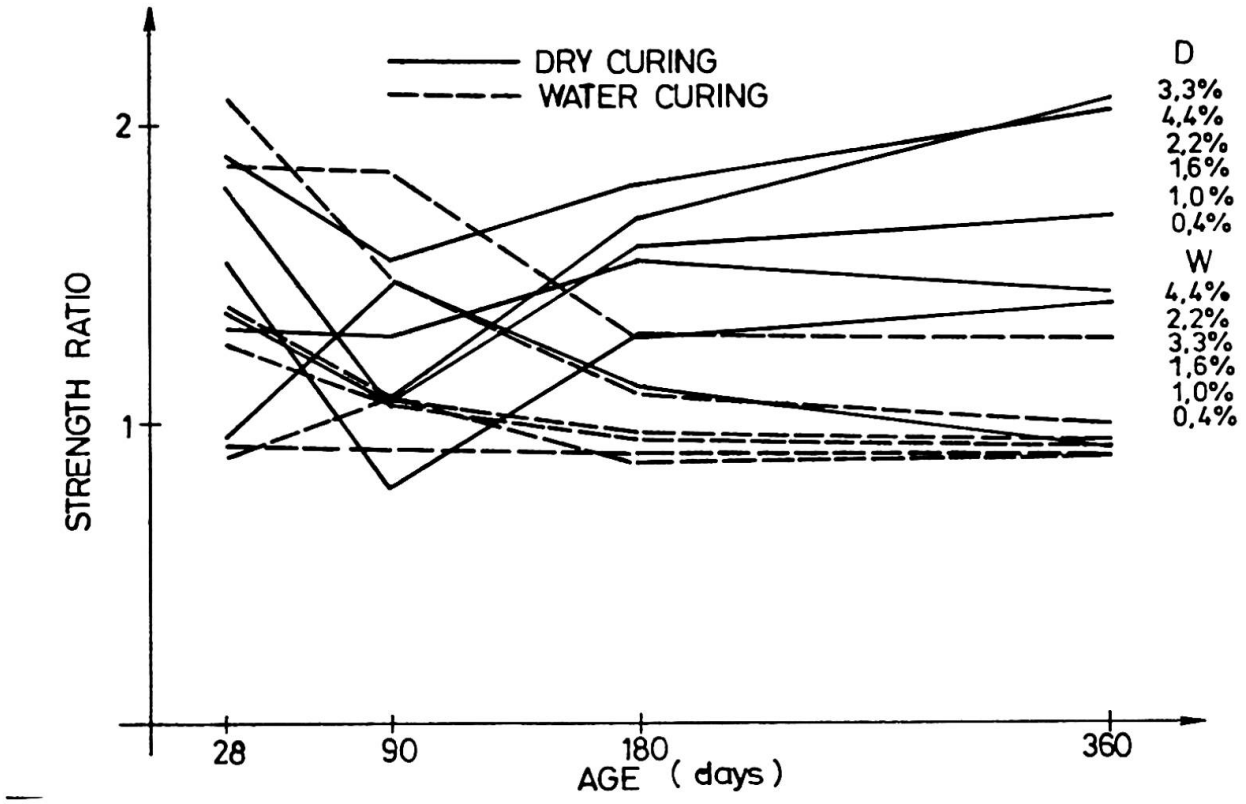

Fig. 2 Strength ratio versus composite age relationship - fibre type: ESAP

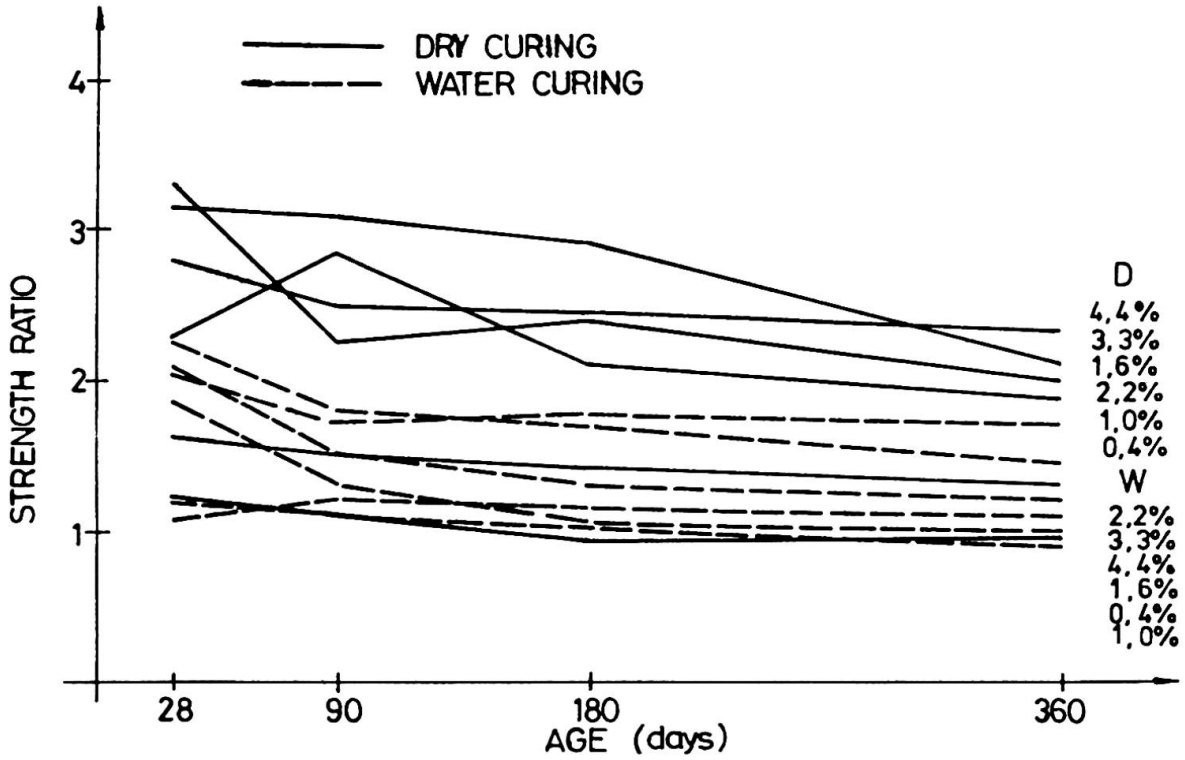

Fig. 3 Strength ratio versus composite age relationship - fibre type: SVŪS 16

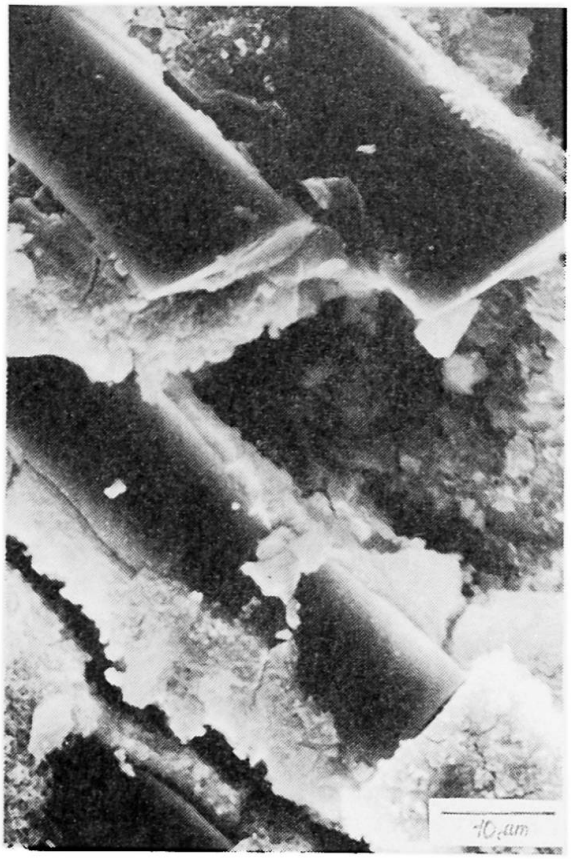

Fig. 4 SEM of REZAL fibres in the cement matrix /360 days, water curing, fibres: 4.4%/

the age of the tested specimen reinforced with a fibre weight fraction of 0.4; 1.0; 1.6; 2.2; 3.3; and 4.4 is plotted. The flexural strength ratio is the ratio

$$\frac{\text{strength of reinforced matrix}}{\text{strength of plain matrix}}$$

The investigations carried out have shown that the specimens stored in water exhibit considerably lower strength than specimens dry cured. The strength of composites of low glass fibre content, stored for 360 days in water, can decrease to the strength of the cement matrix. This phenomenon is in good agreement with results published abroad, as well as with our results obtained earlier [2]. The obtained results show - more pronounced in the case of dry curing - that with the raise of fibre weight fraction, we obtain an increase in the composite strength. The drop

One half of the manufactured specimens was dray cured, and the second half cured in water.

After casting the specimens were cured in moulds for 48 hours in a moist room /20°C, 90 per cent R.H./, and after the moulds were removed, one half of specimens was stored in dry environment /20°C, 60 per cent R.H./, and the second half was stored in water /20°C/. The specimens were tested at the age of 28, 90, 180, and 360 days. The specimens were tested in flexural strength /three point loading being used/. A 25 kN testing machine with a constant loading rate of 6 mm/min. was applied.

2.3. Results and discussion

The results of investigations carried out are summarized in Fig. 1 to 3. In These figures the relationship between the flexural strength ratio and

Fig.5 SEM of ESAP fibres in the cement matrix /360 days, water curing, fibres: 4.4%/

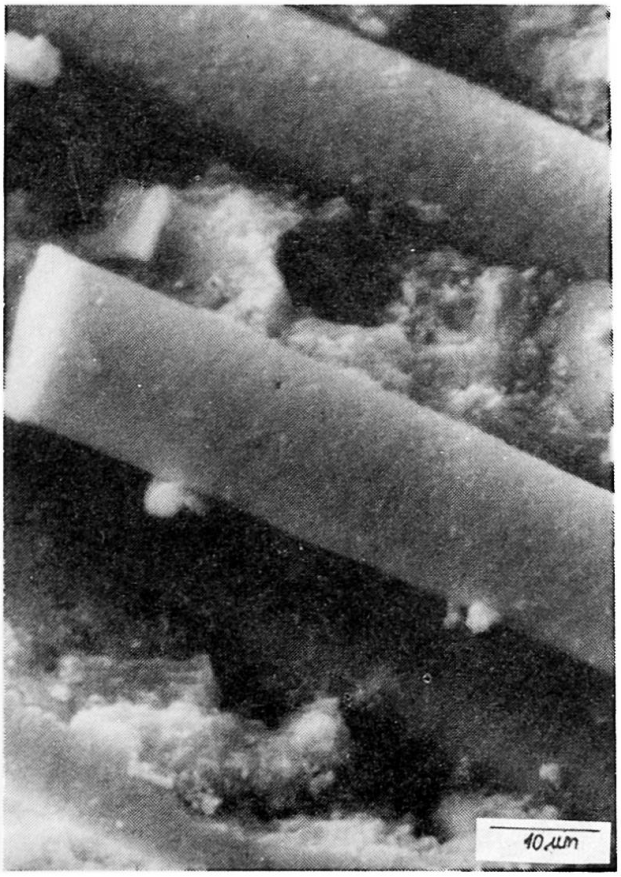

Fig. 6 SEM of SVÚS 16 fibres in the cement matrix /360 days, water curing fibres: 4.4%/

of strength around the composite age of 90 days, in the case of dry curing /see Fig.1 and 2/, can be effected by non uniform shrinkage, or by partial debonding in the fibre-matrix interface, iniciated also by the shrinkage process.

After the strength tests were carried out, samples were taken in order to be investigated under the SEM. According to these investigations we may say that the fibre shape remained unchanged, even in the case of water curing, and that the fibre surface is covered with smaller and larger particles of hydration products /see Fig.4 to 6/.

3. CONCLUSIONS

The investigated glass fibre types have shown a considera bly high alkali resistance. Within the testing period of one year glass fibres of low as well as of high zirkonium dioxyd content show similar behaviour in the cement matrix. Only further investigations, now being carried out, can clear all the problems connected with the alkali resistance of the tested glass fibres.

REFERENCES

1. VANIŠ M., KOMLOŠ K., Contribution to the Methods of Determining the Chemical Resistance of Glass Fibres in Alkaline Media. Proceedings - Durability of Glass Fiber Reinforced Concrete, Symposium, Chicago, November 1985, pp.222-229.

2. VANIŠ M., KOMLOŠ K., Vlastnosti sklenného vlákna typu Rezal, odolného voči alkalickému prostrediu. Sklář a keramik, 36, 1986, august, pp.225-230.

Epoxy-Coated Reinforcement – an Effective Corrosion-Protection System

Armatures recouvertes de résine – une protection efficace contre la corrosion

Epoxy-beschichtete Bewehrung – ein effizienter Korrosionsschutz

David P. GUSTAFSON
Technical Director
Concrete Reinforcing Steel Inst.
Schaumburg, IL, USA

Dr. Gustafson is engaged in the technical promotion of reinforced concrete construction in the USA. He is active in ASTM and ACI committee work in the development of standards for steel reinforcement, design, and construction.

SUMMARY
This paper describes experience in the United States with epoxy-coated reinforcement including coating industry practices, recommended construction practices, and requirements in specifications. Recent laboratory and field research on the corrosion resistance of coated reinforcing bars is cited. Structural performance of concrete members reinforced with coated bars is discussed in terms of bond strength and fire endurance.

RÉSUMÉ
La contribution décrit les expériences faites aux Etats Unis avec les armatures recouvertes de résines, et donne les procédés de fabrication, les recommandations pour la construction et les spécifications requises. On cite les recherches récentes en laboratoire et sur chantier concernant la résistance à la corrosion des armatures enduites de résine. Les performances structurales d'éléments en béton contenant ces armatures sont discutées en ce qui concerne les qualités d'adhérence et la résistance au feu.

ZUSAMMENFASSUNG
Dieser Beitrag beschreibt die in den USA gemachten Erfahrungen mit epoxy-beschichteten Bewehrungen, einschliesslich der Herstellungsverfahren, der Empfehlungen für die Baustelle und der Qualitätsanforderungen. Neuere Labor- und Feldversuche zur Ermittlung der Korrosionsbeständigkeit von beschichteten Bewehrungsstählen werden aufgezeigt. Das Verbundverhalten und der Feuerwiderstand von Bauwerksteilen mit beschichteten Bewehrungen werden diskutiert.

1. INTRODUCTION

In the 1960s, cooperative studies by several state highway agencies, the U.S. Department of Transportation (USDOT), and the Portland Cement Association (PCA) to assess the durability of reinforced concrete bridge decks confirmed that there was a widespread and costly problem of premature deterioration of bridge decks. Corrosion of the reinforcing steel by deicing salts was identified as the main cause of the deterioration. This major problem served as the impetus to accelerate research and develop corrosion-protection methods. The USDOT commissioned the National Bureau of Standards (NBS) to conduct research on the feasibility of using non-metallic coatings on reinforcing bars. NBS evaluated 47 organic coatings [1]. Based on their research, NBS recommended four epoxy powder coatings for use with ribbed bars.

The first application of epoxy-coated bars was a bridge deck in the State of Pennsylvania in 1973. Since 1973, usage in new and replacement bridge decks and in other parts of bridge structures has been continually increasing. Presently, 46 of the 50 state highway agencies use coated bars. States, such as Florida, use coated bars for bridges that are exposed to sea water or salt spray. In recent years, usage has spread to other types of structures, e.g., automobile parking garages, port and marine structures, and wastewater treatment plants. Total usage of epoxy-coated bars in the U.S during 1987 is estimated as 160,000 metric tons.

2. COATING INDUSTRY PRACTICES

For overall economy, the preferred procedure is to coat straight bars and then to fabricate the coated bars. Most of the coating applicators in the U.S. have their equipment arranged to coat straight bars. A few applicators have the capability to coat bent bars. Typically, the coating is applied to bars in a production-line operation which is housed in a plant or factory. Steps in the application process are cleaning of the bars, and application and curing of the coating. Bars are cleaned by abrasive blast cleaning, preheated to about 230°C, and passed through a chamber equipped with electrostatic spray guns that apply the charged dry powder to the grounded bars. The coated bars then pass through a cooling process, typically a water spray bath, to accelerate curing of the coating. The material specification [2] prescribes the requirements for the epoxy powder material, cleanliness of the bars, and the coating application method.

Acceptance tests for thickness, continuity, and adhesion of coating are also prescribed by the material specification. The thickness of the coating after curing must be 0.13 to 0.30 mm. In the continuity test, coated bars are monitored for holidays (pinholes that are not evident to the naked eye) with an electrical detector. The purpose of the test is to assure that the coating has been properly applied to the bars, and that there are a minimum number of tiny cracks or pinholes in the coating. Bonding of the coating to the bar is evaluated by the adhesion test -- a bend test, which also serves to demonstrate practical bendability of coated bars.

Properly-applied coatings are tough, flexible, and adhere so well that coated bars can be shop-fabricated just like uncoated bars. Many fabricators bend bars using pins with nylon collars to protect the coating during bending operations. Damaged coating due to fabrication must be repaired before the coated bars are shipped to the site.

3. CONSTRUCTION PRACTICES

All parties involved with a new construction material should be apprised of the material's characteristics, limitations, special requirements, etc. An effort

has been made to disseminate information about epoxy-coated bars to structural engineers, contractors, and inspectors [3, 4, 5]. Engineers should include requirements in their project specifications to cover job site operations concerning coated bars [6, 7]. The epoxy coating on a bar is hard and relatively durable, but a contractor has to realize that all construction operations must be performed in a manner to minimize damage to the coating. Simply stated, more care must be exercised with coated bars than with uncoated bars. Since requirements in project specifications and recommended construction practices are closely related, these items are discussed together here.

Repair of damaged coating - specify limits on permissible coating damage due to construction operations, and when required, the repair of damaged coating. Current practice permits individual damaged spots up to a certain area or size without requiring repair, the limit is usually in the order of 40 sq mm. Individual damaged spots larger than this limit have to be repaired. Current practice also limits the maximum amount of total coating damage to 2% of the total surface area per metre of the coated bar, i.e., the repaired and unrepaired areas. The patching or touch-up material for repairing damaged coating should conform to the coated bar specification; and the repair work should be done in strict accordance with the patching material manufacturer's instructions.

Handling and placing - specify requirements to minimize coating damage, i.e., handling equipment should have protected contact areas; bundles of coated bars should be lifted at multiple pick-up points to minimize bar-to-bar abrasion from sags in the bundles; coated bars or bundles of coated bars should not be dropped or dragged; and coated bars should be stored on protective cribbing.

Bar supports and tying - bar supports should be made of dielectric material, or wire bar supports should be coated with dielectric material. When reinforcing bars are used as support bars, the bars should be epoxy-coated. Coated tie wire should be specified. Suitable coatings for tie wire are vinyl or epoxy.

Splices - for mechanical connections and welded splices, there will be damaged coating on the bars in the vicinity of the splices. The damaged coating should be repaired. After installation of mechanical couplers or completion of welding, all parts of the connections should be coated with patching material. Adequate ventilation should be provided when welding coated bars.

Field cutting - cutting of uncoated or coated bars, should be done only if permitted by the engineer. Patching material should be applied to the cut ends of coated bars. Coating damage and field touch-up can be reduced by saw cutting bars rather than flame cutting.

Field bending or straightening - include any special requirements for bending or straightening coated bars which are partially embedded in hardened concrete. Damaged coating on the bars should be repaired. If heat is used, adequate ventilation should be provided.

4. PERFORMANCE - CORROSION RESISTANCE

4.1 Laboratory Tests

Several accelerated corrosion laboratory tests have been conducted since the NBS research. In many of the tests, the concrete specimens reinforced with epoxy-coated bars are subjected to cyclic saltwater exposure and drying conditions. Typically, the specimens in laboratory time-to-corrosion tests are not loaded. The performance of coated bars in these types of tests has been very good [8].

Accelerated corrosion tests on precracked, loaded concrete slab specimens also show good performance by epoxy-coated bars [9]. The researchers observed that the coating had chipped off the bar ribs at crack locations and light surface corrosion of the bar was evident. It was the researchers' opinion that the corrosion should be very localized, because the coating should remain intact on a bar away from the cracks, and no cathodes can form to sustain the corrosion process.

4.2 Longer-term field performance

Many practicing engineers would probably agree that it is encouraging that further laboratory tests are confirming the high degree of corrosion-resistance provided by epoxy-coated bars, but an important and practical question is: how are the bars performing in actual structures? Since the use of epoxy-coated bars in bridge decks began only 15 years ago, relatively little published data are available now on their performance in actual structures. A field study of 22 bridge decks in Pennsylvania indicates good performance [10]. The decks were in service for about 10 years. None of the 11 decks with epoxy-coated bars showed any visual signs of deterioration. Four of the 11 decks with uncoated bars exhibited deterioration of the concrete caused by corrosion of the reinforcement.

5. STRUCTURAL BEHAVIOR AND PERFORMANCE

5.1 Bond strength

The question raised most often regarding structural behavior and performance of epoxy-coated bars is: what about their bond strength? That is certainly an appropriate question. The coating on a ribbed bar has a very smooth surface. It is quite comfortable to the touch as compared to uncoated bars. The smooth coating leads, intuitively, to the bond strength question. In the NBS research, bond strength was evaluated by making pull-out tests on 20-mm diameter coated bars. The NBS researchers concluded that the bond strength of coated bars was acceptable if the coating thickness did not exceed 0.25 mm. It should be noted that the NBS research focused on the bridge deck deterioration problem, i.e., the use of relatively small diameter bars in slab elements.

With the increasing usage of coated bars including larger sizes and applications in many other types of structures besides bridge decks, and coupled with the frequently raised questions regarding bond strength, it became apparent that more research was needed. A research project was initiated in 1985 to determine if there is a difference in bond strength between epoxy-coated and uncoated bars, and if so, how much. Beam specimens, with lap-spliced coated or uncoated Grade 400 bars, were load tested [11]. Performance of the lap splices served as the basis for evaluating bond strength. Variables included coating thickness, bar size, concrete strength, and casting position. The coated bars developed approximately 66% of the bond strength of the uncoated bars. All failure mechanisms were splitting of the concrete cover at the splices. Bond strength was essentially the same for the different coating thicknesses. The epoxy coating, whatever its thickness, is essentially a bond breaker of the adhesion bond. The tests showed that adhesion bond is a very important component of total bond strength of ribbed bars in concrete.

Based upon the test results, provisions for tension development length of epoxy-coated bars are being formulated for the 1989 ACI Building Code, i.e., a 50% increase when concrete cover is less than 3 bar diameters or clear spacing between bars is less than 6 bar diameters to control potential splitting fail-through the cover or splitting between bars in a layer; a 20% increase for all

other conditions of cover and spacing; and the combined factor for top bar effect and epoxy coating does not have to exceed 1.7. Since the splice failures in the tests were splitting of the concrete cover, more research will be undertaken to assess the beneficial effect of transverse reinforcement (stirrups or ties) on the bond strength of coated bars.

5.2 Fire endurance

Another question about structural behavior and performance deals with fire endurance. Coated bars are being used in parking garages -- in new construction as well as in the repair and rehabilitation of existing structures. Statutory building codes usually impose a fire rating requirement on enclosed parking garages, particularly on those which comprise the lower levels of commercial or residential buildings. Structural designers' concerns focus on the heating of the epoxy coating and its subsequent effect on bond strength, i.e., when the coating on the bars softens or melts, due to heating, do the bars lose their bond with the concrete? In response to the issue, the Construction Technologies Laboratories (CTL), a Division of PCA, has fire-tested a large two-way slab reinforced with coated Grade 400 bars. The objectives of the fire test were to determine the slab's fire endurance, and compare the slab's structural performance and fire endurance to a companion slab, reinforced with uncoated Grade 400 bars, that had been fire tested previously. The slab with the coated bars performed very well in the fire test. Its fire endurance was about 4½ hours -- comparable to that of the companion slab, and more than satisfactory for use in parking garages where regulations generally require a 1½ to 3-hour fire rating. CTL plans to fire test beams, reinforced with coated bars, in the next phase of the research project.

6. EPOXY-COATED WELDED WIRE FABRIC

It was a natural progression to extend the technology of coated bars to the coating of welded wire fabric. The procedure of coating sheets of fabric parallels the processing of bars with regard to cleaning of the fabric and application of the epoxy powder coating. Coated fabric was first used in an actual construction project about five years ago. Coated fabric is being used in precast prestressed members, in topping slabs and overlays, and in bridge decks. Coated fabric is also used in reinforced earth construction, such as mechanically-stabilized embankments. ASTM is currently preparing a specification for epoxy-coated wire and welded wire fabric.

7. EPOXY-COATED STRAND

Epoxy-coated prestressing strands have been developed [12]. Two basic types of corrosion-resistant strands are commercially available. One type is intended for post-tensioning applications where bond with concrete is not required. The other type is intended for use where bond is an important consideration. The latter type has grit embedded in the outer surface of the coating which provides the coated strand with bond transfer and development length properties equivalent to or better than those of uncoated strand.

Unlike coated bars and welded wire fabric, coated strands are manufactured by a proprietary process. The company, which began development of the coated strands in 1981, will grant licenses to other firms. The strands are coated with epoxy using the electrostatic fusion-bonded process similar to bar and fabric coatings. The coating thickness on strands is nominally 0.76 mm ± 0.13 mm -- much thicker than bar coatings. This greater thickness completely bridges the interstices of the strand and provides a virtually holiday-free coating. The strand coating is considerably more flexible than bar coatings to permit stretching to

large strains during tensioning operations without the formation of holidays. Epoxy-coated strands have been used in a wide variety of prestressed concrete applications and in other corrosive environments, e.g., piles, fender piles, bridge decks and girders, replacement tendons in parking structures, ground anchors (tiebacks), and stay cables.

REFERENCES

1. CLIFTON, J. R., BEEGHLY, H. F., and MATHEY, R. G., Non-Metallic Coatings for Concrete Reinforcing Bars. National Bureau of Standards Building Science Series 65, Aug. 1975, 42 pp.

2. ASTM, Standard Specification for Epoxy-Coated Reinforcing Steel Bars (A 775/A 775M-86). Annual Book of ASTM Standards, Vol. 01.04, 1987, pp. 744-749.

3. GUSTAFSON, D. P., Epoxy-Coated Reinforcing Bars, Concrete Construction. November 1983, pp. 826, 829, 830, 832, 834, and 836.

4. CONCRETE REINFORCING STEEL INSTITUTE, Placing Reinforcing Bars. 5th Ed., 1986, 210 pp.

5. GUSTAFSON, D. P., Inspection and Acceptance of Epoxy-Coated Reinforcing Bars. Concrete Construction, February 1987, pp. 197, 199, and 201.

6. GUSTAFSON, D. P., Specifications for Epoxy-Coated Reinforcing Bars. Concrete Construction, September 1984, pp. 809-812.

7. AMERICAN CONCRETE INSTITUTE, Specifications for Structural Concrete for Buildings (ACI 301-84, Revised 1985), 33 pp.

8. PFIEFFER, D. W., LANDGREN, J. R., and ZOOB, A., Protective Systems for New Prestressed and Substructure Concrete. Report No. FHWA/RD-86/193, April 1987, 133 pp.

9. POSTON, R. W., CARRASQUILLO, and BREEN, J. E., Durability of Post-tensioned Bridge Decks. ACI Materials Journal, July-August 1987, pp. 315-326.

10. WEYERS, R. E. and CADY, P. D., Deterioration of Concrete Bridge Decks from Corrosion of Reinforcing Steel. ACI Concrete International, January 1987, pp. 15-20.

11. TREECE, R. A. and JIRSA, J. O., Bond Strength of Epoxy-Coated Reinforcing Bars. PMFSEL Report No. 87-1, University of Texas at Austin, January 1987.

12. DORSTEN, V., HUNT, F. F., and PRESTON, H. K., Epoxy-Coated Seven-Wire Strand for Prestressed Concrete. PCI Journal, July-August 1984, pp. 120-129.

Einsatz von Hochleistungsverbundwerkstoff im Spannbeton-Brückenbau

Fibre Glass Tendons for Prestressed Concrete Bridges

Armatures en fibres de verre pour des ponts en béton précontraint

Lutz FRANKE
Prof. Dr.-Ing.
TU Hamburg,
Bundesrep. Deutschland

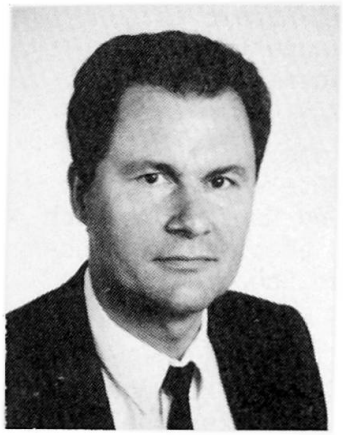

Lutz Franke, geboren 1941, Promotion an der TU Stuttgart, seit 1981 Lehrstuhl für Bauphysik und Werkstoffe im Bauwesen, TU Hamburg-H., Mitinhaber eines Ingenieurbüros in Hamburg.

Reinhard WOLFF
Dr.-Ing.
Strabag Bau-AG, Köln,
Bundesrep. Deutschl.

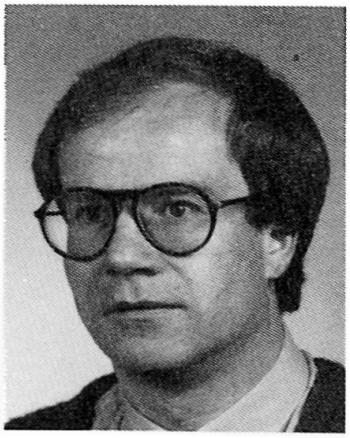

Reinhard Wolff, geboren 1945, Promotion an der TH Darmstadt. Mehrere Jahre im Techn. Büro der Strabag Bau-AG, Köln u. Düsseldorf. Seit 3 Jahren Leiter der Hauptabteilung Technik und Projektbearbeitung der Strabag Hauptverwaltung in Köln.

ZUSAMMENFASSUNG

Der weltweit erste Einsatz von Spanngliedern aus Glasfaserverbundwerkstoff im Spannbetonbau erfolgte bei der Brücke Ulenbergstraße in Düsseldorf. Inzwischen ist die Materialentwicklung weitergegangen. Die Stäbe der neuen Spannglieder auf der Basis von Epoxidharzen haben wesentlich bessere mechanische Eigenschaften. Zur Zeit wird dieses weiterentwickelte Material bei einer Brücke in Berlin eingesetzt. Diese Brücke ist durch eine externe Vorspannung teilweise vorgespannt. Die 19-stäbigen Spannglieder werden mit Hilfe speziell entwickelter Kupferdrahtsensoren und Lichtwellenleiter-Sensoren automatisch überwacht.

SUMMARY

The first use of resin-bonded fibre glass tendons in prestressed concrete construction was in the bridge, Ulenbergstraße in Düsseldorf. Meanwhile the development of materials has continued. The epoxy-resin tendons of the novel prestressing elements have substantially improved the mechanical properties. This further developed material is presently employed in a bridge in Berlin. This bridge is partially pretensioned by an external prestress. The 19 tendons are automatically inspected by the help of specially developed copper wire sensors and beam wave guide sensors.

RÉSUMÉ

La première utilisation dans le monde de barres composites en fibre de verre comme armature de précontrainte a eu lieu dans la construction du pont Ulenbergstraße à Düsseldorf. Entre-temps, le développement du matériau a continué. Les nouvelles barres de précontrainte à base de résine époxide possèdent des propriétees mécaniques sensiblement améliorées. Actuellement ce nouveau matériau est employé dans la construction d'un pont à Berlin. Ce pont est précontraint partiellement par des câbles externes. Les éléments de précontrainte à 19 barres sont contrôlés à l'aide de détecteurs de fils de cuivre et de transmetteurs utilisant des fibres optiques développés spécialement.

1. STABMATERIAL UND WERKSTOFFVERHALTEN

Das Stabmaterial besteht aus Glasfasern, Typ E, die in Epoxidharz eingebettet sind. Um eine möglichst hohe Zugfestigkeit von >1600 N/mm² zu erreichen, ist eine sorgfältige Auswahl des richtigen Rovings aus der Reihe der zur Verfügung stehenden Glasfaserrovings erforderlich. Die Optimierung erfolgt durch Bestimmung der Weibull-Parameter, die die Festigkeitsverteilungen der Glasfasern sowohl in Abhängigkeit von der Dehnung wie auch in Abhängigkeit von der Zeit festlegen. Durchgeführt werden diese Untersuchungen am Rovingmaterial, vgl. [2].

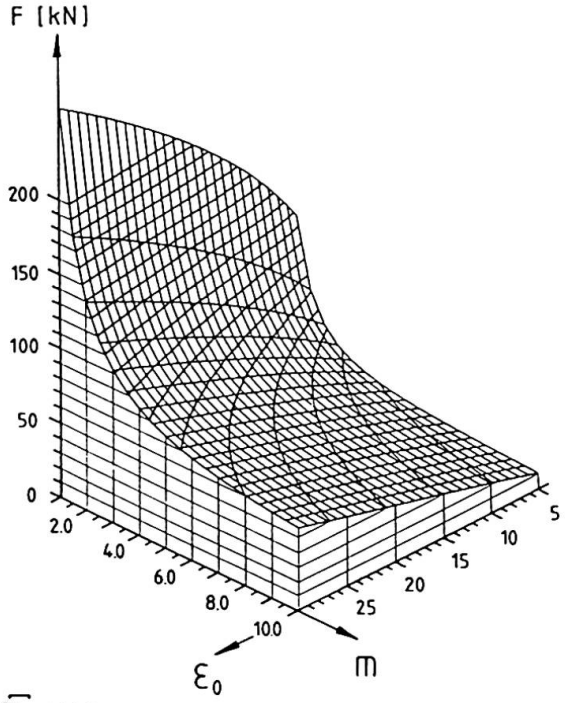

Bild 1 zeigt die Bruchlast F von Stäben Ø 7,5 mm in Abhängigkeit der Rovingeigenschaften (Weibull-Parameter ε_0 und m, Rißwachstumsexponent n = 40), bezogen auf eine Standzeit von 30 Jahren, vgl. [2].

Da das Tragverhalten des Stabmaterials ebenfalls durch die Güte des Verbundes zwischen Glasfasern und Harz maßgeblich beeinflußt wird, sind ebenfalls Messungen der interlaminaren Scherfestigkeit angezeigt im Hinblick auf die Auswahl einer optimalen Schlichte.

Welchen Einfluß die Materialkomponenten auf das Verhalten von GV-Stäben bei mechanischen Beanspruchungen haben können, sollen die Bilder 2a und 2b weiter illustrieren. Die Bilder zeigen die Auswertungen von Zeitstand- und Dauerschwingversuchen an Stäben Ø 7,5 mm.

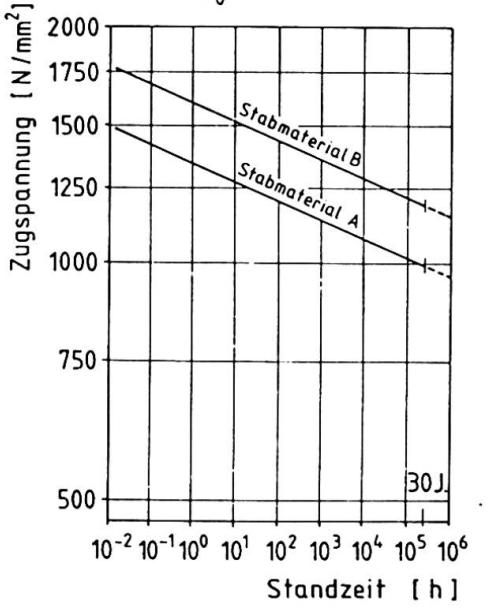

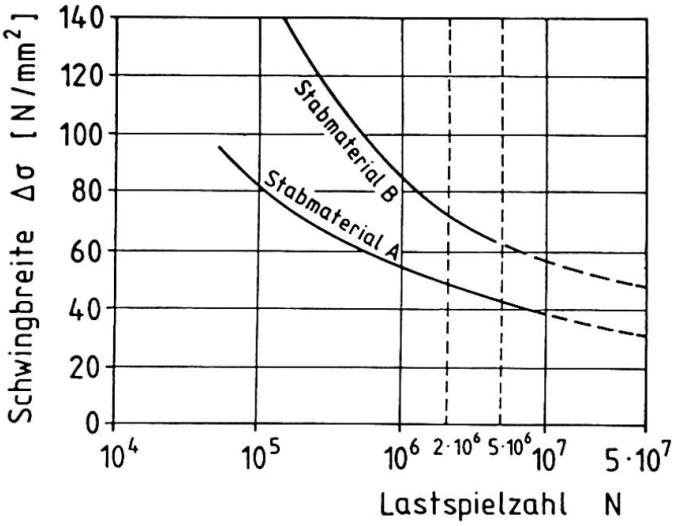

ⓐ Zeitstandfestigkeit ⓑ Dauerschwingfestigkeit

Bild 2 Verhalten von GV-Stäben Ø 7,5 mm bei 20 °C / 55 % rel. F.
Stabmaterial A: E-Glas Typ 1, UP-Harz
Stabmaterial B: E-Glas Typ 2, EP-Harz

2. MEDIENBESTÄNDIGKEIT

Die hohe Medienbeständigkeit des Stabmaterials wird durch die Wahl des Matrixharzes sowie durch zusätzliche Inhibitoren, die u.a. in das Matrixharz eingebettet werden, erzielt. Zur Zeit laufen noch weitere Forschungsarbeiten zu diesem Themenkreis. Als Beispiel für die positive Wirkung von Substanzen auf die Beständigkeit von Glasfasern seien die in Bild 3 dargestellten Ergebnisse angeführt. Es zeigt den Verlauf der Zugfestigkeit von nackten Glasfaser-Rovings nach Lagerung in $Al(OH)_3$ bei 20 °C und 70 °C.

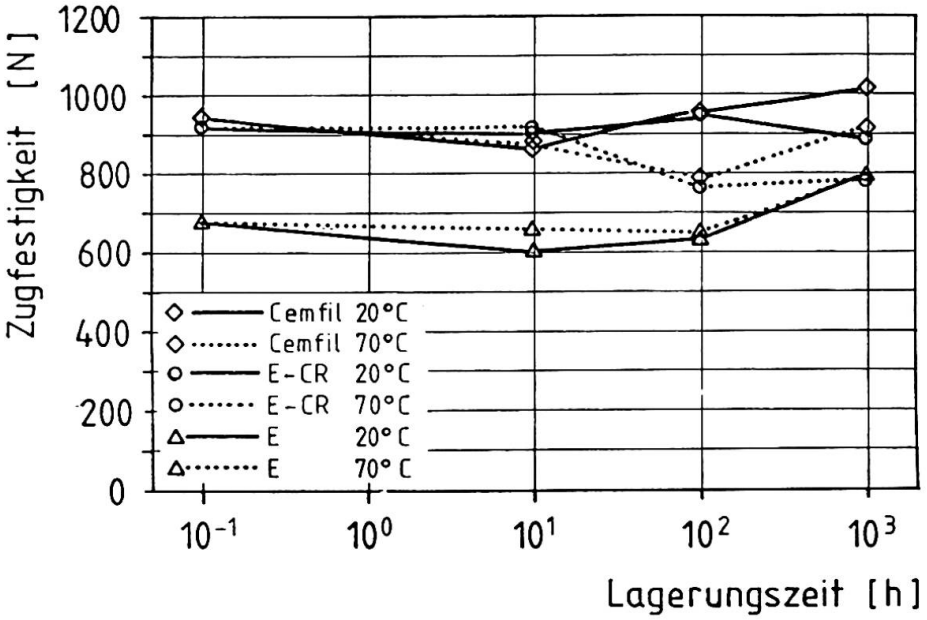

Bild 3

Zugfestigkeit von Glasfasern nach Lagerung in $Al(OH)_3$ (pH = 8,3)

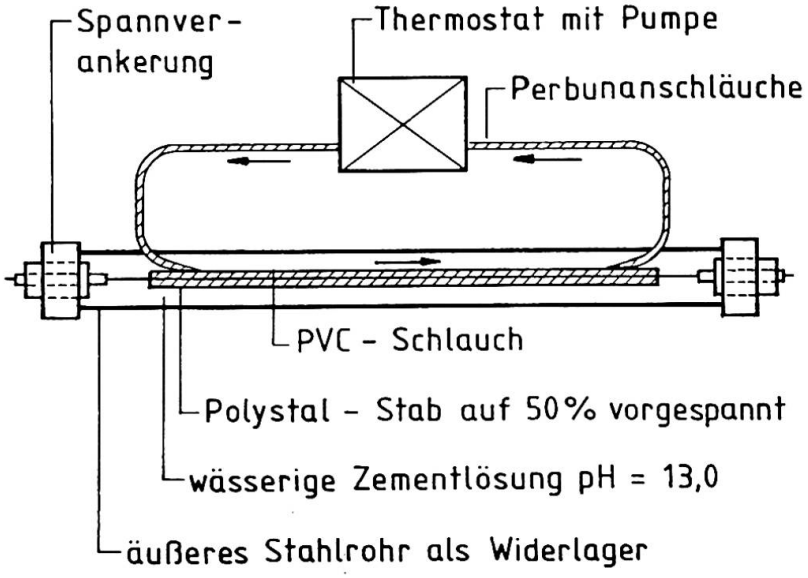

Bild 4

Medienversuchsstand im Labor der Fa. Strabag

Das Verhalten der GV-Stäbe bei Einwirkung ausgewählter Medien wird in Zeitstandversuchen kontrolliert, vgl. Bild 4.

3. BRÜCKE "BERLIN-MARIENFELDE"

Die Brücke Marienfelde in Berlin ist eine zweifeldrige Fußgängerbrücke mit Spannweiten von 22,90 m und 27,58 m. Der Brückenüberbau wird erstmals in Deutschland in teilweiser Vorspannung ohne Verbund ausgeführt.
Der Bruchquerschnitt ist ein zweistegiger Plattenbalken mit einer Bauhöhe von 1,10 m und einer Plattenbreite von 4,80 m (Bild 5). Die Spannglieder bestehen aus Hochleistungsverbundstäben (HLV) auf der Basis von Glasfasern, die in eine Epoxidharzmatrix eingebettet sind. Es handelt sich hier um einen weiterentwickelten Typ der Spannglieder der Brücke Ulenbergstraße in Düsseldorf. Die Spannglieder werden extern zwischen den beiden Stegen geführt und in den Feldern an jeweils zwei Querträgern umgelenkt und an den Mittelstützen über die Querträger hochgeführt.

An dem Institut für Stahlbetonbau der TU Berlin wurde ein Modell der Brücke im Maßstab 1 : 10 aus Mikrobeton hergestellt und erfolgreich getestet [5], Bild 6. Die Mikrospannglieder bestanden ebenfalls aus Glasfaserverbundstäben.

Bei der eigentlichen Brücke werden zum ersten Mal zwei inzwischen ausgereifte Verfahren der Überwachung und Kontrolle der Spannglieder (Strabag) sowie der ganzen Brücke eingesetzt, und zwar durch in den Faserverbundquerschnitt integrierte Kupferdrahtsensoren und Lichtwellenleitersensoren, vgl. Abschn. 4. Auf den Stegen werden zusätzliche Lichtwellenleitersensoren aufgeklebt, die Dehnungen und eventuell auftretende Risse im Beton anzeigen und registrieren.

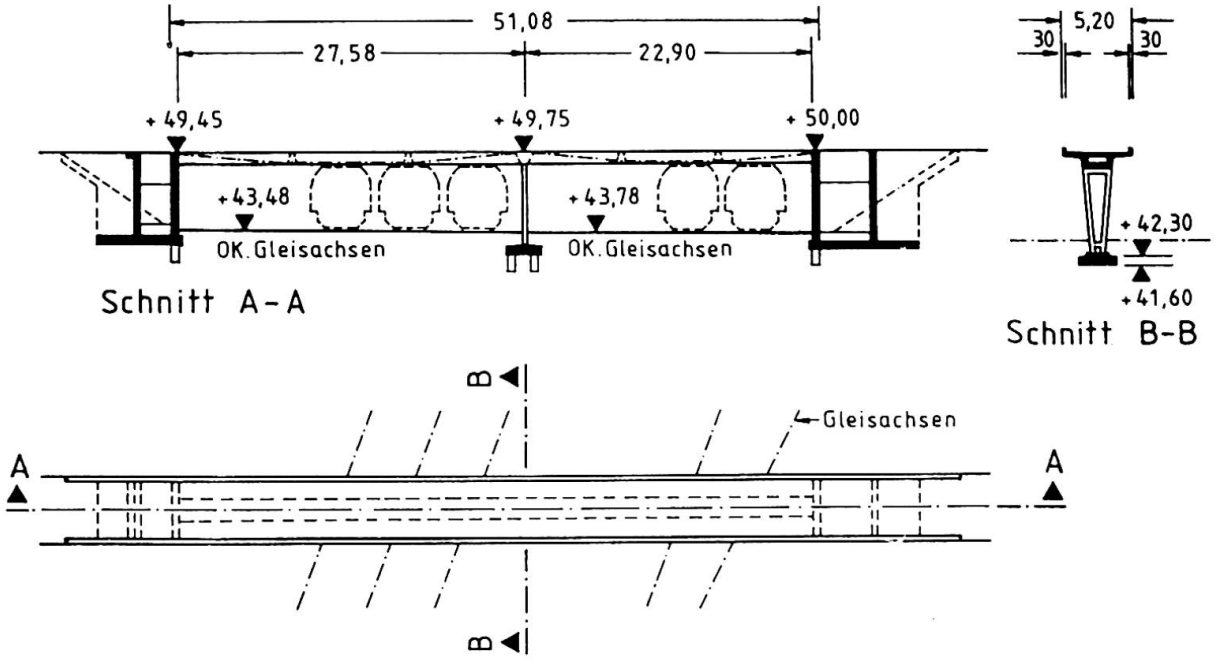

Bild 5 Querschnitte Brücke Berlin-Marienfelde

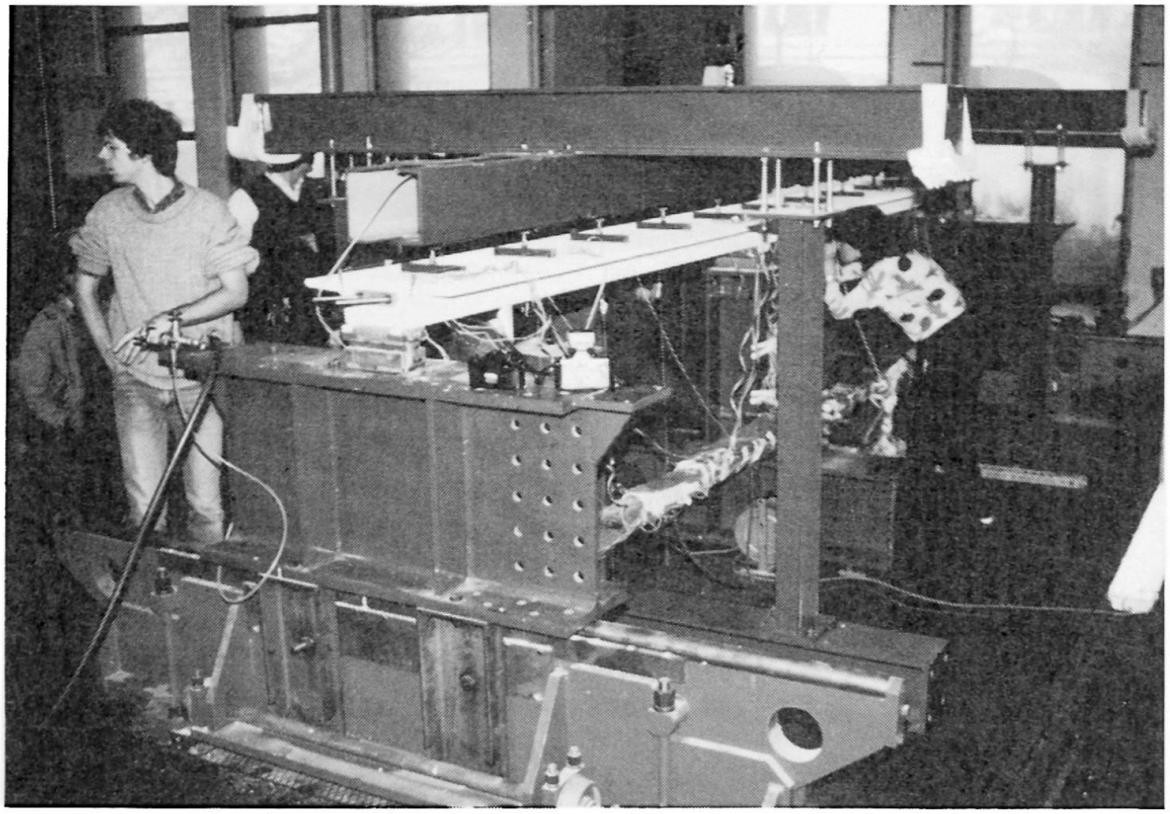

Bild 6 Brückenmodell aus Mikrobeton im Maßstab 1 : 10

4. ÜBERWACHUNG UND KONTROLLE DER SPANNGLIEDER (STRABAG)

Die einzelnen Stäbe der Spannglieder werden durch in den Faserverbundquerschnitt integrierte Kupferdrahtsensoren und Lichtwellenleitersensoren permanent überwacht. Mit Hilfe der Kupferdrahtsensoren kann der Bruch eines Stabes und der Ort des Bruches festgestellt werden. Die Lichtwellenleitersensoren zeigen die Dehnungen des Stabes nach Betrag und Ort an.
Ein Rückschluß auf den im Stab vorhandenen Spannungszustand ist somit ebenfalls möglich. Durch die Installation einer vollautomatisch arbeitenden Meßstellenanlage wird das gesamte Brückenbauwerk fernüberwacht. Eine aufwendige Kontrolle durch Augenschein vor Ort ist somit nur noch im Bedarfsfall erforderlich.

5. AUSBLICK UND ZUSAMMENFASSUNG

Nur durch die ständige Weiterentwicklung des Glasfaserverbundwerkstoffes im Hinblick auf seine Anwendung in der Bauindustrie ist es möglich, diesen Faserverbundwerkstoff sinnvoll für das Vorspannen von Betonbauwerken einzusetzen. Dieser Hochleistungsverbundstab wird immer mehr zu einem Hightech-Produkt, welches eine hohe Zugfestigkeit und eine hohe Medienbeständigkeit in sich vereint. Durch die Integration von Sensoren in den Verbundwerkstoff ist es zum ersten Mal in der Geschichte des Spannbetonbaues möglich, in Spannglieder hineinzusehen, um das Spannungs-Dehnungsverhalten des Spanngliedes und des Bauwerkes permanent überwachen zu können. Eine für die Zukunft der Spannbetonbauweise weitreichende und wertvolle Perspektive.

LITERATURVERZEICHNIS

[1] WAASER, E., WOLFF, R., Ein neuer Werkstoff für Spannbeton, beton 36, 1986, H. 7, S. 245
[2] OVERBECK, E., Zur Bruchfestigkeit und Zeitstandfestigkeit von Glasfasern und unidirektionalen GFK-Stäben, VDI-Fortschrittsberichte, Reihe 5 Nr. 127, VDI-Verl. 1987
[3] FRANKE, L., OVERBECK, E., Dauerschwingfestigkeit hochfester GV-Stäbe im anwendungsorientierten Zugschwellbereich, Bericht des Lehrstuhls für Bauphysik und Werkstoffe im Bauwesen, TU Hamburg-Harburg, 1986
[4] KÖNIG, G., WOLFF, R., Hochleistungs-Verbundwerkstoff für die Vorspannung von Betonbauwerken, IABSE Symposium Paris-Versailles 1987, Vol. 55, S. 419
[5] KALLEJA, H., STAUCH, M., Im Süden Berlins - Bau einer Forschungsbrücke, Forschung Aktuell 4, 1987, Nr. 16-17, S. 43

Application of New Concrete Using Small Pieces of Ice

Application de nouveaux bétons utilisant de petits morceaux de glace

Anwendung einer neuen Betonart unter Beimischung von Eisstücken

Toshiro SUZUKI
Professor
Tokyo Inst. of Techn.
Tokyo, Japan

Toshiro Suzuki, born 1936, received his doctor's degree from the University of Tokyo in 1963. He was awarded the Prize from the Architectural Institute of Japan for his study on steel structure in 1981.

Katsuki TAKIGUSHI
Assoc. Prof.
Tokyo Inst. of Techn.
Tokyo, Japan

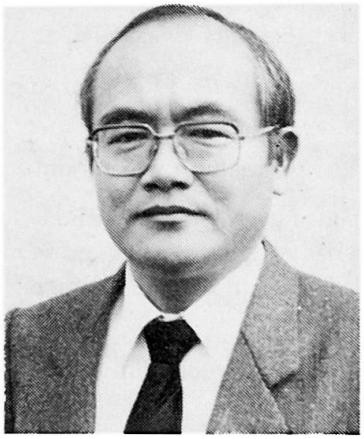

Katsuki Takiguchi, born 1945, received his doctor's degree from Tokyo Inst. of Techn. in 1972. His main research field is concrete structure.

Shin-ichi MIYASHITA
Structural Engineer
Tokyu Construction Co., Ltd.
Tokyo, Japan

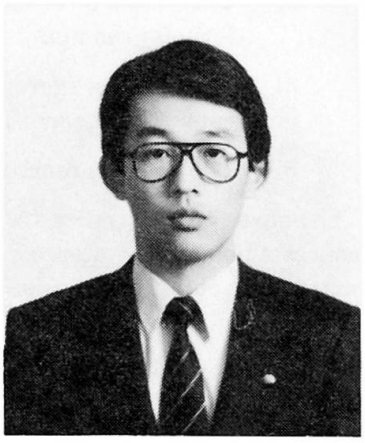

Shin-ichi Miyashita, born 1959 received his master's degree from Tokyo Inst. of Techn. in 1983.

SUMMARY
The new concrete is obtained by using small pieces of ice instead of mixing water at the start of mixing. Various properties of fresh concrete are greatly improved by this new production method. The new concrete had been practically applied to several buildings quite effectively.

RÉSUMÉ
Le nouveau béton est obtenu en utilisant de petits morceaux de glace au lieu de l'eau de mélange au début de mélange. Différentes caractéristiques du béton frais sont considérablement améliorées par cette nouvelle méthode de production. Le nouveau béton a été pratiquement utilisé pour quelques bâtiments d'une manière très satisfaisante.

ZUSAMMENFASSUNG
Die neue Betonart entsteht durch Beimischung kleiner Eisstückchen zum Mischwasser bei Beginn des Mischvorgangs. Dieses neue Verfahren verbessert verschiedene Eigenschaften des Frischbetons erheblich. Für mehrere Bauwerke ist diese neue Betonart mit Erfolg praktisch angewendet worden.

1. INTRODUCTION

A new unique method has been developed for the production of concrete.

This new method takes advantage of small ice pieces and their melting process. The concrete is obtained by substituting small ice pieces for the mixing water, at the start of mixing. The ice should be completely melted prior to concrete placement. The various required properties of concrete during production, including mixing efficiency, placement performance and consolidation ability are greatly improved.

Concrete produced using small ice pieces in lieu of mixing water is characterized by the following advantages.

1) Mixing can be conveniently carried out almost irrespective of the mix proportions.
2) Small ice pieces of a wide variety of shapes, sizes and states can be used.
3) The viscosity of cement paste changes as the small ice pieces melt, reaching an appropriate level for the uniform mixing of special additives, such as fibers.
4) There is no aggregate segregation after uniform mixing because of the change in viscosity caused by the melting of the ice.
5) The hydrate reaction is retarded throughout mixing until final placement.

The above characteristics are advantageous for production of the following types of concrete. High quality concrete using less water, concrete with heavy aggregate, concrete mixed with fibers, concrete mixed with macromolecular materials, pressurized and undrained formed concrete, slow setting ready-mixed concrete, and so on.

The fundamental characteristics of this concrete production method were discussed in the previous papers [1], [2], [3] and [4].

Melting process of small ice pieces should play an important part in this production method. It should be affected by the volume of concrete in the mixer, mixing method and so on, as shown in Fig. 1. The data of large scale experiments and/or practical use of this method are important as well as those of fundamental tests in the laboratory.

As the first objective to apply practically this new method to, cast-in-place concrete / ready mixed concrete had been selected. This paper deals with the properties of the new concrete used in actual buildings.

This method of producing concrete was originally conceived by T. SUZUKI, primary author, and various experiments and examinations were undertaken jointly by T. SUZUKI and K. TAKIGUCHI. S. MIYASHITA lent a helping hand in the tests during practical use of the new concrete.

2. PLANT TRUCK SUPPLYING SMALL ICE PIECES

Transportable plant system supplying small ice pieces into the mixer of ready mixed concrete plant and the first experimental plant truck are shown in the previous paper [4].

After frequent tests and improvements, the plant truck shown in Fig. 2 was made. It is very convenient for experimental concrete works, and is working now without any serious trouble.

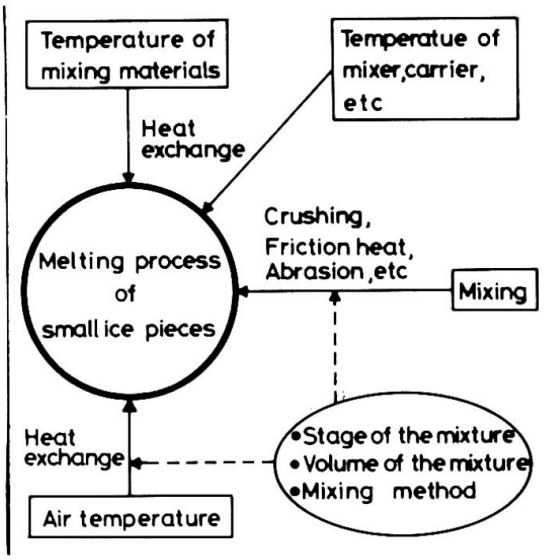

Fig. 1 Factors affecting the melting process of small ice pieces

Weight-measured small ice pieces are blown up into the mixer through a flexible hose. The maximum particle size of ice pieces can be controlled from 3mm to 5mm. The plant can continuously supply the small ice pieces of 200~250kg per a minute. Weight measuring error of the plant is within 1kg/200kg. Blowing up capacity is 15~20m height. Atmospheric temperature under which the truck can be operated ranges from −15°C to 35°C.

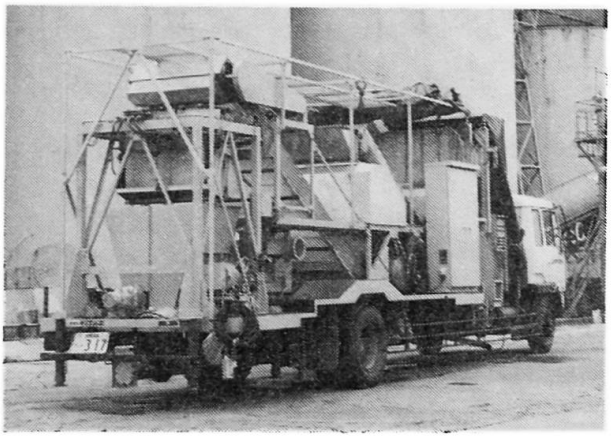

Fig. 2 Plant truck supplying small ice pieces

3. COLD WEATHER CONCRETE

Concrete mixed, transported, placed and cured under condition of low temperature should be prevented from damage by freezing at an early age.

(Low water-cement ratio)−(well mixed)−concrete having two properties mentioned below can be produced by the new method.

i) Freezing does not occur easily.

ii) Strength can be recovered even in case that the concrete has been suffered early freezing.

Strength recovery of early frozen concrete was discussed in the previous paper [1].

An experiment of cold weather concrete was carried out, in February 1987 in Hokkaido. The atmospheric temperature was about −5°C. The outline of the experiment is shown in Fig. 3.

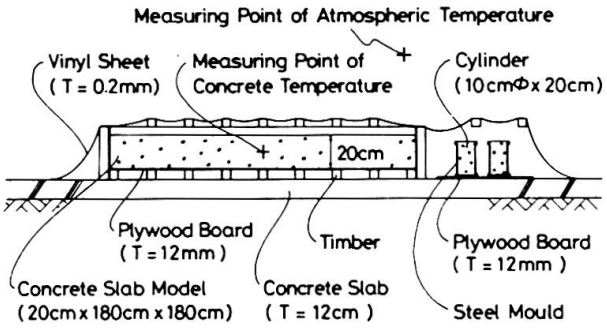

Fig. 3 Outline of experiment

The mix proportion of the concrete was : normal portland cement 448kg/m^3, powdery snow 161kg/m^3 in lieu of mixing water, land sand (2.5mm) 679kg/m^3, river gravel (25mm) 1163kg/m^3, AE water reducing agent 1.12kg/m^3. Water−cement ratio was 33%.

In case of cold weather concrete production, the temperature of aggregate should be controlled carefully. The fine aggregate temperature was 3°C. The coarse aggregate temperature was raised up to 40°C~50°C.

With the pan-type / forced mixing type / 3m^3 / mixer, 1m^3 concrete was mixed for 3 minutes. The slump of the concrete mixed up was 4.5cm.

Concrete of 2m^3 by two mixing was transported by the 4.5m^3 truck agitator. After 45 minutes transportation, the concrete was placed into the formworks. The concrete placing situation is shown in Fig. 4.

Fig. 4 Concrete placing under − 5°C

After the completion of surface finishing of the concrete slab model and cylinders, concrete was covered with flimsy vinyl sheet as shown in Fig. 3, and left at the site. The concrete temperature history and the atmospheric temperature history are shown in Fig. 5.

After 3 days curing, the cylinders and core test specimens cut out from the slab model were tested. The compressive strengths of cylinders and core test specimens were almost equal and were about 20MPa.

High quality concrete / (low water-cement ratio) – (well mixed) – (early freezing proof) – concrete can be produced by the proposed method using small pieces of ice.

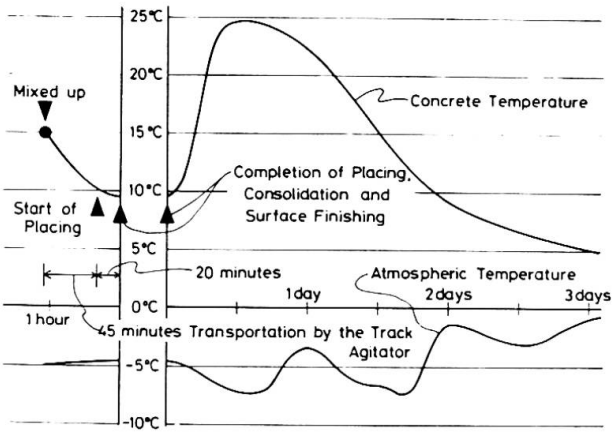

Fig. 5 Temperature history

4. PRACTICAL APPLICATION TO HOTEL BUILDING

The concrete produced by the new method was practically used in a hotel building, in Akita – prefecture in March 1987.

The atmospheric temperature rangéd from −3°C to 0°C during the concrete works. The concrete was placed in columns, walls, beams and slabs. As the concrete works had to be done under the cold weather, early freezing proof concrete was required. At the same time, over 15cm slump value of the concrete at pumping was required.

Concrete of water-cement ratio 46% was produced. The mix proportion was : normal portland cement 358kg/m^3, crushed ice (3mm) 161kg/m^3, (1/2) sand from sand dune and (1/2) river sand (5mm) 616kg/m^3, river gravel (25mm) 1104kg/m^3, AE water reducing agent 3.58kg/m^3.

The temperature of the gravel was raised up to 40~50°C.

With pan type / forced mixing type / 2m^3 / mixer, 1m^3 concrete was mixed for 2 minutes as one batch mixing. The concrete was transported from ready mixed concrete plant to the building construction site by 6m^3 truck agitator.

Slump value, temperature and air content of the concrete are indicated in Fig. 6. Needless to say, mix proportions of the new concrete and of conventional concrete were equal.

It was confirmed by this practical use that the proposed method improves the workability of fresh concrete.

The hotel building completed is shown in Fig. 7.

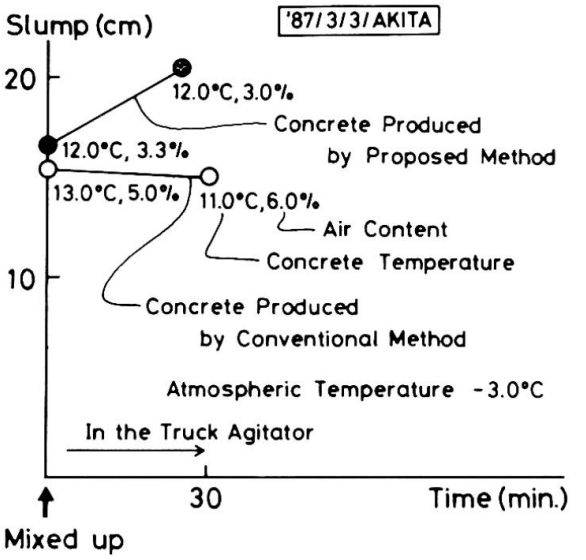

Fig. 6 Slump of the concrete produced by proposed method and of conventional concrete

5. HOT WEATHER CONCRETE

It was confirmed that this method can be used quite effectively in the concrete works under high atmospheric temperature, as described in the previous paper [4].

In August 1987, the new concrete was used in reinforced concrete slab of a warehouse in Osaka. In most cases, sea sand and crushed gravel have to be used in Osaka area. To get the same workability, more water is needed in the sea sand concrete than in the river sand concrete. To get the same workability, more water is needed in hot weather concrete than in mild weather concrete, because of slump loss.

In Osaka area, the concrete production method which can reduce the water is seriously required. Especially in hot season, the situation of concrete production is just so.

The mix proportion of the concrete used in the slab construction was : normal portland cement 311kg/m^3, crushed ice (5mm) 174kg/m^3, sea sand (2.5mm) 791kg/m^3, crushed gravel (20mm) 1023kg/m^3, AE water reducing agent 0.78kg/m^3.

With the variable speed type / horizontal twin shafts type / forced mixing type / 2.5m^3 / mixer, 2m^3 concrete was mixed for 2 minutes.

The concrete was transported by 4.5m^3 truck agitator. The atmospheric temperature was 28°C.

Slump, temperature and air content of the concrete are indicated in Fig. 8, together with those of the same mix proportion conventional concrete.

The concrete was placed in the formworks as shown in Fig. 9.

High workability of the concrete produced by the new method was confirmed as shown in Fig. 8.

As shown in Figs. 6 and 8, the slump value of the concrete produced with small ice pieces became larger as time passed, though the ice pieces were perfectly melted when the concrete was mixed up. This is one of the distinctive properties of the concrete with small ice pieces.

The strength of the concrete produced by the new method was discussed in the previous paper [4]. Curing period discussed in the previous paper [4] ranged from 1 day to 91 days. Curing conditions were in 20°C water, in the water at the site, in air, in mould and under sealing. Water–cement ratio ranged from 40% to 63%.

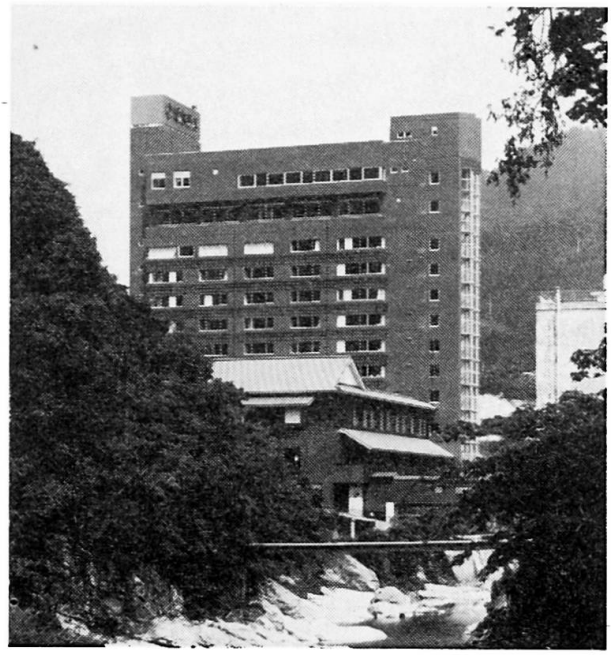

Fig. 7 The hotel building

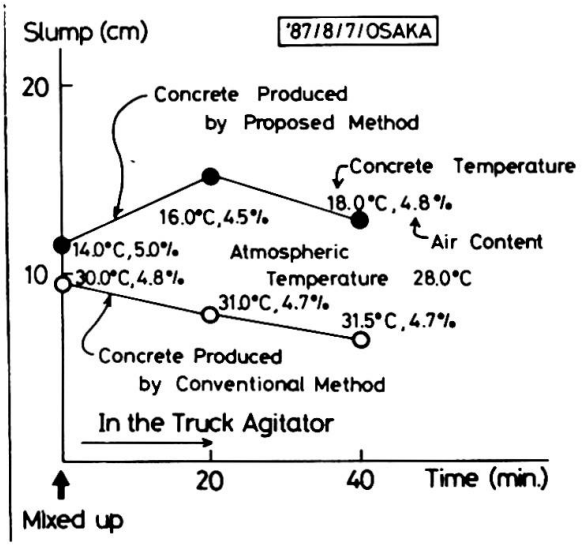

Fig. 8 Slump of the concrete produced by proposed method and of conventional concrete

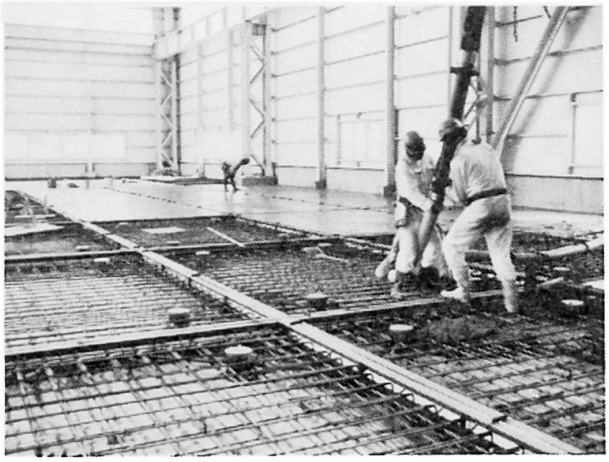

Fig. 9 Concrete placing under 28°C

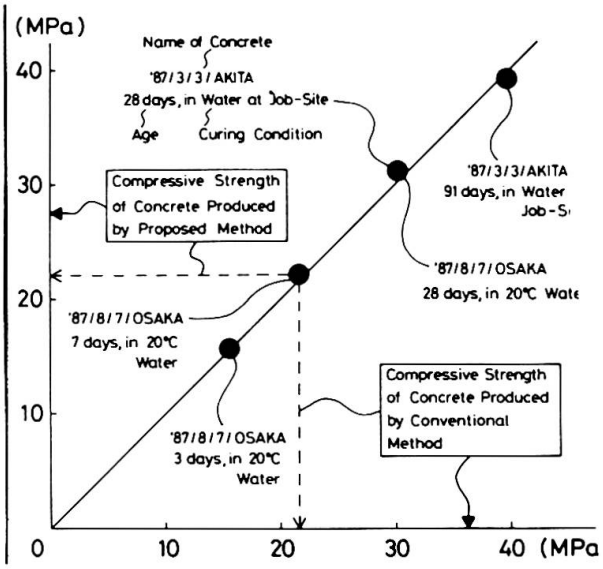

Fig. 10 Compressive strength of the concrete produced by proposed method and of conventional concrete

It was concluded in the previous paper [4] that the strength of concrete produced by proposed method is equal to that of the same mix proportion conventional concrete.

Plotted points in Fig. 10 mean that weight–measuring errors of small ice pieces and of mixing water did not occur during the production of the concrete described in this paper. It is not necessary to be anxious about weight–measuring error in evaluating the data shown in Figs. 6 and 8.

6. CONCLUSION

The new concrete production method using small pieces of ice was practically applied to actual building concrete works quite effectively.

Workability of fresh concrete is improved much by the new method.

The new method is powerful especially for hot weather concrete and for cold weather concrete.

ACKNOWLEDGEMENT

Kindhearted supports of Dr. Fujio MATSUSITA, a managing director of Tomoegumi Iron Works Ltd., and of Dr. Tsukasa AOYAGI, a director of NIKKEN SEKKEI Ltd. are gratefully acknowledged.

REFERENCES

1. SUZUKI T. and TAKIGUCHI K., Well Mixed Concrete Using Small Ice Pieces in lieu of Mixing Water. Nikkei architecture, 4–21 1986, pp.80–85 (in Japanese).
2. SUZUKI T. and TAKIGUCHI K., A New Concrete Production Method Using Small Ice Pieces. Transactions of The Japan Concrete Institute Vol. 8, 1986, pp. 81–88.
3. SUZUKI T., TAKIGUCHI K. and HOTTA H., Characteristics of Concrete Produced by New Method Using Small Ice Pieces. Transactions of The Japan Concrete Institute Vol. 8, 1986, pp. 89–96.
4. SUZUKI T. and TAKIGUCHI K., A New Concrete Production Method Using Small Pieces of Ice. IABSE Sym. Paris–Versailles 1987 Report, Vol. 55, pp. 339–344.

High Strength Concrete

Béton à haute résistance

Hochfester Beton

Manuel F. CÁNOVAS
Head of Constr. Dep.
Polythecnic University
Madrid, Spain

M.F. Cánovas, obtained his construction engineering degree at the Sueprior Polythecnic School of the Army in Madrid. For twenty five years he was involved in research works at the Instituto Eduardo Torroja in Spain, and now is responsible for the Material Research Laboratory at the Escuela de Ingenieros de Caminos de Madrid.

SUMMARY
This paper describes the work carried out to obtain high strength concretes. The work is divided into two parts; firstly, the parameters which influence the strength of these concretes are studied, and secondly using these parameters as an approximate guide along with special aggregates, superplasticers and silica fume, high strength concrete is obtained.

RÉSUMÉ
Cette contribution décrit les travaux réalisés pour obtenir des bétons de haute résistance. Le travail est divisé en deux parties: dans la première partie on étudie les paramètres qui ont une influence sur la résistance de ces bétons, et la deuxième partie a pour but d' obtenir des bétons de haute résistance en s'appuyant sur ces paramètres et en utilisant des agrégats spéciaux, des superplastifiants et de la fumée de silice.

ZUSAMMENFASSUNG
In diesem Bericht werden die Untersuchungen zur Herstellung von Beton mit hohen Festigkeitswerten beschrieben. Der Bericht besteht aus zwei Teilen: im ersten werden die Einflußfaktoren auf die Festigkeitswerte analysiert; im zweiten Teil wird beschrieben, wie diese hohen Festigkeitswerte auf Grund der genannten Einflußfaktoren und der Zugabe von Zuschlagstoffen mit besonderen Eigenschaften, Superverflüssigern und Silikastaub erreicht werden.

1. INTRODUCTION

Not long ago the maximum compression strength of concrete could be considered to be about 50 N/mm^2 and structural concretes of 25 N/mm^2 were frequently used.

The needs imposed by construction of higher buildings, prestressed bridges of long spans, concretes with good performances against shell penetration,etc., have led to more attention being given to higher compression strength concretes and nowadays we can obtain concretes of 60 N/mm^2, which have at the same time a good workability due to the use of superplasticers. These concretes have been applied in high buildings especially in the USA and in some prestressed bridges in Japan. The simultaneous use of superplasticers and silica fume permits considerably higher strengths to be reached.

The study carried out in the Escuela de Ingenieros de Caminos, Canales y Puertos at the Polythecnic University of Madrid, which we summarize in this paper, have had the aim of analyzing which are the most convenient parameters in order to obtain concretes of high strength.

2. METHODOLOGY

This work can be divided into two phases:

2.1 First phase

In this phase we have used a high initial strength Portland cement.

We have used rounded gravel and crushed gravel aggregates in order to observe the influence of the surface texture of aggregates on the compressive strength of the concrete. Also, differents maximum sizes of aggregates have been used to observe the influence of this parameter on the concrete strength.

The compression tests have been carried out at after periods of 28 and 60 days. It is necessary to take into consideration that these types of concrete generally reach the service load in structural elements after a period of 28 days and also that it is important to carry out the tests after long periods in order to observe the evolution of the pozzolanic activity of the silica fume.

2.2 Second phase

The second phase of our work is based on the results of the first one, but in this phase we have used new aggregates, superplasticer admixture and silica fume.

The coarse aggregates used in this second phase consisted of good limestones from different areas of Spain and ophites from Navarra (Spain).

The superplasticer admixture used was a sulphonated napthalene formaldehyde condensate (SNF) and the pozzolanic addition to the concrete was silica fume in water suspension at 50 %.

The workability of the concretes was measured by means of the Abrams cone.The slump was between 5 and 8 cm.

The ages for compression tests of concretes were 28 and 60 days.

3. INVESTIGATIONS

3.1. First phase

3.1.1. Design

The cement used in all the concretes was P-550 ARI which corresponds to a high initial strength Portland cement with 55 N/mm^2 minimum compression strength at 28 days on the RILEM-ISO-CEMBUREAU.

The cement contents were: 350, 400, 450, 500 and 550 kg/m^3.

The fine aggregate was silica river sand having a fineness modulus of 2.98.

The coarse aggregates were natural rounded river gravel and crushed river gravel.

Aggregates with 40, 20 and 10 mm. of maximum size were used.

In these concretes we have used neither admixtures nor silica fume.

Two fine aggregate/coarse aggregate ratios have been used: 2.00 and 1.50.

The water contents were that necessary for reaching a good workability with a slump between 5 and 8 cm.

The compression tests were carried out after 28 and 60 days.

The specimens used were 7.5Ø x 15 cm. cylinders cast in steel moulds.

3.1.2. Test results

The results of compression tests are represented on figures 1 and 2; every one is the average of six tests.

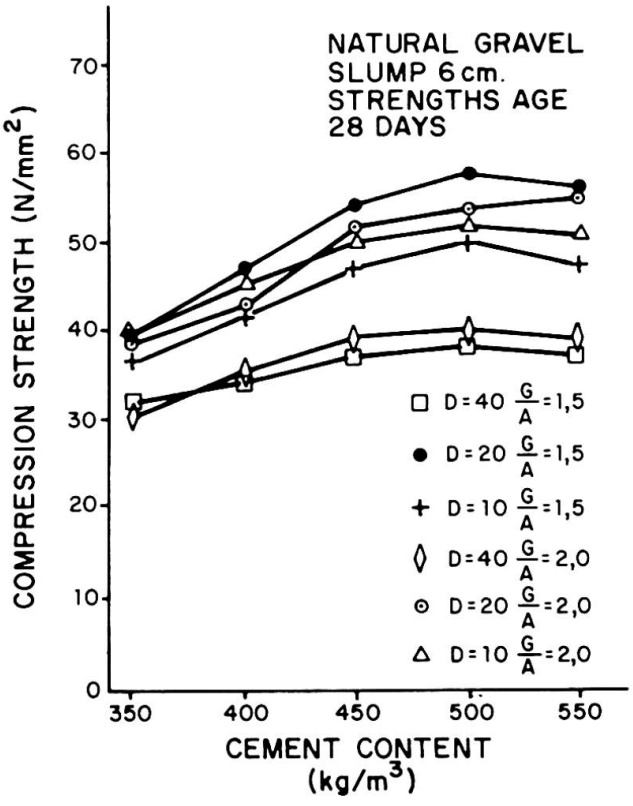

Fig.1

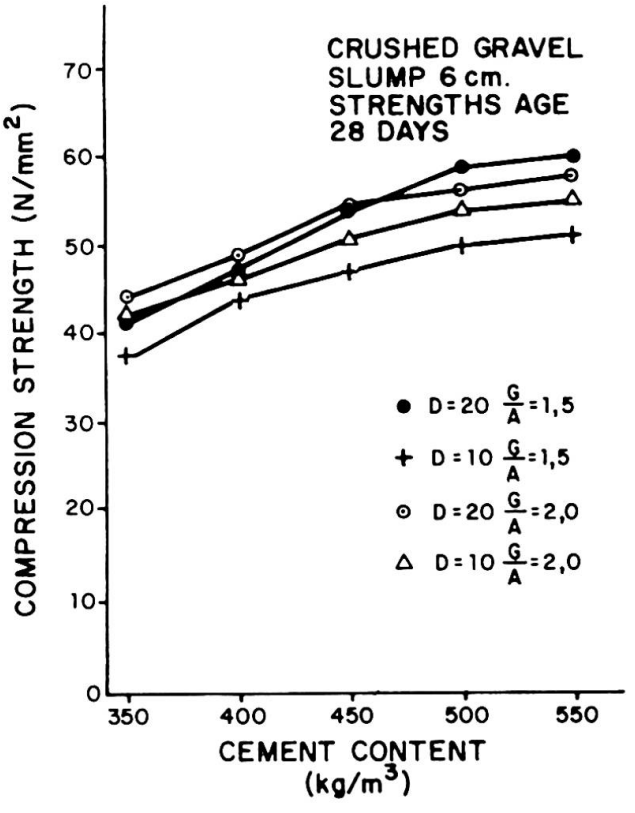

Fig.2

3.1.3. Conclusions

It can be observed in this phase of the study how concrets, with growing cement contents, increase their compression strengths in a linear way until a maximum content of 500 kg/m^3. when the strengths tend to stabilize.

It is also observed that aggregates of 20 mm maximum size give the maximum compression strength followed by 10 mm. The worse aggregate was 40 mm. maximum size.

We have also found that concretes with a fine aggregate/coarse aggregate ratio of 1.5 give the best results from the compression strength behaviour.

Observing the behaviour of rounded and crushed aggregates from the tests we conclude that crushed aggregates gave the maximum strengths.

It has been found that cleanness of aggregates is very important; with water washed aggregates the compression strengths reached are higher than with those not subjected to this treatment.

3.2. Second phase

3.2.1. Design

The cement used in this second phase was the same as that used in the first one.

The cement contents were limited to 400, 450, 500 and 550 kg/m^3.

All the concretes used crushed aggregates with 20 mm. maximum size aggregate and with a fine aggregate/coarse aggregate ratio of 1.5.

The coarse aggregates used were crushed limestones from different areas of Spain, natural crushed gravel and crushed ophites.

The fine aggregate were in one case silica river sand with a fineness modulus of 2.98 and water washed ophites with a fineness modulud of 3.00 in other case.

Some concretes used superplasticer admixture type SNF and others used a mix of this admixture plus silica fume in water suspension at 50 %.

The water content in concretes were the necessary for reaching a good workability with slumps between 5 and 8 cm.

The ages for compression tests of concretes were 28 and 60 days.

3.2.2. Test results

The results of compression tests at 28 and 60 days, together with the cement contents, type of aggregate, admixture and silica fume per cents, are shown in table 1.

Concrete type	Cement content kg/m^3	Aggregate type	Admixture %	Silica fume %	Compression strength N/mm^2	
					28 days	60 days
D	400	Limest. 1	2.0	-	56.8	66.2
	450	"	1.5	-	59.9	67.6
	500	"	1.5	-	60.1	71.7
E	400	Limest. 1	2.0	10	57.4	70.6
	450	"	1.5	10	62.6	73.8
	500	"	1.5	10	64.7	76.6
F	400	Limest. 2	2.0	10	59.3	70.5
	450	"	1.5	10	64.5	71.5
	500	"	1.5	10	65.9	74.8
G	400	Gravel	2.0	10	59.8	72.0
	450	"	1.5	10	63.2	73.5
	500	"	1.5	10	63.7	74.1.
H	400	Ophite	2.0	-	62.5	74.6
	450	"	1.5	-	69.8	81.2
	500	"	1.5	-	72.3	86.3
J	400	Ophite	2.0	10	69.3	82.5
	450	"	1.5	10	84.2	98.0
	500	"	1.5	10	85.3	102.2

Table 1

The results of tests on concrete of types H and J are presented in the figures 3 and 4.

3.2.3. Conclusions

In this second phase it is observed how the use of superplasticers produces a notable increase in the compression strength of the concrete with reference to the first phase and how the simultaneous use of superplasticer and silica fume permits strengths of approximately 100 N/mm^2 to be reached, especially when high quality and clean aggregates are used.

4. FINAL CONSIDERATIONS

In our study we have tested on hundred and sixty different concrete mixes. These tests have led us to the following final conclusions necessary for obtaining high strength concretes:

- Use high strength Portland cement.
- High strength, crushed and clean aggregates are necessary.

- The cement content must be between 450 and 500 kg/m^3.
- Good quality fine aggregate with a fineness modulus less or equal to 3.00 are recommended.
- The fine aggregate/coarse aggregate ratio used must be near to 1.5.
- Reduce the quantity of mix water by using superplasticers, so that the water/cement ratio is near to 0.30.
- Use silica fume in order to improve the workability of concretes and to increase the strength especially at ages greater than 28 days.
- Vibrate the concrete energitically.
- Carry out a well controlled wet curing of concrete, especially during the first fifteen days.

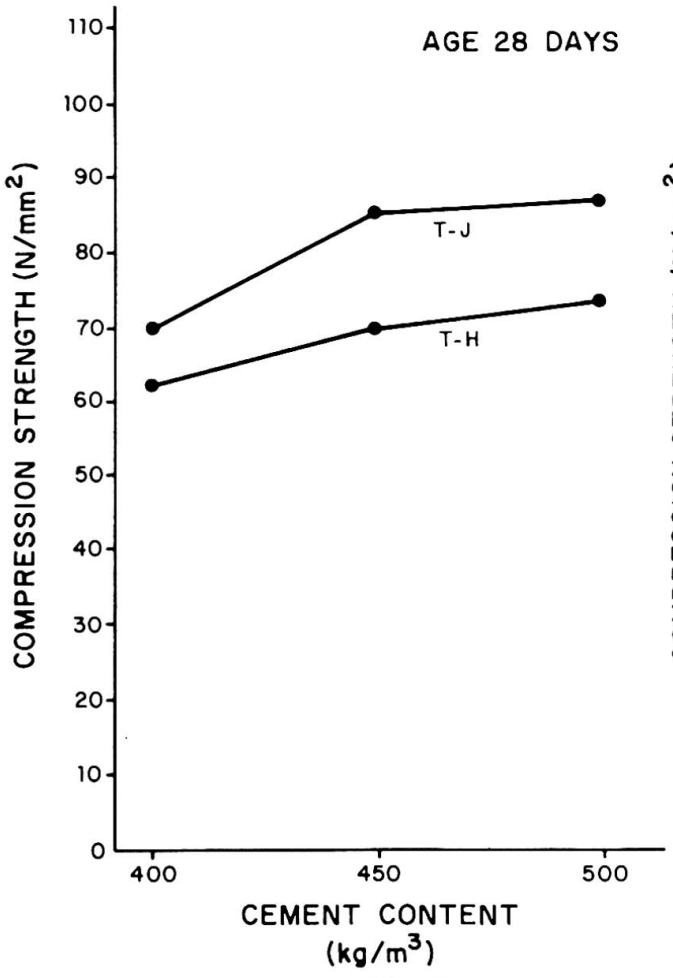

Fig.3

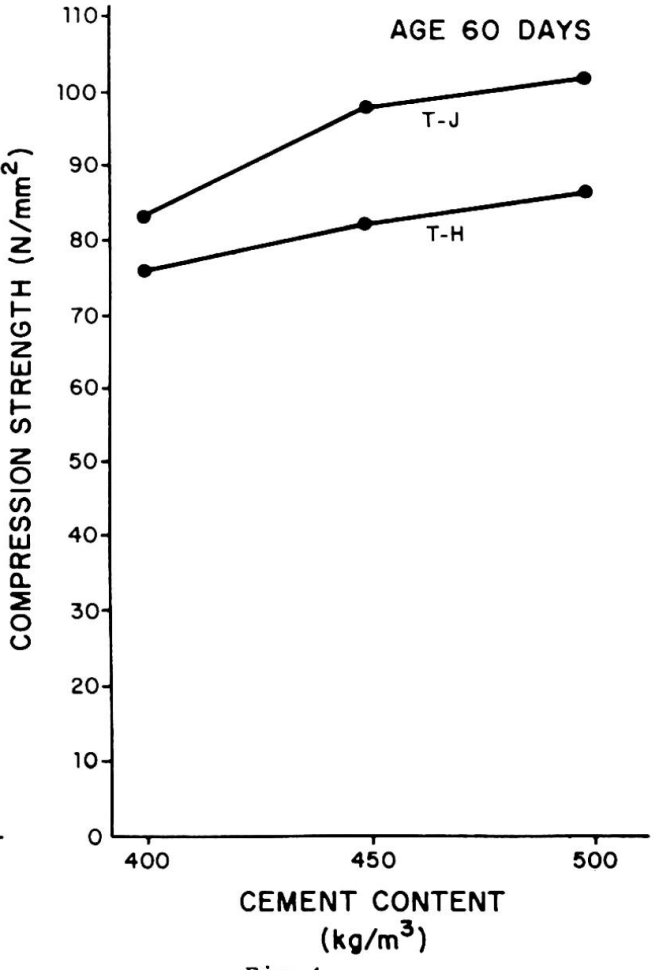

Fig.4

REFERENCES

1.- HOLLISTER, S.C.., Urgend Need for Research in High-Strength Concretes. ACI Journal, Proceedings, Vol.73, núm.3. March 1.976

2.- CARRASQUILLO, R.L., The Production of High-Strength Concrete. Report núm 78. Department of Structural Engineering. Cornell University, Ithaca, May 1.978.

3.- SAUCIER, K.L., High Strength Concrete. Concrete International, Vol 2,núm 6. June 1.980.

Fracture Mechanics Parameters as Criteria for Use of Mortars

Paramètres de la mécanique de rupture comme critères d'application

Parameter der Bruchmechanik als Anwendungskriterien von Mörtel

Ryszard FRACKIEWICZ
PhD
Wroclaw Polytechnic,
Wroclaw, Poland

Ryszard Frackiewicz graduated from Civil Engineering Department, Wroclaw Polytechnic, Poland, in 1978. He got his PhD degree in materials engineering in 1983 and since then he has been an assistant professor in Civil Engineering Institute. He is interested in fracture mechanics of cement matrix composites, acoustic emission and fibre reinforcement.

Danuta WALA
PhD
Wroclaw Polytechnic,
Wroclaw, Poland

Danuta Wala graduated from Department of Chemistry, Wroclaw Polytechnic, Poland, in 1968. In 1975 she obtained her PhD degree in ceramics. Since 1978 she has been an assistant professor in Civil Engineering Institute. Her field of interest is ceramics and brittle fracture mechanics.

SUMMARY
Research has been carried out on cement matrix mortars and on fibre-reinforced mortars. The materials tested were of very different microstructures. Both standard and fracture mechanics parameters have been measured. The strong relationship between the microstructure and fracture behaviour of the materials has been observed. Unfortunately, on the basis of the results obtained, it seems impossible to improve all the material characteristics simultaneously.

RÉSUMÉ
La contribution présente les recherches sur les mortiers de ciment et sur les mortiers de fibres. Les matériaux examinés se caractérisaient par une microstructure fortement différente. On a déterminé les propriétés traditionnelles de ces matériaux ainsi que les paramètres de la mécanique de rupture. Il existe une étroite relation entre la microstructure des matériaux et les mécanismes de rupture. Les résultats des essais ont montré qu'il n'ést malheureusement pas possible d'optimiser simultanément toutes les caractéristiques sur un même échantillon.

ZUSAMMENFASSUNG
En wurden Untersuchungen durchgeführt an Zementmörteln und an faserbewehrtem Zementmörtel. An den einzelnen Probekörpern von sehr unterschiedlicher Mikrostruktur wurden die klassischen Materialeigenschaften und die Parameter der Bruchmechanik untersucht. Es besteht ein enger Zusammenhang zwischen der Mikrostruktur eines Zementmörtels und seinem Bruchverhalten. Die Versuche haben aber auch gezeigt, dass es leider nicht möglich ist, an einem Prüfkörper alle Materialeigenschaften gleichzeitig zu optimieren.

1. INTRODUCTION

In hitherto civil engineering practice a standard procedure, based mainly on measurements of compressive and flexural strengths, has been used for assesment of properties of cement matrix structural materials. The higher and higher service demands on materials subjected to cyclic or dynamic loads has caused that new research procedures and techniques were seeked for to enable an estimation of their structural applicability by means of fracture toughness parameters. As a result, numerous efforts were undertaken in order to transform brittle fracture mechanics methods developed and tested for glass, ceramics and metals to the area of brittle concrete-like materials [1].

This paper reports on results of a research program designed to answer a question if it is possible to model microstructures of cement pastes and mortars in such a way that both their standard strength and fracture tougness are high.

2. MATERIALS

The research has been carried out on cement matrix composites of maximum aggregate size 2.5 mm and on fibre reinforced mortars. The materials were of different amount and size of aggregate, kind of stone /quartz, basalt/, porosity, water-cement ratio and kind of fibres /steel, plastic/. Table 1 containes mix proportions and the other microstructural data of the materials tested.

3. TESTING TECHNIQUES

Standard and fracture mechanics parameters of materials tested have been obtained by the following means:
-flexural strength, R_g,: cuboids 0.04x0.04x0.16 m, 0.10 m span;
-compressive strength, R_s,: halves of the broken cuboids;
-Young's modulus, E, and Poisson's ratio, ν,: ultrasonic method;
-critical stress intensity factor, K_{Ic},: 3-point bending of notched beams, Instron 1126 testing machine; [2]
-fracture surface energy, γ_f,: Davidge-Tappin method [3];
- subcritical crack growth velocity, v,: double torsion method, 0.01x0.09x0.16 m plates with initial notch and groove; the $v=AK_I^n$ relation has been assumed [4].

Fracture mechanics parameters of brittle materials enable to work out diagrams of their service lives and to design proof tests that can eliminate, before the real application in service, all the specimens that contain flaws of diameter too long to let the material work under the service stress for a desired period [5]. Fracture mechanics parameters of materials tested are given in table 2.

4. RESULTS

4.1 Flexural strength

Within the range of the materials tested it is noticable that the higher the porosity and an amount of aggregate the lower the flexural strength. This decrease is more intensive for the mortars of uniform sizes of sand. For 60% amount of sand the highest flexural strength is observed for a standard mortar containing quartz aggregate of 0÷2.5 mm size. Fibres substantially increase the flexural strength of mortars.

No.	Mix proportions aggr.	w/c	Density g/cm^3	Porosity %	E 10^{10}J/m^2	ν	Admix.
1	standard	.5	2.20	8.4	4.3	.34	-
2	-	.3	1.91	8.7	3.1	.33	-
3	-	.4	1.67	15.0	2.1	.20	-
4	-	.5	1.60	16.7	1.6	.26	-
5	-	.5	1.06	21.5	.7	.20	Al powder
6	fq12	.4	2.01	11.5	2.9	.27	-
7	fq30	.4	2.06	15.4	3.1	.30	-
8	fq60	.5	2.11	16.8	3.2	.32	-
9	mq60	.5	2.24	14.0	3.1	.33	-
10	cq12	.4	2.02	13.6	3.8	.33	-
11	cq30	.4	2.09	12.6	4.0	.36	-
12	cq60	.5	2.20	10.6	4.3	.37	-
13	fb12	.4	2.02	15.1	3.0	.26	-
14	fb30	.4	2.03	18.5	3.1	.27	-
15	fb60	.5	2.09	22.5	3.4	.28	-
16	cb12	.4	1.96	14.6	4.0	.34	-
17	cb30	.4	2.15	13.6	4.3	.35	-
18	cb60	.5	2.32	12.9	4.8	.36	-
19	standard	.53	2.27	10.88	4.3	.33	steel fib.
20	—"—	.53	2.24	10.11	4.3	.33	plast.fib.
21	standard basalt	.53	2.49	11.21	4.3	.34	steel fib.

Tab.1 Mix proportions and microstructural data of mortars.
f-fine /0-.5mm/, m-mean /.5-1.0mm/, c-coarse /1.0-2.5mm/
q-quartz, b-basalt, 12,30,60-average volume amount of sand /%/.

No.	R_g MPa	R_s MPa	K_{Ic} MNm$^{3/2}$	γ_f Jm^{-2}	n	S_n	-logA	S_A
1	8.6	35.2	.64	12.8	9	12	57	8
2	11.9	52.1	.52	6.3	9	6	56	4
3	9.1	45.0	.44	2.2	15	6	87	5
4	7.7	36.1	.45	1.8	19	7	110	5
5	2.8	10.4	.21	9.6	-		-	
6	11.9	53.0	.66	8.4	11	8	68	7
7	10.2	42.6	.58	11.0	6	10	39	9
8	5.5	31.3	.44	13.1	6	15	49	13
9	5.7	30.1	.58	23.2	-		-	
10	9.8	50.9	.54	11.9	20	10	119	8
11	9.0	56.2	.56	23.5	17	13	102	11
12	6.6	42.5	.48	30.0	10	20	62	15
13	11.5	53.0	.72	15.6	18	11	110	8
14	10.2	50.3	.69	16.2	6	15	40	13
15	5.7	42.0	.65	21.1	27	22	159	18
16	10.4	55.7	.66	19.4	30	11	177	9
17	9.8	68.1	.62	31.5	11	18	68	15
18	7.6	43.7	.69	73.8	6	24	40	22
19	14.5	38.7	1.44	670.0	-		-	
20	7.5	33.3	.63	70.0	-		-	
21	12.5	52.0	1.36	540.0	-		-	

Tab.2 Standard and fracture mechanics parameters of mortars.
S-mean standard deviation /%/

4.2 Compressive strength

Compressive strength of the mortars decrease with the increase of porosity and a volume shear of fine aggregate. Materials containing coarse aggregate exhibit their maximum compressive strengths at about 30% vol. amount of sand. The highest compressive strength /68.1 MPa/ has been obtained for a mean size coarse aggregate mortar /30% vol./. Addition of fibres does not substantially increase the compressive strength of the mortars.

4.3 Young's modulus

Young's modulus of the mortars decrease with the increase of porosity and slightly increase with the increase of the volume shear of sand.

4.4 Fracture mechanics parameters

K_{Ic} decrease with the increase of porosity of the materials tested. The higher the amount of fine quartz sand the lower the K_{Ic}, while for the basalt aggregate the influence of the volume changes of sand seem negligible. It is clearly visible that in all cases basalt aggregate effects in higher K_{Ic} values than the quartz sand. Admixture of steel fibres /1.5% vol./ increase the K_{Ic} values of the mortars of 110% /see No.19, No.21/. Fracture toughness of the materials /assesed by means of n and -logA/ increase with the porosity. The highest toughness exhibit the mortars of low w/c ratio, high percentage of microporosity and of coarse basalt aggregate at about 10% vol. /No.16/.
Effective fracture surface energy γ_f decrease for the lower values of porosity and considerably increase for the higher porosities /No.2-No.5/. The increase of volume amount of all the kinds of aggregates increase γ_f. This effect is clearly visible for the coarse basalt grains. Admixture of steel fibres /1.5%vol./ effects in the increase of γ_f from 12.8 J/m^2 to 670 J/m^2.

5. CONCLUSIONS

On the basis of the results obtained it is possible to establish a relationship between the mortars' microstructures and their standard mechanical properties. For the micro-concretes K_{Ic}, n, -logA and γ_f can be considered the materials' constants describing their toughness to subcritical crack growth and to impact damage. The best way to increase the fracture toughness of the cement matrix materials is to increase the values of K_{Ic}, n and -logA. Within the range of materials tested attempts to model the microstructures of the mortars in order to obtain the highest possible values of all the three parameters simultaneously have failed. For the cement composites subjected to cyclic loads the optimalization of their microstructures should increase the values of γ_f. Unfortunately, it is a difficult process because generally the microstructural parameters that are responsible for the high γ_f values decrease both R_g and K_{Ic}.
Application of the cement matrix materials for any specific working conditions, along with flexural and compressive strengths, should take into account the fracture mechanics parameters, still bearing in mind the necessity of a deliberate compromise between all the materials characteristics.

REFERENCES

1. MINDESS S. Application of Fracture Mechanics to Cement and Cocrete. Proc. 81st Annual Meeting of the American Ceramic Society, Cincinatti, Paper 1-SII-79, /1979/. .

2. MINDESS S., NADEAU J.S. Effect of Notch Width on K_{Ic} for Cement Paste. Cem.Concr.Res. 6/4/529-34,/1976/.

3. DAVIDGE R.W., TAPPIN G., The Effective Surface Energy of Brittle Materials. J.Mat.Sci. 3, 165-73, /1968/.

4. NADEAU J.S., MINDESS S., HAY J.M., Slow Crack Growth in Cement Paste. J.Am.Cer.Soc. 57/2/51-54, /1974/.

5. EVANS A.G., WIEDERHORN S.M., Proof Testing of Ceramic Materials - an Analytical Basis for Failure Prediction. Int.J. of Fracture, 10/3/379-92,/1974/.

Leere Seite
Blank page
Page vide

Fluage des bétons à très hautes performances

Kriechen von hochfestem Beton

Creep in Very High Strength Concrete

François de LARRARD
Ing. de Recherche
LCPC
Paris, France

Paul ACKER
Chef, section BBAP
LCPC
Paris, France

Yves MALIER
Chef, Division MSOA
LCPC
Paris, France

Alex ATTOLOU
Technicien Supérieur
LCPC
Paris, France

RÉSUMÉ
Cet article relate des essais de fluage pratiqués pendant 18 mois sur un béton de 100 MPa de résistance à 28 jours. Analysant les origines physiques des faibles valeurs mesurées, on en déduit des règles simples de formulation pour obtenir des bétons à fluage très réduit. On montre enfin sur un exemple la réduction des pertes de précontrainte escomptable dans des structures utilisant ce nouveau matériau.

ZUSAMMENFASSUNG
Dieser Artikel beschreibt die Kriechversuche, welche über die Dauer von 18 Monaten an einem Beton mit einer 28-Tage-Festigkeit von 100 MPa durchgeführt wurden. Aus der Analyse der physikalischen Ursachen für die niedrigen Messwerte werden einfache Rezepte zur Aufbereitung von Betonen mit stark verringertem Kriechen abgeleitet. An einem Beispiel wird schliesslich die Verminderung der Vorpannungsverluste aufgezeigt, die in Strukturen aus diesem neuen Baustoff festzustellen ist.

ABSTRACT
This article recounts creep tests carried out over an 18-months period on a concrete having a 28-day strength of 100 MPa. Through analysis of the physical origins of the low values measured, simple mix-design rules for producing low-creep concrete are derived. Finally, an example is given to illustrate the reduction in losses of prestress that can be expected in structures in which this new material is used.

On s'intéresse dans cet article au fluage des bétons à très hautes performances (THP). Ces matériaux, de haute compacité, ont des compositions classiques, à quelques additifs près (adjuvants fluidifiants et ultrafines); ils présentent par conséquent un surcoût modéré par rapport aux bétons ordinaires. Leurs propriétés sont illustrées sur l'exemple du tableau 1.

	Granulats calcaires du Boulonnais 5/20	0/5	Sable de Seine	Ciment CPA55 HTS	Fumée de silice	Fluidifiant	Eau	Affaissement au d'Abrams	Résistance en comp. à 28 j.
Béton TPH2	1265	326	326	421	42,1	7,59	112	> 20 cm	101 MPa
Béton témoin	1224	315	315	410	-	-	181	15 cm	55 MPa

Tableau 1: Composition et propriétés d'un béton à très hautes performances et d'un béton témoin [1].

Essais de fluage

Les éprouvettes cylindriques (longueur 1 m, diamètre 16 cm) sont conservées sous enveloppe étanche jusqu'à l'âge de 28 jours. Certaines sont alors revêtues de résine, alors que d'autres sèchent dans une ambiance constante (20°C, 50 %, H.R.). Les éprouvettes de fluage sont chargées à 30 % de leur charge de rupture instantanée, et l'on suit leur déformation, depuis l'âge de 28 jours jusqu'à la fin de l'essai. Les résultats apparaissent sur le tableau 2.

Par rapport à un béton témoin de mêmes composants mais sans additifs, on constate que **les retraits** (après 28 jours) **sont divisés par 2, ainsi que le fluage propre** (déformation par unité de contrainte, se produisant sans échange d'eau avec l'extérieur, déduction faite du retrait libre de l'éprouvette non chargée). Le retrait au jeune âge, en l'absence d'échanges d'eau, est par contre majoré [2]. **Le fluage de dessiccation**, c'est-à-dire ce qu'il faut ajouter au fluage propre et au retrait total pour retrouver la déformation de l'éprouvette séchante et chargée, **est quant à lui supprimé.**

En terme réglementaire, le "coefficient de fluage", c'est-à-dire le rapport de la déformation différée à la déformation instantanée, passe de 1,70 pour le béton ordinaire à 0,55 pour le béton THP (au bout de 18 mois d'essai).

Interprétation physique

WOLSIEFER [3] et SEKI et al. [4] ont aussi observé une réduction globale du fluage, quoique dans de moindres proportions. Ici nous proposons une explication physique de ce phénomène.

	B.O.	B.T.H.P.
Module instantané (MPa)	36.800	53.400
Retrait endogène (micro-déformations)	**220**	**100**
Retrait de séchage (micro-déformations)	**150**	**80**
Fluage propre :		
. déformation totale (micro-déformations)	385	315
. déformation par unité de contrainte (10^{-6} MPa^{-1})	23,3	10,5
. rapport de la déformation différée à la déformation instantanée	0,86	0,55
Fluage de dessiccation :		
. déformation totale (micro-déformations)	375	35
. déformation par unité de contrainte (10^{-6} MPa^{-1})	22,7	1,2
. rapport de la déformation différée à la déformation instantanée	0,84	0,00
"Kfl":	**1,70**	**0,55**

Tableau 2: résultats à 18 mois

Quel qu'en soit le mécanisme élémentaire, il est admis que le **fluage propre** se produit dans la pâte de ciment durcie, plus précisément dans les hydrates de cette dernière (qui comprend également les "grains de HADLEY", c'est-à-dire le reste du clinker non hydraté). Du fait de la faible quantité d'eau de gâchage utilisée pour le béton THP, la quantité d'hydrates (en volume total) est plus faible que dans le béton ordinaire. La loi de Pickett [6] laisse prévoir alors une réduction du fluage propre en raison de la puissance 1,7 de celle de la proportion d'hydrates (cf. fig.1), prédiction confirmée par l'expérience. A contrario, BUIL et ACKER [7] ont trouvé un fluage propre inchangé sur un béton à hautes performances qui comportait le même volume d'hydrates que le témoin.

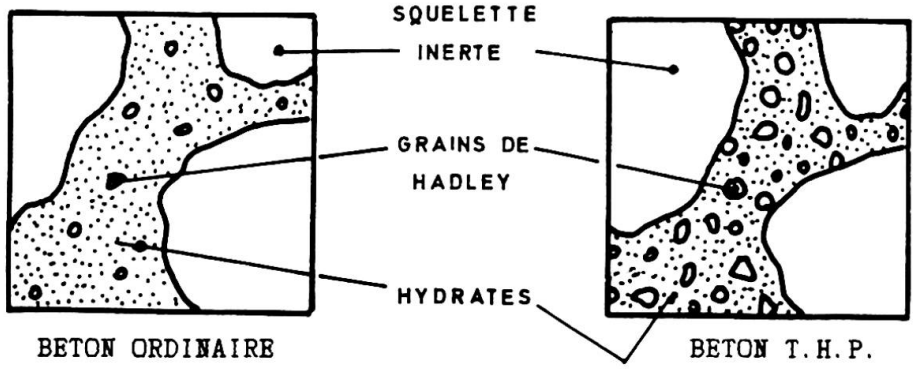

Figure 1: constitution des bétons à l'état durci.

Quant au **fluage de dessiccation**, il nous faut, pour expliquer sa quasi-disparition, avancer une hypothèse sur son origine. Selon ACKER [5], le séchage d'une éprouvette non chargée provoque un gradient de teneur en eau, lequel engendre un champ de contraintes suffisamment intense pour provoquer une fissuration de peau (cf. fig.2). La superposition d'une compression limite alors cette fissuration, qui ne relaxe plus les contraintes nées du séchage. La déformation globale est donc majorée, par rapport à la somme du fluage propre et du retrait macroscopique observée sur l'éprouvette fissurée.

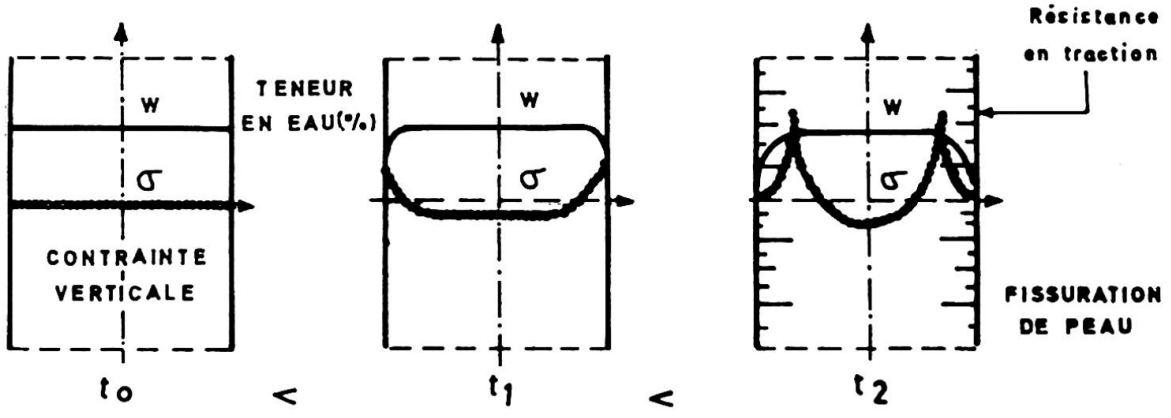

Figure 2: micro-fissuration de peau du béton ordinaire [5]

Si l'on admet que ce mécanisme explique la majeur partie du fluage de dessiccation, on comprend le comportement du béton THP: du fait de sa faible quantité d'eau évaporable (voir fig.3), et de sa meilleure résistance en traction, le séchage ne suffit pas à provoquer de fissuration de peau (comme on a pu s'en assurer par observation directe, avec un grandissement de 50).

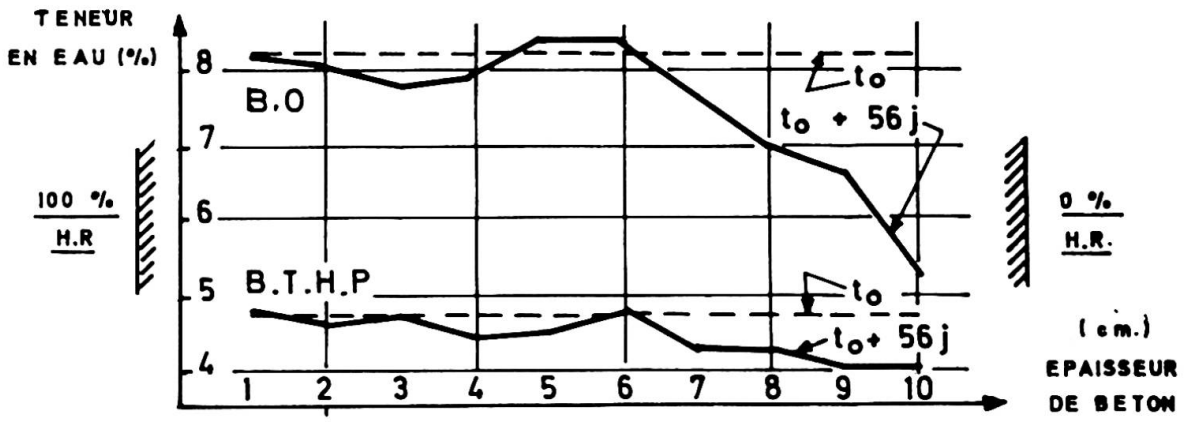

Figure 3: évolution de la teneur en eau dans des éprouvettes soumises au séchage [8].

Conséquences sur la formulation de bétons à faible fluage

On doit donc minimiser le volume d'hydrates contenu dans un béton, ainsi que sa teneur en eau évaporable, pour réduire le plus possible son fluage. **Une règle simple de formulation est donc de réduire le plus possible le dosage en eau** *: c'est en effet ce dernier qui contrôle la quantité d'hydrates formée, la réaction d'hydratation s'arrêtant par déficit d'eau. Une optimisation de la granularité du squelette, ainsi qu'un usage massif d'adjuvants [1,9] rend possible l'obtention de bétons maniables à 100-115 l d'eau par m3. Ces bétons restent modérément dosés en ciment (400 à 450 kg/m3) mais contiennent des particules ultra-fines en ajout, qui se substituent à une partie de l'eau présente entre les grains de ciment [9].

Conséquence dans les structures de génie civil

La réduction des sections, autorisée par des contraintes importantes en service, n'est possible qu'en l'absence de risque d'instabilité élasto-plastique. Pour des charges de faible durée d'application, on ne peut compter que sur une augmentation relative de module d'environ 50 %. Par contre, pour les charges permanentes telles que le poids propre, prédominantes pour les portées moyennes et grandes, **l'accroissement du module différé est de l'ordre de 150 % !**

Quant aux pertes de précontrainte, on peut voir sur le tableau 3 le résultat du dimensionnement en parallèle, avec deux matériaux (béton ordinaire et THP), d'une poutrelle précontrainte par fils adhérents: **les pertes de la poutre en THP sont légèrement plus faibles, malgré des pertes instantanés plus importantes**. Par ailleurs, le gain en poids est supérieur à 40%

Conclusion

En observant des règles simples de formulation, on peut aujourd'hui fabriquer, avec une faible proportion d'additifs "nobles" (fluidifiants, ultrafines telles que la fumée de silice), des bétons de "très hautes performances" à fluage réduit. C'est une condition souvent nécessaire pour que ces matériaux conduisent à des structures non seulement plus durables, mais aussi plus économiques, car plus légères et consommant moins de matières.

Bibliographie

[1] **de LARRARD F.** : "Formulation et propriétés des bétons à très hautes performances". Rapport de recherche LPC n°149, Paris, 1987.

[2] **PAILLERE A.M., BUIL M., SERRANO J.J.**: "Durabilité du béton à très hautes pérformances: incidence du retrait d'hydratation sur la fissuration au jeune âge". De la science des matériaux au génie des matériaux, III, pp.990-997, Chapman et Hall Ed., 1987.

[3] **WOLSIEFER J.** : "Ultra high-strength Field placeable concrete in the range 10.000 to 18.000 psi (69 to 124 MPa)". ACI Annual Convention, Atlanta, pp 1-23, January 1982,

* Nota: cette règle n'est pas une "tautologie" dans la mesure où de fortes résistances peuvent aussi être obtenues avec un dosage en eau usuel, mais une très forte proportion de liants (voir par exemple [3]).

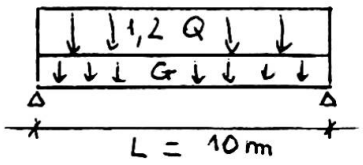

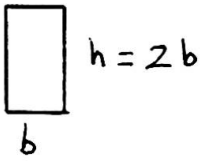

PROBLEME POSE:

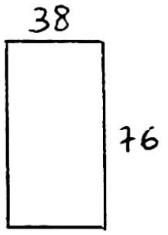

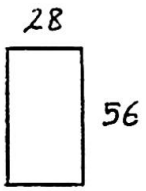

	SOLUTION B.O.	SOLUTION B.T.H.P.
Béton:	f_{c28} = 45 MPa	f_{c28} = 90 MPa
Précontrainte:	21 T15	24 T15
Pertes instantanées:	≃ 8 %	≃ 12 %
Pertes différées:	≃ 19 %	≃ 11 %
Pertes totales:	≃ 27 %	≃ 23 %

Tableau 3: dimensionnements comparés d'une poutrelle en béton, précontrainte par fils adhérents [1]

[4] **SEKI S., MORIMOTO M., YAMANE M.** : "Recherche expérimentale sur l'amélioration du béton par l'incorporation de sous-produits industriels". Annales de l'ITBTP n°436, Juillet-Août 1985.

[5] **ACKER P.** : "Comportement mécanique des bétons : apports de l'approche physico-chimique". Thèse de Doctorat de l' ENPC, Paris, 1987.

[6] **PICKETT G.** : "Effect of Aggregates on shrinkage of concrete and a hypothesis concerning shrinkage". ACI Journal proc. 52, p. 581-590, 1956.

[7] **BUIL M., ACKER P.** : "Creep of a silica-fume concrete". Cement and Concrete Research, Vol.15, pp. 463-466, 1985.

[8] **BOUSSION R., GABILLY Y.**: "Contribution à l'étude des teneurs en eau et des migrations d'eau dans les bétons". Fiche 1.30.11, Rapports du LRPC d'Angers 10/85 & 24 /86,

[9] **de LARRARD F., MOREAU A., BUIL M., PAILLERE A.M.**: "Improvement of mortars and concrete really attributable to condensed silica-fume". Supplementary paper, 2nd international conference on fly ash, silica-fume, slag and other pozzolans in concrete, Madrid 1986.

Lightweight Concrete from Flyash

Béton léger avec des cendres volantes

Leichtbeton aus Flugasche

P.D. AGARWAL
Superintending Engineer
P.W.D., U.P.,
Lucknow, India

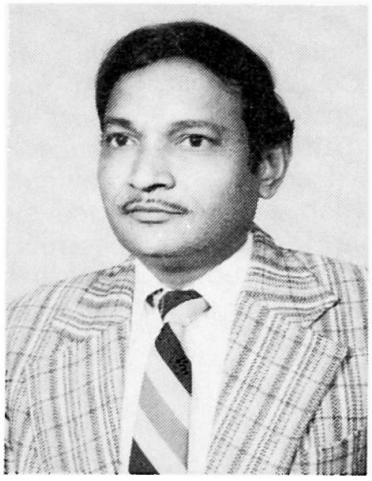

P.D. Agarwal, born 1940, received his Civil Engineering degree at the Roorkee University, India. He was Director Research Institute U.P., P.W.D. for three years. He is member of Indian Roads Congress. He has his experience in the design, construction and management of many bridge, road and building projects.

SUMMARY
Lightweight Concrete of suitable strength can be produced from flyash and lime on addition of certain chemicals, and by autoclaving. Production costs of lime flyash. 'Foam Concrete' and 'Pressed Concrete' were found to be cheaper than for conventional lightweight concrete. These foam concrete blocks can be used in non-load bearing walls and partitions. Pressed Blocks can be used even in load bearing structures.

RÉSUMÉ
Du béton léger de résistance suffisante peut être produit à l'aide de cendres volantes et de chaux, en ajoutant certaines substances chimiques, et à l'aide d'un durcissement sous pression. Les coûts de production de "béton mousse" ou de "béton pressé" sont inférieurs à ceux d'un béton léger ordinaire. Les briques en béton mousse sont utilisées pour des murs non porteurs ou des séparations. Les briques en béton pressé peuvent également être utilisées pour des murs porteurs.

ZUSAMMENFASSUNG
Leichtbeton von annehmbarer Festigkeit kann hergestellt werden aus Flugasche und Kalk, unter Beigabe gewisser chemischer Substanzen, und mittels Dampferhärtung. Die Produktionskosten von Schaumbeton und Pressbeton aus Flugasche und Kalk sind günstiger als diejenigen von normalem Leichtbeton. Die Würfel aus Schaumbeton werden verwendet für nichttragende Wände und Abtrennungen. Die Würfel aus Pressbeton können auch für tragende Bauteile eingesetzt werden.

1. INTRODUCTION

Flyash is a by-product of pulverised coal fired thermal power station. It is being treated as a waste and its disposal is causing a serious problem of space and atmospheric pollution. As per an estimate a thermal power station of 1000 MW capacity produce about 0.10 to 0.12 million tons of flyash annually. Simple open space storage of this waste product may require about 1250 Cubic Meter of space.

Pulverised Fuel ash discharged by a thermal power station is generally of two type. Main part is about 70-75 percent consisting of very fine ash mostly finer than 76 micron, 15 to 20 percent of the total discharge gets collected at the bottom of boiler and is known as bottom ash. This study deals with the finer part which is generally known as Fly Ash. Efforts were made at the U.P., P.W.D. Research Institute, Lucknow, India to utilize this waste product in manufacturing Foam Concrete and Pressed Concrete. Keeping in view the cost considerations, lime was used as binder instead of Portland Cement. Inherent pozzotanic property of the flyash was utilised in the process. Some chemical accelerators were added to achieve early strength. Autoclaving (Steam curing under pressure) was resorted to so as to further expedite the development of strength. Products achieved were found acceptable for use in construction industry. Foam Concrete blocks were found to have as cube crushing stength of about 60 to 100 Kg/Square Cum, and Pressed concrete Blocks were found to have a crushing strength of about 100 to 250 Kg/Sq.Cum.

2. MATERIALS

Following materials were used in the study.

2.1 Fly ash

Laboratory analysis of the Flyash used is given in Table a(A) and 1(B) below:-

Table - 1(A)

PHYSICAL CHARACTERISTICS OF FLY ASH USED

Sl. No.	Name of Test	Value obtained with fly ash				Value as per I.A. 3819 (Part-1)	Remarks
		Panki Distt. Kanpur	Obra Distt. Mirza-pur	River side Kanpur	Hardwaganj Distt. Aligarh (Old plant)		
1	2	3	4	5	6	7	8
1.	Lime resctivity in Kg/cm^2	76.55	56.08	24.71	25.95	40	(Minimum)
2.	Compressive strength of 1:4:15 fly ash: Cement : Standard sand mortar as compared to 20 days strength of plain 1:3 cement : Standard sand mortar percent						
	29 days	81.3	82.0	-	76.6	80	(Minimum)

1	2	3	4	5	6	7	8
	90 days	100.1	100.9	-	92.0	100 (Minimum)	
3.	Fineness by B.S. 170 sieve percent retained	40	4.0	35.0	30.0	-	
4.	Fineness by Blain's air Permeability appertatus						
	Cm^2/gm	3768	4308	2260	2683	3200(Minimum)	

* FLY ASH from Panki Kanpur was chosen for use.

TABLE - 1 (B)

CHEMICAL ANALYSIS OF FLY ASH USED

(a)	Loss on Ignition	6.0	%
(b)	Soluble Silica	2.784	%
(c)	Insoluble Silica	58.530	%
(d)	Calcium Oxide	1.153	%
(e)	Mg. Oxide	0.204	%
(f)	$R_2 O_3$	2.290	%
(g)	Insoluble Matter	29.039	%

2.2 Ordinary white lime - class C

2.3 Accelerators:-

2.3.1 Sodium Silicate of Commercial quality.

2.3.2 Calcium Chloride of Commercial quality.

2.4 Foaming Agent - Aluminium Powder of Commercial quality.

3. PROCESURE

3.1 Foam concrete

3.1.1 Flyash passing through 200 mesh was taken and mixed thoroughly with lime in a ratio 3 Flyash to 1 lime.

3.1.2 Sodium Silicate and Calcium Chloride in equal quantities were dissolved into water. Quantity of Sodium silicate and Calcium Chloride was 4.25 percent each of the mix.

3.1.3 The slurry (with about 60% water) of Flyash, lime and accelerators was added with foaming agent (Aluminium Powder) at the rate of 0.025 percent by weight. The entire mass was thoroughly mixed to ensure proper spread of minute quantities of additives.

3.1.4 The mix was poured into moulds and the moulds were stored in a room. Moulds were opened next day (after about 18 Hours) and left in the open air under a shed.

3.1.5 After 48 Hrs of moulding the cubes were subjected to Autoclaving with steam pressure of 14 Kg. per Sq. Cm for eighteen hours.

3.1.6 The cubes were taken out of the chamber after 18 Hrs and were allowed to dry for about 12 Hrs.

3.1.7 The compressive strength was then determined by Universal Testing Machine. The results obtained in one of series of experiment are given in Table No. 2 below:

3.1.8 The Table No. 2 also contains the density in Kg/Cubic Metre. It may be observed that the blocks obtained were of light weight.

TABLE No. 2

LABORATORY TEST RESULTS OF FOAM CONCRETE

SL No.	MOULD NUMBER	MIX.	Strength in Kg. Per Sq cm.	Weight in gms	Density Kg. Per cum
1	2	3	4	5	6
1.	IV/A_1	Fly-ash = 700 gm Lime = 233 gm Na_2 Sio_3, $Cacl_2$ Al. Powder	102.24	298	868.8
2.	IV/A_2	-do-	80.8	101	808.0
3.	V/A_1	Fly-ash = 300 gm Line = 100 gm Na_2 Sio_3, $Cacl_2$ Al. Powder	92.54	103	824.0
4.	V/D_1	Fly-ash = 300 gm Lime C = 100 gm Na_2 Sio_3, $Cacl_2$ Al. Powder	86.35	100.2	801.60
5.	C/D_2	-do-	89.89	100.0	800.00
6.	IV/C_1	Fly-ash = 700 gm Lime C = 210 gm Na_2 Sio_3, $Cacl_2$ Al. Powder	86.73	29.0	845.00
7.	IV/C_2	-do-			
8.	VII/F	Fly-ash = 300 gm Lime C = 100 gm Na_2, Sio_3, Ca Cl_2 Al. Powder	92.55	101	808.0
9.	VII/G_1	Fly-ash = 300 gm Lime C = 100 gm Na_2, Sio_3, Ca Cl_2 Al. Powder	94.82	102	816.0
10.	VII/G_2	-do-	94.37	100.2	801.6

1	2	3	4	5	6
11.	VIII/G_3	Fly-ash = 300 gm Lime C = 100 gm Na_2, Sio_3, Ca Cl_2 Al. Powder	78.2	105.0	840.0
12.	X/8	Fly-ash = 758 gm Lime C = 233 gm Na_2, Sio_3, Ca Cl_2 Al. Powder	93.87	100.0	808.0
13.	X/D_1	Fly-ash = 700 gm Lime C = 233 gm Na_2 Sio_3, Ca Cl_2 Al. Powder	88.0	106.0	848.0
14.	X/D_2	Fly-ash = 700 gm Lime C = 233 gm Na_2 Sio_3, Ca Cl_2 Al. Powder	78.0	107.0	856.00
15.	X/D_3	-do-	79.8	106.0	848.00

3.2 Pressed Concrete Blocks

3.2.1 The process was the same as given in para 3.1 except that no foaming agent was added to it. The moulding was done under manual pressure. The consistency of the mix was kept such that it did not flow under its own weight but required nominal presure to get properly moulded.

3.2.2 The results of cube strength are given in table No.3 for one of the series of tests. It may be seen that mix ratios tried were 1:3 and 1:4 i.e. one part lime and three/four parts flyash.

3.2.3 The fall in cube strength due to decrease in the percentage of lime is not very significatn but the economy so achieved in quite significant.

TABLE No. 3

LABORATORY TEST RESULTS REGARDING FOAM CONCRETE

Sl No.	Mould	MIX	Strength in Kg. Per Sq.cm.
1	2	3	4
1.	X/G_1	Fly-ash = 700 gms Lime C = 233 gms Na_2 Sio_3, Ca Cl_2	240.0
2.	X/C_2	Fly-ash = 700 gms Lime C = 233 gms Na_2 Sio_3, Ca Cl_2	236.73
3.	X/G_3	Fly-ash = 700 gms Lime C = 233 gms Na_2 Sio_3, Ca Cl_2	248.0
4.	XI/D_1	Fly-ash = 700 gms Lime C = 175 gms Na_2 Sio_3, Ca Cl_2	228.3
5.	XI/D_2	-do-	232.36

4. PROBABLE REACTIONS

4.1 Strength of lime mortars is attributed mainly to the process of carbonation. But the process of carbonation, when carbon dioxide is solely taken from atmosphere, is confined to the outer layer only. Under such a situation the pozzolanic material present in the lime mortar does not, by and large, participate in the strength development.

4.2 When lime flyash concrete blocks are subjected to steam preassure in an outoclave the fine silica present in the flyash (Pozzolanic material) reacts with lime. This hydrothermal reaction between silica and lime yields various Calcium Silicate Hydrates - One of them being Tobermorite.

4.3 Quartz (Silica) available in normal way in the flyash-lime mixture reacts extremely slowly due to slow dissolution in water. Consequently strength development is not only very slow but incomplete also. To overcome this problem moderately reactive silica in the form of gels were supposed to be helpful. sodium Silicate and Calcium Chloride were added to the lime-flyash paste. This addition enhenced the quantity of calcium silicate in the paste, and also introduced silica gel into it.

4.4 Autoclaving with high stream pressure and with these additives imparted reasonable strength to the lime flyash blocks to make them suitable for structural use.

4.5 It is not considered fit to give much of the chemistry and reactions involved in the process due to space limitations. But these are available in various research works specially those of G.E. Bessey, H.F.W. Taylor, R. Kondo and others.

5. ACKNOWLEDGEMENT

The help and work of Sri. A.P. Jain, Sri R.P. Porwal and Bankey Lal is gratefully acknowledge.

REFERENCE

1. Lee F.M., The Chemistry of Cement and Concrete.
2. Short A., and Kinmburgh W., Light weight Concrete.

Water Permeability and Strength of Concrete

Perméabilité à l'eau et résistance du béton

Wasserdurchlässigkeit und Festigkeit des Betons

Ali ZREGH
Dr.Eng.
Al-Raya Al-Khadra Univ.
Tripoli, Libya

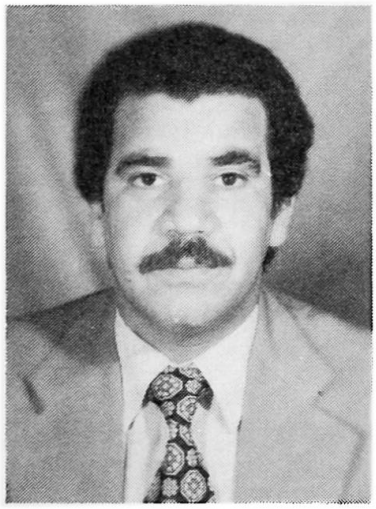

Ali Zregh born 1947 in Tripoli, B.Sc. MSCE and Ph.D. involved as a young engineer in design and construction of housing projects in Libya in the early 70's. Now as a staff member in Civil Engineering Dep. he is the Head of this department. He is a member in the local engineering societies and ACI, ASCE, SEA and others.

SUMMARY
Concrete is permeable when water can pass through its internal matrix under pressure. Permeability in concrete may be responsible for the disintegration of concrete. In this paper 30 different mixes were investigated. Variable water to cement ratios and cement contents were considered. Results and findings are reported at the end. A guideline to design a watertight concrete can be gained from this paper.

RÉSUMÉ
Le beton est considéré perméable lorsque l'eau sous pression peut pénétrer à travers sa matrice interne. La perméabilité du béton peut être á l'origine de sa désagrégation. Dans cette contribution, 30 différents mélanges de béton ont été considérés. Les paramètres variables ont été la rapport eau/ciment et la quantité de ciment contenue dans le mélange. Les résultats et les conclusions sont présentés, ainsi que des directives pour exécuter un béton imperméable.

ZUSAMMENFASSUNG
Beton ist durchlässig, wenn Wasser durch seine Zementmatrix dringen kann. Die Durchlässigkeit von Beton kann verantwortlich sein für dessen Zersetzung im Laufe der Zeit. In der beschriebenen Studie sind 30 verschiedene Betonmischungen untersucht worden. Die Versuchsparameter waren der Wasser/Zementfaktor und der Zementgehalt. Der Beitrag erläutert die Versuchsergebnisse und die Schlussfolgerungen. Es werden Richtlinien zur Herstellung eines wasserundurchlässigen Beton gegeben.

INTRODUCTION

Permeability is caused by existance of pores in the cement paste and the aggregate voids, because not all space between the aggregate particles becomes filled with solid cementations and fine materials. Furthermore to achieve a workable mix much more water is added than that required for the hydration of cement. Destruction of hardened concrete from freezing and thowing in presence of water, and corrosion of reinforcement subjected to moisture and air are problems related to the permeability of concrete. Burry and Domome [1] investigated penetration rates of sea water into concrete under pressure and concluded that penetration was found to be proportional to time to power 0.45. Datta in his ref. [2] concluded that if a relatively impermeable concrete is produced, the rate of chemical attack is drastically reduced thereby considerably delaying the rate of corrosion of reinforcement. Other researchers [3] and [4] indicated that the permeability of concrete is not a single function of its porosity but depends upon the size, shape and continuity of the pores and upon water to cement ratio. In this paper an attempt is made to investigate the behavior of concrete permeability with varying water to cement ratio and the cement content. Normal weight concrete with local "Libyan" materials were used. The materials properties are according to standards. Results and finding related to permeability and concrete strength are presented at end.

FACTORS AFFECTING PERMEABILITY OF CONCRETE

Three important factors may cause the concrete to be permeable:

1. The Constituent Materials:

   i - The fineness of cement improves the cohesiveness of mixes and hence the water tightness of concrete. It also controls the shrinkage and cracking. Cement with slow hydration and hardening characteristic tends to increase the permeability of concrete.

   ii - Water Cement Ratio:

   The permeability decreases as voids decreases but for plastic workable mixes the permeability increases as the water cement ratio increases as reported in ref. [1].

   iii - Aggregate and Cement:

   Both the cement paste and the aggregate contains pores that can permit liquid to pass through. Dense clean very well graded and fine grained aggregate yields a solid impermeable concrete. The greater the maximum size of aggregate for a given "W/C" water to cement ratio the greater the permeability as reported in ref. [2].

   iv - Admixtures:

   The main purpose of water proofing agents is to close the pores of the concrete matrix as lime soaps, butyle aluminium calcium or ammonium soaps, and also stearates or others.

2. Method of Preparation:

   Honey combing or differential settlements of newly placed fresh concrete can cause cracks. Workable, homogenous and well compacted concrete will minimize these defects.

3. Curing:

   If concrete is kept wet at early age the continued hydration of cement results in gel development which reduces the size of voids and increases the water tightness of concrete.

EXPERIMENTAL WORK:

All 30 mixes were designed according to the standards. Each of ingredients was compared to the ASTM specification. The cement properties met ASTM C150 while the aggregate met ASTM C33 and ASTM C-74. The 30 mixes were varied in both the cement content and water to cement ratio. Six cement contents were used starting from 2.45 KN/m^3 to 4.90 KN/m^3. That is at 0.49 KN/m^3 interval. At each case six water to cement ratios were varied starting from 0.45 to 0.70. Three mixes were omitted from both the lowest cement content and the highest cement content due to the workability problems. The aggregate to cement ratio was calculated for the 1st mix and found to be equal the value of 8.0 while in the last mix was found to be equal to the value of 3.25.

A total of 240 standards cubes "150 mm x 150 mm x 150 mm" were casted. Eight cubes for each mix were tested as follows: One cube per mix was tested for 3 days strength test, and one cube was tested for 7 days strength and 3 cubes were tested for 28 days strength. The last 3 cubes were tested for permeability test.

PERMEABILITY TEST:

Testing procedure was according DIN-1048. A constant pressure was applied to six specimens at each time. The water pressure was kept to 0.7 MPa. Percolation volume readings were taken at each half hour interval.

The coefficient of permeability K_c was determined from Darcy's law.

$$K_c = \frac{Q}{A} \times \frac{L}{H} \qquad (1)$$

Where

K_c = permeability coefficient m/sec.

Q = rate flow (m^3/sec)

A = cube cross-sectional area (0.15 m x 0.15 m)

L = specimen depth (0.15 m)*

H = water head above specimen (71.35 m)

Therefore equation (1) becomes:

$$K_c = 9.342^* \times 10^{-8}\ Q \quad \text{m/sec.} \qquad (2)$$

TEST RESULTS AND DISCUSSION:

Fig. 1 shows the 28 days compressive strength for the 30 different mixes versus the water to cement ratio and the cement content. As the "W/C" water to cement ratio increases the compressive strength decreases, and as the cement content decreases the compressive strength increases. This is due to the increase of aggregate to cement ratio.

A typical behavior of concrete permeability "water percolation rate to fill up voids" at 6 hours is shown in Fig. 2. As W/C increases the percolation rate increases for a constant cement content. The permeability increases as the cement content increases. Fig. 3 shows the same trend of permeability but at 24 hours. A combination of 30 min., 6 hours and 24 hours permeability coefficient "K_c" is illustrated for a constant cement content. K_c values are larger in the early stage since voids are to be filled first. It is important to notice that permeability does not mean leakage.

The lower the cement content the lower the K_c values are, and this is due to pores in the cement paste. This can be seen from Fig. 3 which illustrates also the permeable "leakage" and impermeable mixes. The lowest K_c value "0.76 x 10^{-4}, m/sec occured at the mix of which had W/C = 0.45 and cement content of 2.94 KN/m^3.

The same mix in Fig. 1 had the highest compressive strength which is equal to 46.1 MPa.

CONCLUSIONS AND RECOMMENDATIONS

1. A low value of cement content associated with a lower value of W/C yields both impermeable and high strength concrete, however trial mixes are recommended.
2. A value of $K_c = 4 \times 10^{-11}$ m/sec after 24 hours meant the concrete is impermeable under 0.7 MPa pressure.
3. Watertight concrete without any admixtures added does not exist because of the pores in both cement paste and aggregate particles.
4. More research is required on permeability and admixtures effect.

REFERENCES:

1. BURY and DOMONE, Role of Research in the Design of Concrete Offshore Structures. Offshore Technology Conference paper No. 2132, Vol.1, Houston, 1974.
2. T.K. DATTA, Durability of Concrete in Ocean Environment. Proc. of the 2nd International Conference in Concrete Technology. Tripoli, Oct. 1986.
3. NEVILLE A.M. Properties of Concrete, Pitman Publishing Co., 1973.
4. W.H. TAYLER, Concrete Technology and Practice. Aust. Division Research, C.S.I.R.O.

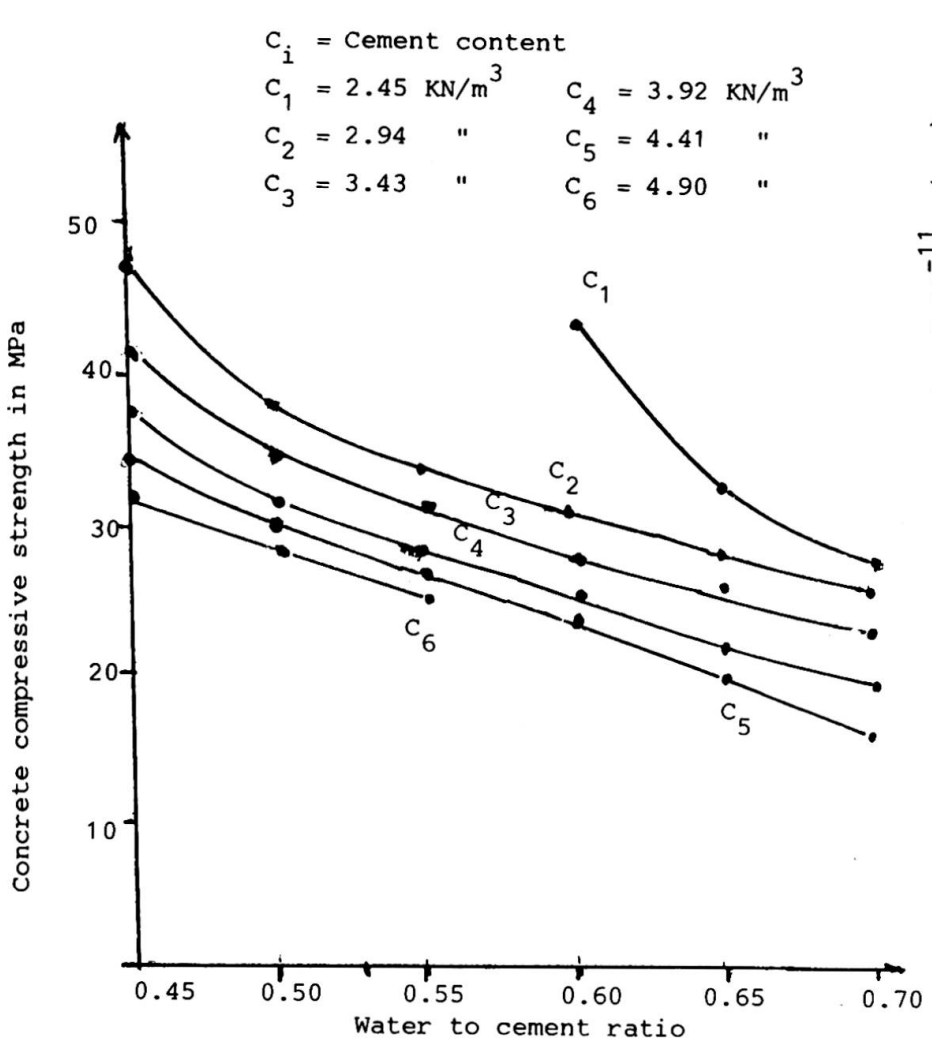

Fig. 1 : Cement content effect on concrete strength

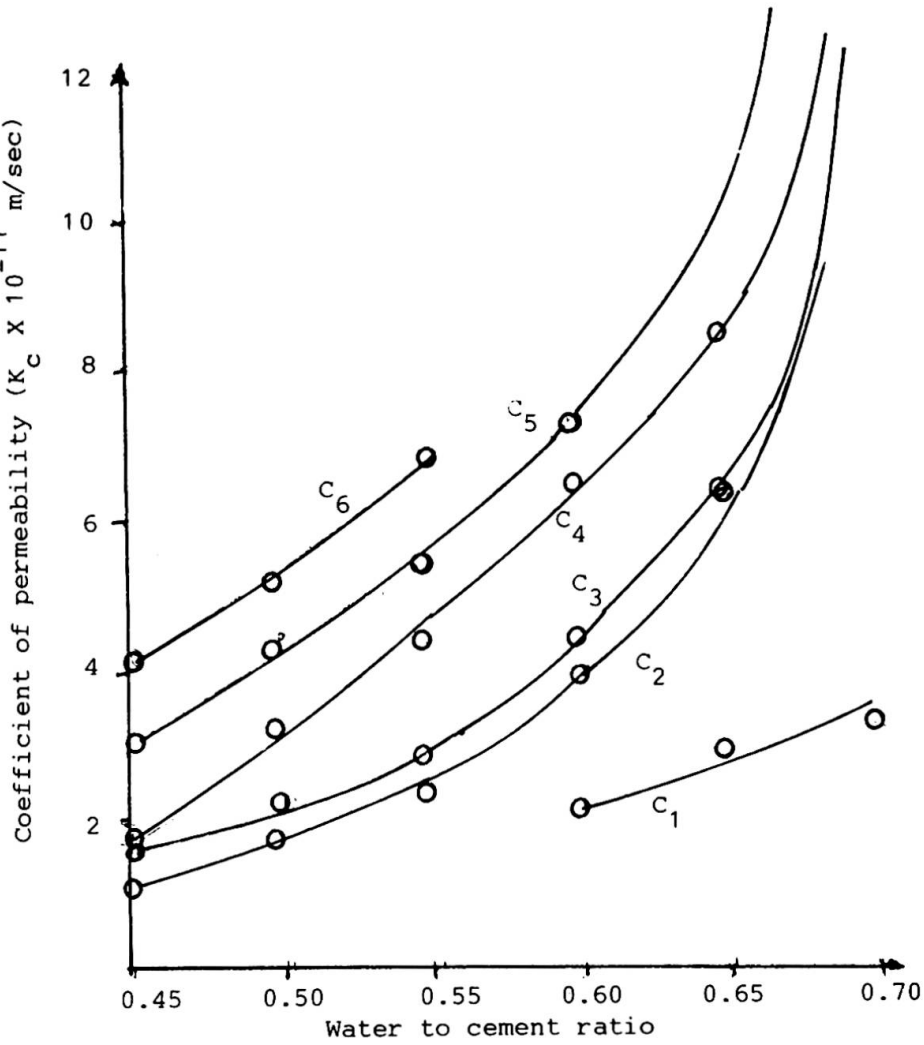

Fig. 2 : Cement content effect on permeability 6 hours test.

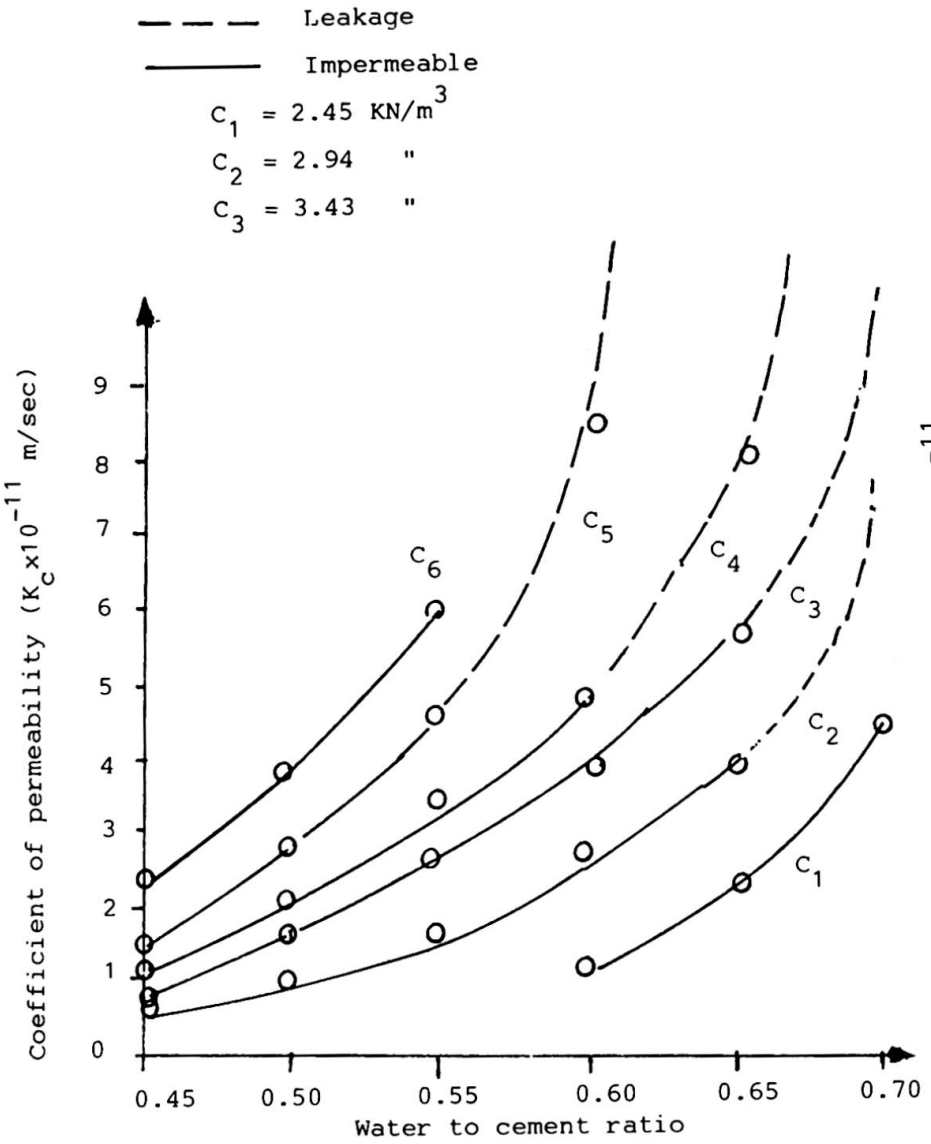

Fig. 3 Cement content effect on permeability 24 hours test.

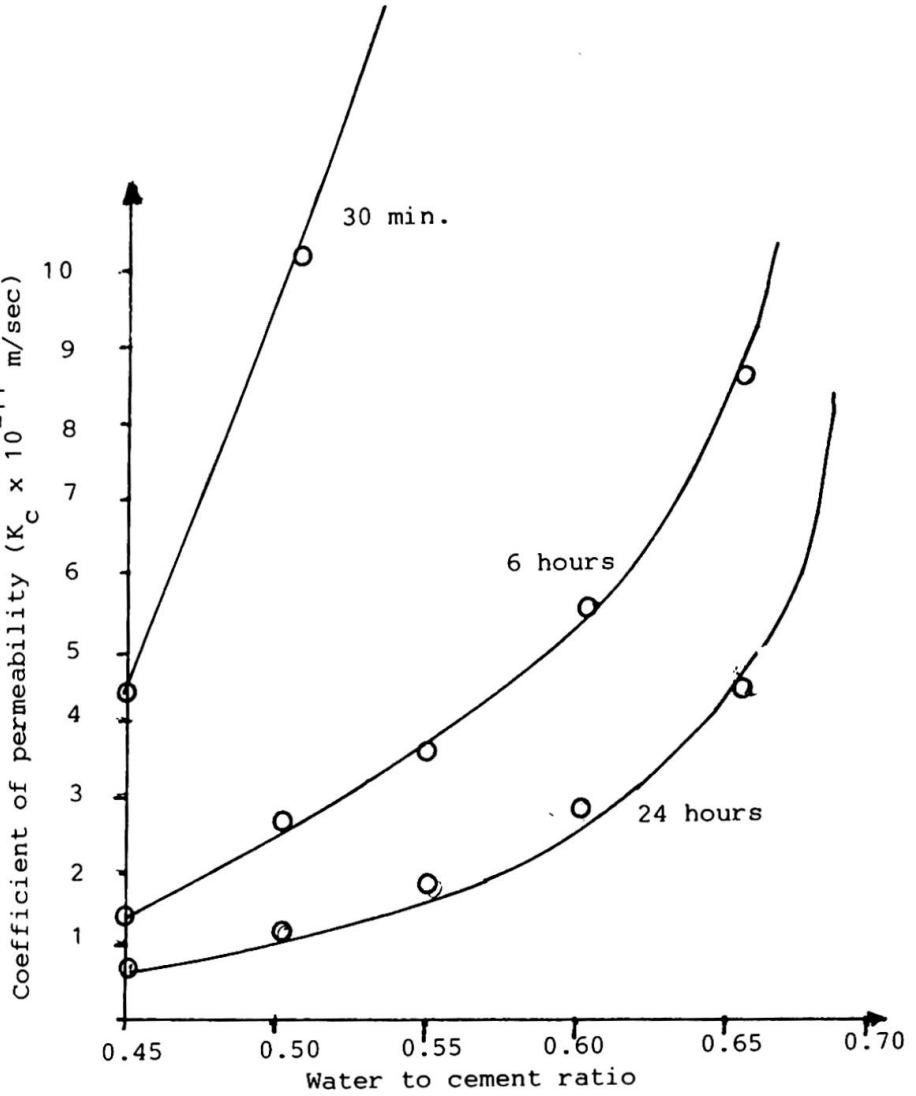

Fig. 4 Time effect on permeability for "C_2" cement content.

Retractable Roof Olympic Stadium Montreal

Toiture rétractable du Stade Olympique de Montréal

Einziehbares Dach des Olympiastadions Montreal

Luc LAINEY
Dr.Ing.
Lavalin
Montreal, Canada

Jörg SCHLAICH
Prof. Dr.Ing.
Schlaich und Partner
Stuttgart, Fed. Rep. of Germany

Normand MORIN
Dr.Ing.
Lavalin
Montreal, Canada

Rudolf BERGERMANN
Dipl.Ing.
Schlaich und Partner
Stuttgart, Fed.Rep. of Germany

SUMMARY
The 20 000 m^2 retractable roof of the Montreal Olympic Stadium consists of a Kevlar fabric suspended from a 168 m high inclined tower. 46 winches and other mechanisms are used to lift the roof to the top of the tower. The engineering and construction of this unusual structure have recessitated a number of innovative technical solutions.

RÉSUMÉ
Le toit rétractable du Stade Olympique de Montréal est constitué d'une toile de Kevlar de 20 000 m^2 suspendu à un mât incliné d'une hauteur de 168 m. Quarante-six treuils et autres mécanismes permettent de le remonter dans un espace réservé à la partie supérieure du mât. La conception et la réalisation d'un tel ouvrage ont fait appel à des solutions techniques innovatrices à plusieurs égards.

ZUSAMMENFASSUNG
Das einziehbare Dach des Olympiastadions in Montreal besteht aus einem Kevlargewebe von 20 000 m^2, das an einem 168 m hohen Turm befestigt ist. 46 Winden und andere mechanische Einrichtungen ermöglichen das Heben und Einziehen des Dachs in einen dafür vorgesehenen Raum im oberen Teil des Turmes. Ein derartiges Bauwerk konnte nur mit neuartigen technischen Mitten konzipiert und ausgeführt werden.

1. INTRODUCTION

The 20 000 m^2 fabric roof of the Montreal Olympic Stadium closes an elliptical opening of 220 X 140 m in the existing concrete roof covering the grandstands. It is suspended from a 168 m high inclined tower with an average angle of 30 deg. from the vertical. Even though the initial concept of architect R.Taillibert was followed, the original design was considerably reworked especially regarding the snow load and all the lifting mechanisms. Indeed, strong concerns about the feasibility and reliability of the snow melting system considered in the earlier design required an increase of the nominal snow load from the initial 0.45 kN/m^2 to 1.65 kN/m^2. The consequences of this change include a complete redesign of the suspension system and the hardware pieces, an optimized geometry, a strengthening of the fabric joints and major modifications to the mechanisms retracting the roof. (See fig.1)

Special attention was given throughout the design to reconcile such diverging objectives as having a flexible and easily foldable structure during retraction and obtaining a very stiff and stable roof supporting heavy loads in the closed position. An effort was also made to isolate the mechanisms from the structural parts carrying heavy wind and snow loads.

Fig.1 Overall View of the Stadium

2. ROOF AS A STATIC STRUCTURE

2.1 General description

The roof is roughly ellipsoïdal in shape and is suspended by 26 points, looking like Chinese hats distributed over the entire roof surface. On the periphery of the ellipsoïd, the fabric is attached to circular edge cables which join together at anchoring plates called boomerangs.

A normal surface reaction at each suspension point is achieved by a suspension cable connecting the suspension point to the top of the tower and one or two liaison cables linking two suspension points or a boomerang.

2.2 Membrane Material

The original membrane material is a PVC coated Kevlar 49 fabric with a Panama weaving. The breaking strength is 600 kN/m in the warp and 550 kN/m in the fill. The strain at 20% of breaking load under biaxial tension is about 1.4%. The compensation factors are 1.5 and 3.5‰ in the warp and the fill respectively which characterize an extremely stiff behaviour.

In order to improve the durability of the material, both faces were coated with a film of polyurethane. The final total thickness is about 2.5 mm and the mass per unit area close to 2.9 kg/m^2. Over 400 fabric samples are exposed on the concrete roof and will periodically be submitted to cyclic folding to monitor the actual aging of the fabric with time.

2.3 Suspension Point

The top of the Chinese hats (See fig. 2) consists of a cast steel piece to which are attached suspension and liaison cables. Forty small steel cables, called "suspenders", spread out from the bottom part of this piece. The lower end of every suspender is attached to a cast steel clamp that holds the Kevlar fabric.

These clamps are made out of two halves bolted together and shaped to squeeze a pocket of Kevlar fabric where an aluminium cylinder is inserted. The suspenders are covered with a translucent polyester PVC coated fabric for water tightness and skylight effect at each of the 26 suspension points (See fig. 2).

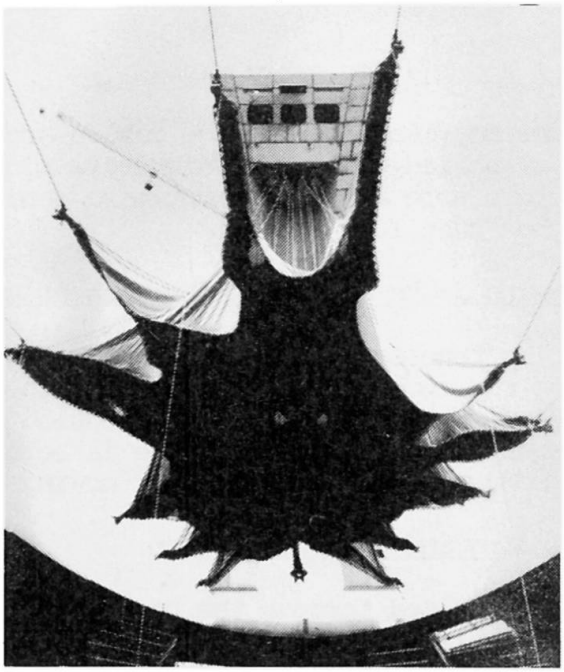

Fig.2 Hats during Erection

2.4 Boomerang and Anchorage

The boomerangs are cast steel pieces having in general a saddle for the continuous edge cable, connectors for the hauling and the liaison cable and a large cylindrical hole which receives a pin up to 300 mm in diameter to make the anchorage. The inside of the hole is covered with a reinforced teflon in order to create a good hinge around the axis of the pin.

The anchoring structure attached to the concrete has some funnel shaped plates and the boomerang itself carries some rollers to guide it into its anchorage (See fig. 3).

2.5 Edge

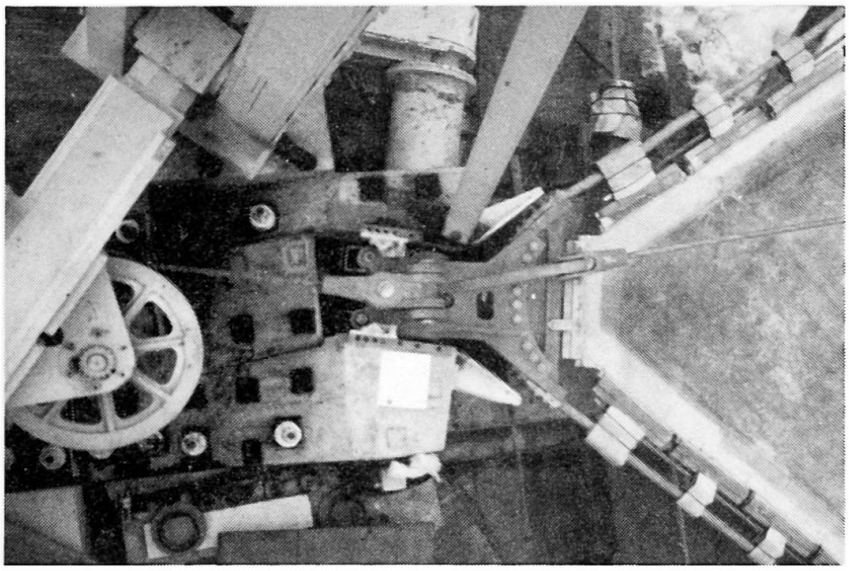

The attachment of the fabric on the edge cable consists of a series of cast steel fabric clamps similar in principle to the ones used for the hats. In order to preserve the flexibility of the edge, only one of four fabric clamps is rigidly attached to the cables. The three others have U shaped connectors which allow a free bending of the cable during the retraction. These connectors can only transfer radial forces.

Fig.3 Boomerang and Anchorage

The tangential forces which appear under wind or snow load are carried by a small "tangential cable" attached to all the fabric clamps which runs parallel to the edge cable (See fig. 3).

2.6 Suspension and liaison cable

All the suspension, liaison and edge cables are lock coil ropes with two or three layers of shaped wires. The diameters range from 37 to 95 mm. Special design parameters were adopted to optimize bending flexibility while maintaining a modulus higher than 160 000 MPa.

2.7 Prestressing Jacks and Top Anchorages of suspension cables

The prestressing tension in the membrane is applied through 12 centerhole jacks located at the top anchorage of the suspension cables. Extending the piston by 0.7 to 1.0 m is enough to increase the tension in the fabric from about 3 kN/m to 10 kN/m. When the hydraulic pressure is released, the piston sits directly on the cylinder body via a large ring gear moving on the piston.

2.8 Shape Finding and Cutting Pattern

The shape was optimized through the use of mathematical models to achieve a state of uniform biaxial stress in the fabric under prestressing. The cutting pattern was prepared to fit this state. The end product is an anticlastic shape built from 76 main strips cut in 3.1 m wide rolls. Around the hats, the assembly of the main strips leaves circular holes 12.5 m in diameter. A conical shape with a circular generating line joins the periphery of this opening to the fabric clamps at bottom of the suspenders.

Due to the extreme stiffness of the material, a high precision of less than $\pm$2 mm was required in the cutting of the strips. For the cutting patterns, a compensation factor was applied in either main directions of fibers according to the results of the biaxial tests (see 2.2). Along the edges, the fabric was "decompensated" up to 7.5‰ to fit the stiff edge as well as to avoid any circonferential tension in the fabric close to the edge.

2.9 Loading and Analysis

The final maximum uniform snow and wind loads are 1.65 kN/m^2 and 0.70 kN/m^2 respectively, based on codes and wind tunnel tests. In cooperation with Prof. Linkwist of Stuttgart University, a number of static F.E. analysis were performed to determine the stresses and deformation over the entire roof surface under various combinations of wind and snow.

2.10 Membrane assembly

The assembly joints between kevlar strips are either sewn (15 stitches) or High Frequency (H.F.) welded and sewn (26 stitches) to meet strength requirements of up to 100% of the base material. Unique H.F. welding machines and 15 needle long arm sewing machines were specially designed and built for the execution of these joints which required hundreds of mechanical tests to perfect. The accuracy of the assembly is better than $\pm$2 mm per joint. All joints are coated with polyurethane for water proofing and U.V. protection. After completion of the work in the assembly plant, the 65 ton membrane was transported in a single piece to the stadium for the attachment of the hardware.

3. MECHANISMS

3.1 Lifting Sequences

The roof is operated by 26 hoisting cables in series with suspension cables in addition to 17 hauling cables attached to the boomerangs. Each cable is connected to a winch.

When the roof opens, the prestressing tension is first decreased by lowering the 12 hydraulic cylinders. The hauling winches are then activated to separate the boomerangs from their anchoring pins; an electrically driven mechanism pulls out the pin. Immediately after, the boomerangs are lifted using sheave elevators as described in 3.5.

Then, the hoisting winches slowly lift the fabric into a specially designed space in the mast called the "niche". Simultaneously, the hauling winches keep an antagonist tension. In addition a circular cable called a "lasso" connects all boomerangs, giving a better control on their position (See fig. 4).

All the sequences are automatically controled by computer in order to closely follow the predetermined intermediate positions. The lowering sequence is exactly the reverse of the lifting one.

Fig.4 Roof during Retraction

In the final stage, an additional cable pulls the boomerang closest to the tower to the inside of the niche and at the same time, the lasso is tightened to bring the membrane into its final parking position. Wind tunnel tests show that the stability of the membrane during the lifting is satisfactory for wind speeds up to 25 km/h.

3.2 Hoisting system

The hoisting and the suspension cables are rolled up from their anchoring position at the top of the tower to the hoisting winches located at the base of the tower. The hoisting cables are round strand rope with diameter and length up to 57 mm and 294 m respectively. To avoid rubbing against the many guiding rollers, the connection piece between the hoisting and the suspension cable is equipped with wheels rolling on parallel tracks

3.3 Hauling system

From the boomerang, each hauling cable is guided to its winch through by two sheaves. The first one, close to the anchorage, is hinged around one axis to accommodate the variation of inclination of the cable when the boomerang moves up. The second one is fixed and guarantees a proper fleet angle on the drum of the winch. The hauling cables are similar to the hoisting cables but with a diameter up to 70 mm. All hauling winches are hydraulic and behave like counterweight of variable mass.

3.4 Lasso

Two lasso winches are located at the bottom of the niche. Each is able to store 400 m of cable and has a 700 kN pulling capacity. The lasso is a single cable 850 m long, 57 mm in diameter.

The lasso is going out of the niche through the first winch. It is then deviated by one vertical and one horizontal sheave over to the boomerang closest to the tower and then thru a "lasso saddle" hanging from all the other boomerangs. It circles around the stadium and goes back to the second winch in a symmetric way. A typical lasso saddle includes a sheave and two arms hinged in the plane of the sheave. In the parking position, all saddles are touching each other.

3.5 Other mechanisms

Apart from the prestressing jacks and the driving mechanisms of the pins at the boomerangs, an additional mechanism was needed to prevent the contact between the edge cable and the fixed roof during the retraction. For that purpose, the first deviation sheave of the hauling cable is installed on a movable support sliding on tracks 3 to 4 m high bolted on a frame. This support is electrically driven with 4 screws.

4. CONTROL SYSTEM

Up to 46 winches have to be synchronized during retraction. Every cable is equipped with a measuring device of the winded or unwinded length and with a number of limit switches for safety.

All winches have their own Local Programmable Computer which manage some basic logic. Three larger Local Programmable Computers and two micro computer dispatch the instructions and coordinate the complete operation. They also allow the communication with the operators and display system status, informations and faults. Some changes to the calculated sequences can be undertaken by the system itself to keep the actual sequence within fixed boundaries.

5. CONCLUSION

The Montreal Olympic Stadium Retractable Roof has been finally completed after three years of engineering, manufacturing and construction efforts. Dealing with unusually large dimensions and an extremely complex geometry has required innovative solutions out of standard guidelines. The end product is a prototype of an hybrid structure being at the same time a large span suspended roof and a huge machine.

Ice: A Future Structural Material of the North?

La glace: un matériau futur de construction pour le Nord

Eis: ein zukünftiger Baustoff für den Norden?

Peter G. GLOCKNER
Prof. of Civil and Mechanical Eng.
University of Calgary
Calgary, AB, Canada

Born in Hungary, Dr. Glockner came to Canada in 1949. He obtained his B.Eng. from McGill, and further degrees in the U.S. For over 30 years he has taught at universities in Alberta and acted as a consultant. He has over 250 publications.

Walerian SZYSZKOWSKI
Assoc. Prof. of Mechanical Eng.
University of Saskatchewan
Saskatoon, SK, Canada

After graduation in 1974, Dr. Szyszkowski taught and did research at the Technical University of Warsaw. In 1982 he came to The University of Calgary and in August 1986 took up his present position. His research area is solid/applied mechanics.

SUMMARY
A nonlinear 3-dimensional constitutive model describing the behaviour of ice, including its three creep stages, its strain softening at constant strain rate and its tensile brittleness, is briefly reviewed. The properties of reinforced ice, with spun fibreglass yarn as reinforcement, are sketched and a possible use for it in constructing reinforced ice domes indicated.

RÉSUMÉ
Cette contribution décrit une loi tridimensionnelle et non-linéaire du comportement de la glace, en incluant les trois phases de fluage, la relaxation sous l'effet d'un raccourcissement à vitesse constante et la fragilité en traction. Sont également décrites les caractéristiques de la glace armée de fibres de verre et une application pour la construction de coques en glace.

ZUSAMMENFASSUNG
Ein kurzer Überblick über ein nichtlineares dreidimensionales Stoffgesetz für Eis wird gegeben, der dessen Materialeigenschaften, einschließlich der drei Kriechenphasen, des Dehnungserweichens unter konstanter Dehngeschwindigkeit und der Zugsprödigkeit beschreibt. Die Eigenschaften von mit Glasfaserzwirn bewehrtem Eis werden beschrieben und eine mögliche Anwendung für Eisschalenbau aufgezeigt.

1. INTRODUCTION

The demand for improved performance characteristics of common structural materials under increasingly stringent/hostile environments has resulted in research and development work leading to completely new structural materials or to significant improvements in their mechanical, chemical, electrical or transmissivity properties. For example, mechanical alloys have been produced which have ultimate/yield strength characteristics far superior to those produced by traditional thermal/chemical processes. Fibre reinforced plastics and resins, new and improved ceramics and various other new or improved materials are increasingly used in the latest products of microelectronics and other branches of technology.

The need for more economical and improved materials also forces us to look at traditional materials available abundantly in nature to see whether they can be used and/or their use increased. One abundant material in cold regions is ice which has been studied extensively by engineers and physicists, establishing its crystal structure and its physical properties [1-3]. Less attention has been paid to its mechanical/strength characteristics and its behavioural features which affect its use as a structural material [7,8].

This paper briefly sketches a constitutive model which describes the characteristic features of ice behaviour [4-6], including the three-stage creep under constant stress, strain-softening under constant strain-rate, and its brittleness. Stress-strain nonlinearities and hereditary effects are also included. Next properties of reinforced ice are briefly reviewed. The reinforcing is spun fibreglass yarn. As a possible application of ice as a structural material, the construction of reinforced ice domes, using a novel construction/erection technique whereby water is sprayed onto an inflatable [7-9], is sketched.

The aim of the paper, thus, is to give a brief review of information available on this abundant and potentially important material thereby, hopefully, fostering further research and bringing about its acceptance as a common structural material with an accompanying substantial increase in its use. Is this a 'challenge' for structural engineers during the last decade of this millennium and the first years of the 21st century?

2. A UNIFIED CONSTITUTIVE MODEL FOR ICE

From a structural viewpoint ice exhibits the full range of features characteristic of structural materials, the most important of which are elasticity, viscosity and brittleness. Experiments indicate that the effects of viscosity manifest themselves in strain hardening during the primary creep stage, strain softening at advanced stages of deformation and partial recovery after unloading. A well-known property of ice is its brittleness in tension leading to stress-anisotropy at advanced stages of deformation. The constitutive model sketched here simulates all of these significant features of ice behaviour. It is of the hereditary type and is chosen with two primary objectives in mind: 1. The number of material parameters contained in the model must be 'reasonable' and 'determinable' from experimental data; 2. A resulting theory using this constitutive model must be 'tractable' and 'calculable' by means of some reasonable effort.

In view of these objectives each of the material parameters used in our constitutive law should have specific physical meaning. The stress-anisotropy/brittleness feature is handled by introducing a damage function which is assumed to be tension stress dependent and is intended to simulate internal microcracking. The Volterra-type integrals are treated approximately by means of a nonlinear Kelvin body with some imposed similarity conditions [6].

On the basis of experimental data from tests on 'laboratory' ice, the following general characteristics are assumed in modelling ice behaviour: 1. A linear

instantaneous response, typical of the behaviour of linearly elastic isotropic materials. 2. Material isotropy, extending and being acceptable for some range into the viscous deformation, including the primary and secondary creep stages. 3. Isotropy terminating with the appearance of microcracking at some advanced stage of deformation, a stage which can be related to the start of the accelerating/third phase of creep. 4. The accelerating creep stage for compression may be rather long while for tension this stage may disappear almost completely, leading to very rapid fracture. All of these features are indicated schematically on Figure 1 for uniaxial tests in tension and compression.

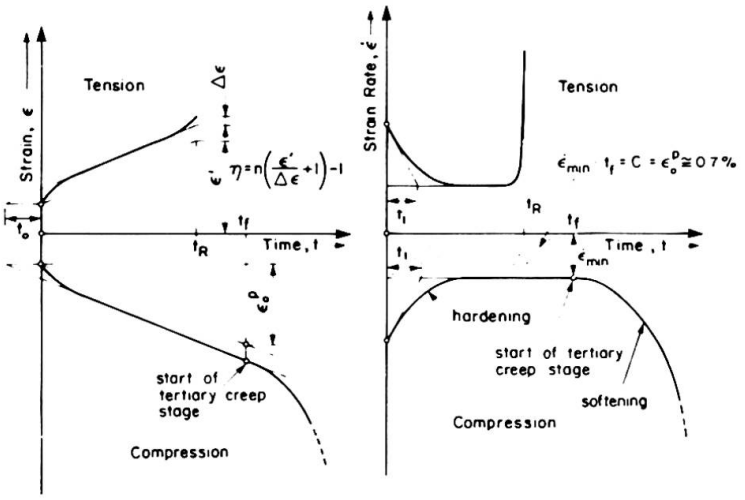

Fig 1 Some Characteristic Features for Tension and Compression Creep Test Curves of Ice

2.1 The Constitutive Model

Starting from a general uniaxial strain/stress relation for time-dependent materials, a three-dimensional nonlinear constitutive law, simulating the above-listed characteristic features of ice, was derived in [6], expressing the strain rate, $\dot{\varepsilon}_{ij}$ in the form

$$\dot{\varepsilon}_{ij}(t) = \dot{\varepsilon}^{e}_{ij} + \dot{\varepsilon}^{r}_{ij} + \dot{\varepsilon}^{p}_{ij} \qquad (1)$$

where the elastic, reversible and permanent viscous strain rate portions $\dot{\varepsilon}^{e}_{ij}$, $\dot{\varepsilon}^{r}_{ij}$, $\dot{\varepsilon}^{p}_{ij}$ are given, respectively, by

$$\dot{\varepsilon}^{e}_{ij} = \frac{1}{E_o}\left[(1+\mu)\dot{\sigma}_{ij} - \mu\dot{\sigma}_{kk}\delta_{ij}\right]; \quad \dot{\varepsilon}^{p}_{ij} = \frac{1}{\nu_2}\left[\frac{\tilde{\sigma}_{ij}(t)}{1-\omega(t)}\right]^{n} \cdot \left\{1+\alpha\left[\frac{\varepsilon^{p}_{ef}(t)}{\varepsilon^{p}_{o}} - 1\right]^{a}\right\} \qquad (2a,b)$$

$$\dot{\varepsilon}^{r}_{ij} = \frac{1}{\nu_1}\frac{d}{dt}\int_{o}^{t}\left[\tilde{\sigma}_{ij}(\tau)\right]^{n}.j(t-\tau)d\tau; \quad \frac{dj}{dt} < 0; \quad j(0) = 1; \quad j(t)\Big|_{t\to\infty}^{\to 0} \qquad (2c)$$

and where E_o and μ are Young's modulus and Poisson's ratio, respectively, n, ν_1, ν_2 and the function j(t) are used in describing the first two stages of creep, with the latter (function) being (approximately) characterized by the stress-independent parameters t_o and t_1 (see Fig. 1) while α, a and ε^{p}_{o} are material constants chosen to help define the tertiary compressive creep phase. The 'effective' viscous stress, $\tilde{\sigma}_{ij}$, is given in terms of the stress deviator, s_{ij} and its second invariant S, by

$$\tilde{\sigma}_{ij} = s_{ij}\left\{\frac{3}{2}\left|\frac{S}{s_{ij}}\right|^{n-1}\right\}^{1/n}; \quad s_{ij} = \sigma_{ij} - \frac{1}{3}\sigma_{kk}\delta_{ij}; \quad S^2 = \frac{3}{2}s_{ij}s_{ij} \qquad (4ab,c)$$

where δ_{ij} denotes the Kronecker delta and where $\varepsilon^{p}_{ef}(t) = \left[\frac{2}{3}\varepsilon^{p}_{ij}\,\varepsilon^{p}_{ij}\right]^{\frac{1}{2}}$.

The damage function, $\omega(t)$, is assumed to be tensile stress dependent so that the damage rate, $\dot{\omega}(t)$, assumed to be a function of the 'true' stress and the current damage, can be written in the form [6]

$$\dot{\omega}(t) = K\left|\frac{\sigma_{max}}{1-\omega}\right|^{\Gamma} \cdot \frac{1}{(1-\omega)^{\eta-\Gamma}} \qquad (5)$$

where K, Γ and η are three material parameters required in defining the tensile tertiary creep stage and where σ_{max} denotes the largest tensile stress and is assumed to be zero for compression. From Fig. 1 we note that η represents the ductility of ice at/near brittle failure. For $\sigma_{max} = \sigma_o = \text{const}$, one can integrate Equ. (5) to obtain an expression involving the rupture time, t_R, (for

which $\omega = 1$) in the form $(1+\eta)Kt_R\sigma_o^{\Gamma} = 1$, which allows determination of K and Γ from a log-log plot of t_R vs σ_{max}.

Note that this constitutive law was derived by assuming, 1) the viscous nonlinearity of the material in the form of a power law (Norton's law), defined by n; 2. microcracking/anisotropy affects only the permanent and not the reversible viscous strain rate. Note also that $\dot{\varepsilon}^e_{ij}$ and $\dot{\varepsilon}^p_{ij}$ are functions of the current stress rate, $\dot{\sigma}_{ij}$, and the current stress, σ_{ij}, respectively, while $\dot{\varepsilon}^r_{ij}$ is a function of the entire stress history. Equ. (1) can be obtained, formally, by postulating the existence of a scalar functional, $P(\sigma_{ij})$, with the physical meaning of a complementary power potential [6].

Reducing our constitutive law, Equ. (1), to the uniaxial case and using numerical values for the thirteen material parameters, as given in [6], we simulated the behaviour of ice under constant stress (creep), under constant strain rates and under loading/unloading conditions and compared our predictions with experimental data, as shown on Fig. 2. As one can see, this constitutive model

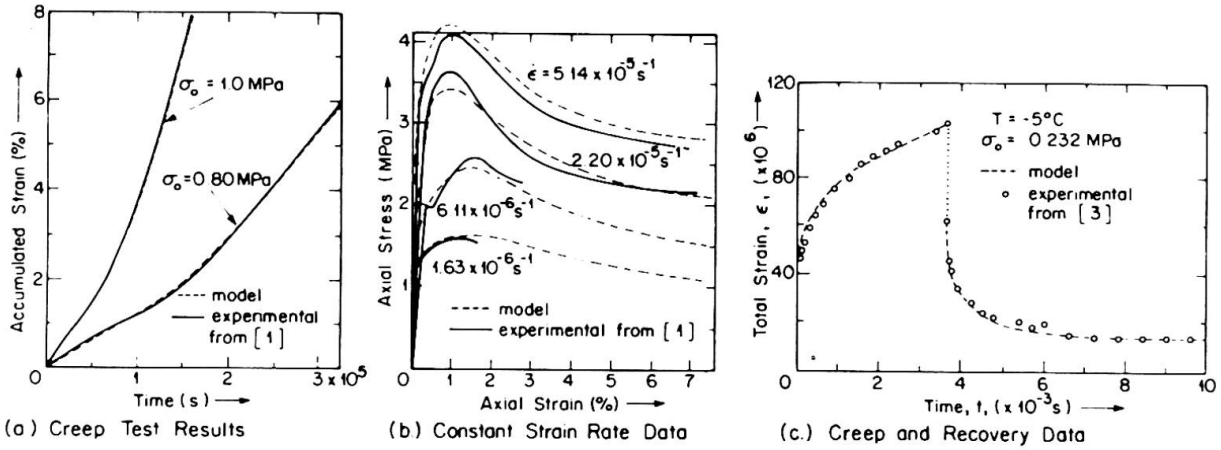

Fig. 2 Comparison of Model Predictions with Experimental Data for Ice

simulates the characteristic behavioural features of ice, including creep at advanced stages of deformation, strain softening and recovery upon unloading, quite well. The model can also be used in formulating a von Kármán-type nonlinearly viscous plate theory which was used to predict the time-deflection-strain-stress behaviour of a long ice plate undergoing cylindrical bending and subjected to uniform compressive stresses applied along its longitudinal edges [6] (see Fig. 3).

3. REINFORCED ICE AND A POSSIBLE USE

If ice is to become a widely used structural material its tensile and flexural strength, like that of concrete, will have to be enhanced by suitable/economical reinforcement. Unfortunately, there is no commonly known/adopted reinforcing material for ice at the present time. When we first thought of reinforcing ice [7-9] various materials, including wire and nylon string were considered. In the end, we decided to use spun fibreglass yarn (#ECG 150-4/8) with an average diameter of 0.87 mm and a specified average breaking strength of 570 N. This material was used in all reinforced ice samples and in the construction of reinforced ice domes. Results from tensile tests on 3 pieces of spun fibreglass yarn are shown in Fig. 4a. The load-strain curve is initially very flat but becomes linear at higher loads with a modulus of elasticity (approximately) of 42 GPa when the nominal diameter of the yarn is used in calculating stress.

The yarn was used to reinforce tensile test specimen formed in a specially fabricated mold. The test series included 15 specimens with different amounts

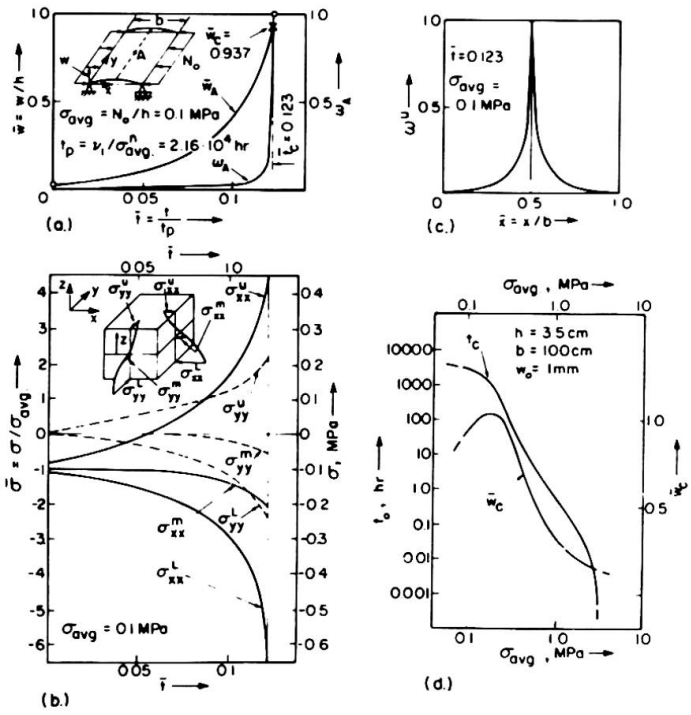

Fig. 3 Some Numerical Results for Ice Plate

of yarn. As one can see (Fig. 4b), for plain ice the 'initial cracking stress' was also the ultimate stress, while for the reinforced specimen, the reinforcement inhibited initiation/propagation of cracking, as a result of which the initial tensile cracking stress was increased by approximately 25% as compared to that for the unreinforced specimen.

A possible area of application of reinforced ice is in the construction of temporary and semi-permanent enclosures for shelters, storage areas, repair and workshops along pipeline right-of-ways, and/or enclosures at mining and exploration sites. Reinforced ice domes may even be suitable for covering/enclosing recreational areas in northern communities. Since cold regions are often rather inaccessible, a construction/erection procedure was suggested [7-9] whereby water is sprayed onto an inflatable, below

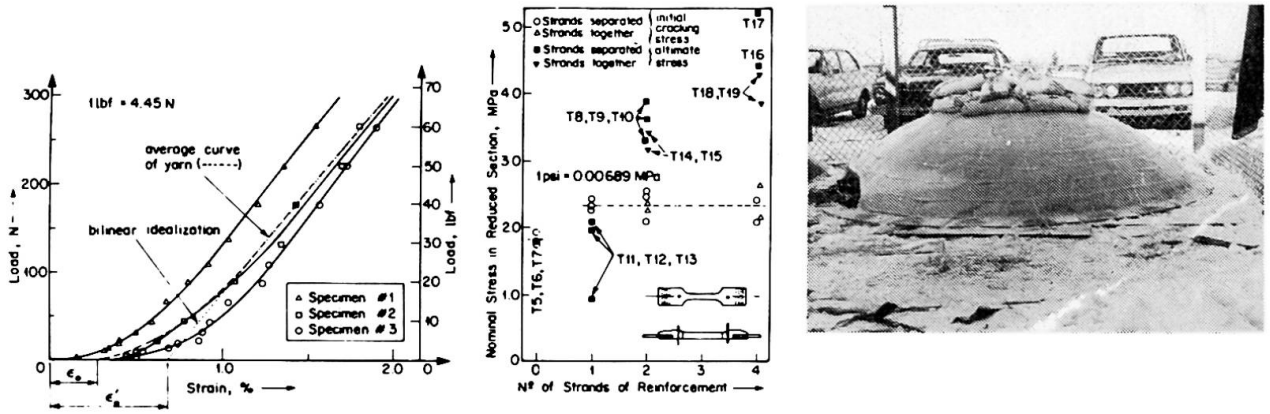

(a) Load Strain Curves for Three Specimen of Spun Fiber-Glass Yarn [9]

(b.) Some Tensile Test Results [9]

(c.) Ice Dome Nº2

Fig. 4 Some Test Data on Reinforced Ice and the Ice Dome

freezing temperature, to form a reinforced ice dome. A number of model ice domes were constructed at The University of Calgary using this erection technique [9]. A network of spun fibreglass yarn was used as reinforcement to inhibit thermal cracking.

Dome #2 is shown in Fig. 4c partially loaded. The useful life-span of such domes, naturally, depends not only on the state of stress in the structure, but also on any imperfections present and on the environmental conditions, particularly the temperature.

4. CONCLUSIONS

From our analytical and experimental studies to date, it is apparent that reinforced ice can become a useful structural material for cold regions. Spun fibreglass yarn may have potentials as reinforcement for ice. Further tests are required to determine the properties of the composite and the effectiveness of the reinforcement which may be enhanced by pretensioning.

Tests on small-scale reinforced ice domes indicate that spraying water onto an inflatable may be a practical and economical erection technique for such structures.

Before ice is accepted as a common structural material, more tests and analytical investigations will have to be carried out in order to gain a better understanding of its behaviour, particularly its response to multi-axial stress and to temperature variations.

REFERENCES

1. Mellor, M., Cole, David M., "Stress/Strain/Time Relations for Ice Under Uniaxial Compression", Cold Regions Sci. and Technol., 6, 1983, pp. 207-230.

2. Jacka, T.H., "The Time and Strain Required for Development of Minimum Strain Rates in Ice", Cold Regions Sci. and Technol., 8, 1984, pp. 261-268.

3. Ting, S.K., Sunder, S.S., "Constitutive Modelling of Sea Ice with Applications to Indentation Problems", M.I.T., CSEOE Report No. 3, Oct. 1985.

4. Szyszkowski, W., Dost, S. and Glockner, P.G., "A Nonlinear Constitutive Model for Ice", Int. J. Solids Structures, 21, No. 3, 1985, pp. 307-321.

5. Szyszkowski, W. and Glockner, P.G., "Modelling the Time-Dependent Behaviour of Ice", Cold Regions Science and Technology, 11, 1985, pp. 3-21.

6. Szyszkowski, W. and Glockner, P.G., "On a Multiaxial Constitutive Law for Ice", Mechanics of Materials, 5, 1986, pp. 49-71.

7. Glockner, P.G., "Reinforced Ice Domes: Igloos of the 21st Century?", Proc. on "HOUSING: The Impact of Economy and Technology", Pergamon Press, 1981, pp. 887-908.

8. Stanley, R.G. and GLockner, P.G., "The Use of Reinforced Ice in Constructing Temporary Enclosures", Marine Science Communications, 1, No. 6, 1975, pp. 447-462.

9. Stanley, R.G., "An Experimental Investigation of Reinforced Ice Domes", M.Sc. Thesis, Dept. of Civil Engineering, The University of Calgary, Nov. 1975.

10. Stanley, R.G. and Glockner, P.G., "Some Properties of Reinforced Ice", Proc. Conf. on Materials Engineering in the Arctic, M.B. Ives (ed.), ASM, Metals Park, Ohio, 1977, pp. 29-35.

11. Szyszkowski, W. and Glockner, P.G., "Modelling the Mechanical Properties of Ice", Proc. Sixth Int. Offshore Mechanics and Arctic Eng. Symp., 4, V.J. Lunardini et al (eds.), American Society of Mechanical Engineers, 1987, pp. 159-165.

ACKNOWLEDGEMENTS

The results presented here were obtained in the course of research sponsored by the Natural Sciences and Engineering Research Council of Canada, Grant No. A-2736.

Structural Sandwich Panels at Low Temperature

Panneaux sandwich à basse température

Sandwichtragelemente bei tiefen Temperaturen

Paavo HASSINEN
Senior Research Scientist
Techn. Res. Centre of Finland,
Espoo, Finland

Paavo Hassinen, born 1952 received his civil engineering degree at the Helsinki University of Technology in 1976. He is currently engaged in research on steel structures and bridges.

Antti HELENIUS
Research Scientist
Techn. Res. Centre of Finland,
Espoo, Finland

Antti Helenius, born 1954 received his civil engineering degree at the Helsinki University of Technology in 1980 and he is currently studying the behaviour of light weight structures.

Jouni HIETA
Research Scientist
Techn. Res. Centre of Finland,
Espoo, Finland

Jouni Hieta, born 1951 graduated from Oulu University in 1978. He is currently doing research on sandwich structures and core materials.

Anders WESTERLUND
M.Sc. (Tech)
Helsinki Univ. of Technology,
Espoo, Finland

Anders Westerlund, born 1962 graduated from the Helsinki University of Technology in 1987. For his Master's thesis he studied the behaviour of viscoelastic sandwich structures.

SUMMARY

Sandwich panels with thin sheet metal faces and a plastic foam core often experience between the faces high temperature gradients which cause deflections and stresses. The mechanical properties of some plastic foams and the design principles for thermal stresses are reviewed in this paper. The magnitude of the stresses due to temperature gradients is presented by examples that are calculated according to the traditional theory of elasticity and also considering the creep of the core.

RÉSUMÉ

Il existe souvent un risque de variation de température entre les surfaces des panneaux sandwichs composés de couches minces ou profilées métalliques avec des noyaux en mousse plastique. Cela cause des déformations et des contraintes dans les panneaux. Cet article analyse des qualités de rigidité de certaines mousses plastiques et explique des principes de calcul pour les contraintes de température. L'intensité des contraintes causées par la variation de température est illustré par des exemples de calcul effectués sur la base de la théorie d'élasticité traditionnelle, en tenant compte de l'effet du fluage du noyau en mousse plastique.

ZUSAMMENFASSUNG

Zwischen den Schichten von Sandwichtragelementen mit Deckschichten aus Stahlfeinblech und Kernschichten aus Schaumstoff entstehen oft hohe Tempreraturdifferenzen, die Verformungen und Spannungen verursachen. In diesem Beitrag werden die mechanischen Eigenschaften von einigen Schaumstoffen und die Berechnungsprinzipien von Tempreraturspannungen vorgestellt. Die Grösse der durch die Temperaturdifferenz verursachten Beanspruchungen wird durch Berechnungsbeispiele veranschaulicht, die nach der traditionellen Elastizitätstheorie gerechnet werden, in denen aber auch das Kriechen der Kernschicht berücksichtigt wird.

1. INTRODUCTION

High and rapid temperature differences occur in sandwich panels with thin metal faces and a plastic foam core because of the good insulative core layer. The differences produce large curvatures to the cross section, and furthermore, deflections and in most cases also stresses to the panel. The stresses depend on the shear stiffness of the core layer, which is usually considered to be a structurally elastic part of the cross section. Most structural foams creep under a long term load and the creeping reduces the shear stiffness of the core and also the thermal stresses of the panel. The creeping of the core can be taken into account by reducing the shear modulus by the well known creep factor. In this case the elastic theory can be still used in the calculations. Influence of the creeping can also be examined more comprehensively by using viscoelastic constitutive laws for the core layer.

Generally the creep rate of structural foams increases with the temperature. In temperatures lower than the room temperature the mechanical properties of the foams are also different. Therefore, it is important in structural desing to evaluate the thermal stresses as accurately as possible and to compare them with the relevant strength values at low temperatures, where the load bearing capacity as well the insulative properties of the panels are actually needed.

To increase the knowledge of the mechanical properties loading tests were carried out with some potential core materials at temperatures +20, -40 and -60 ^{o}C in the Laboratory of Structural Engineering at Technical Research Centre of Finland (VTT). The long term behaviour of sandwich beams with different core materials were studied at room temperature with the facilities of some Finnish companies. To analyse sandwich panels a special purpose program was written, which is based on finite element method and experimental creep functions.

2. MECHANICAL PROPERTIES OF SOME PLASTIC FOAMS

In the experiments there were only a limited number, 3 - 4 pieces, of specimens from each structural foam in each test and at each temperature. The results show that excluding the XPS foam the compressive strengths and moduli slightly increase with the decrease of temperature (Fig. 1). They maintain the shape of their original σ-ε curve, which means that the foams have also high ultimate compressive strain without a tendency to brittleness.

Depending on the material the shear strength increases or decreases slightly at low temperatures, but the strength level remains about the level at +20 ^{o}C. The shear moduli follow the compressive moduli with the temperature. An important property in sandwich panels is also the tensile strength in the flatwise direction of the panel. In the tests this stength was close to its original level at +20 ^{o}C. But by the increase of the tensile moduli the foams became more brittle against the tensile forces.

The long term behaviour of sandwich beams with different core materials were studied only at room temperature. The nonlinearity in the long term creep function was examined by changing the shear stress level in the core (Fig. 2). All the stress levels were above the long term design stress level in usual structures, where the highest stress at the serviceability limit state is about 40 % of the characteristic short term strength. The test results of EPS foam show clearly nonlinearity above the stress level 0.4-times the characteristic short term strength. The design stresses have to be kept in the stable area below this stress limit. All the creep functions of the PIR foams have about the same shape, only their level is increasing slightly with the shear stress. The latter

result follows from the low shear strength of the joint between polyisocyanurate foam and steel face, for which reason the shear strength of the foam itself could not be totally utilized.

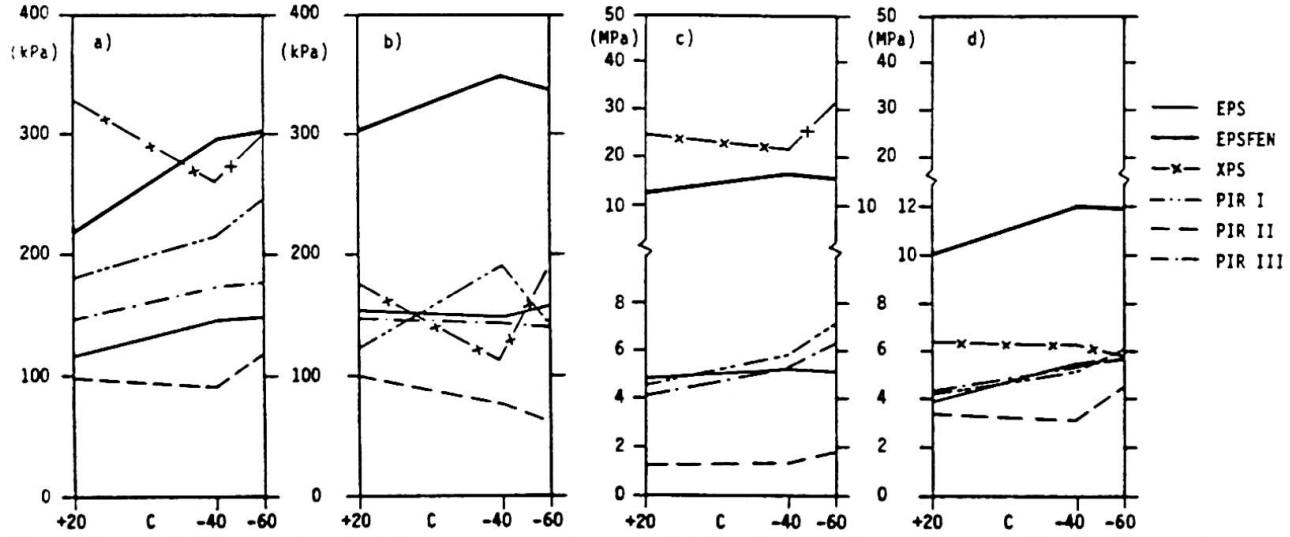

Fig. 1. a) Characteristic compressive and b) shear strengths and c) characteristic compressive and d) shear moduli of polystyrene, EPS ($\bar{\rho}$ = 19.5 kg/m^3), phenol filled polystyrene, EPSFEN ($\bar{\rho}$ = 40.8 kg/m^3), extruded polystyrene, XPS ($\bar{\rho}$ = 32 kg/m^3), polyisocyanurate, PIR I ($\bar{\rho}$ = 42.5 kg/m^3, batch mould), PIR II ($\bar{\rho}$ = 40.6 kg/m^3, continuous laminator), PIR III ($\bar{\rho}$ = 38.2 kg/m^3, continuous laminator).

The creep curves in literature show that the creeping becomes slower at low temperatures /1/. The following creep function, determined at room remperature, is suitable to describe the creep of commonly used core materials

$$J(t) = \frac{1}{G} + J_1 \, t^n \qquad (1)$$

where G denotes the short term shear modulus and J_1 and n are parameters. t is the time.

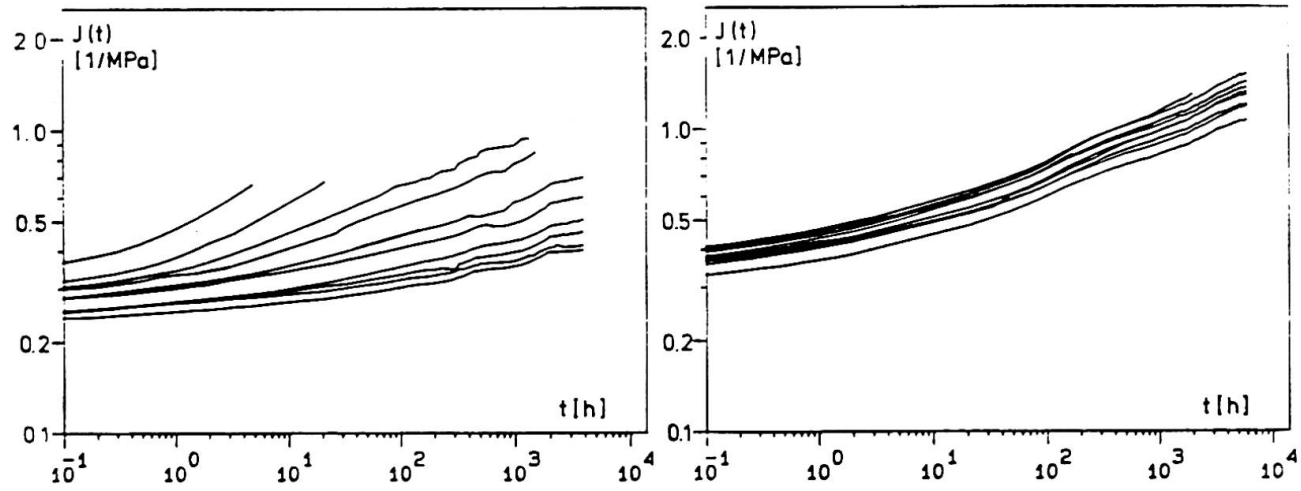

Fig. 2. Shear creep functions of a) an expanded polystyrene (τ_{ko} = 145 kPa) and b) a polyisocyanurate (τ_{ko} = 70 kPa) foam determined in beam tests. The foams are the same as EPS and PIR II in Fig. 1. The stress level of the functions is 0.4, 0.5, 0.6, 0.7 or 0.8 τ_{ko}. τ_{ko} represents the characteristic short term shear strength at temperature +20 °C. In the figures curves of two specimens have been drawn at each stress level.

3. THERMAL STRESSES IN SANDWICH PANELS

3.1 Analysis of sandwich panels

The finite element solution of sandwich beams with thick or profiled face layers is based on the following homogenous differential equations.

$$w^{(6)} - (\frac{\lambda}{L})^2 w^{(4)} = 0$$
$$\gamma^{(4)} - (\frac{\lambda}{L})^2 \gamma^{(2)} = 0 \qquad (2)$$

where w is the deflection, γ the shear strain in core, primes denote differentation with respect to x that is directed along the axis of the panel. L is the length of the panel. The thick-wallness parameter λ is given by

$$\lambda^2 = \frac{BSL^2}{B_S B_D} \qquad (3)$$

where B_D and B_S are the bending stiffnesses of the faces alone and due to the sandwich action. B is the total stiffness of the cross-section, $B = B_D + B_S$. S is the shear stiffness of core S = GA, where A is the effective shear area and G the shear modulus.

Using the solutions of the equations (2) and the linear elastic relation between the strains and stresses and further the equation of equilibrium M' = Q equation (4) can be written for a finite element.

$$\{F\} = [K]\{d\} \qquad (4)$$

The equations (2) are also valid in the case of a viscoelastic core provided that the shear modulus G is replaced with timedependent "secant modulus" G_S, that is the ratio of the shear stress and the shear strain γ. In the finite element formulation G_S is assumed to be constant in an element.

In the viscoelastic case the displacements are obtained by time integration. Assuming the state at time t_1 known and the load constant in the interval from t_1 to t_2 the displacement at t_2 can be iterated from the equation

$$[K]_1\{d\}_2^{n+1} = \{F\} - ([K]_2^n - [K]_1)\{d\}_2^n \qquad (5)$$

where $\{F\}$ is the loadvector and the subscripts 1 and 2 refer to times t_1 and t_2 and the superscripts denote the iteration cycles.

Practically the same results as by the viscoelastic finite element method can be found in linear viscoelastic cases by replacing the shear modulus by a time dependent shear modulus G(t) = 1/J(t) in the elastic analysis. However, the calculations of structures caused by variable loads are very laborious. The viscoelastic finite element analysis is the only possibility, if the second order effects caused by the axial loads or the stress dependent creep functions are to be included in the analysis.

3.2 Examples

In the first example a thin faced two span sandwich panel is exposed to a temperature gradient of 80 ^{o}C. In the first loading case the temperature difference

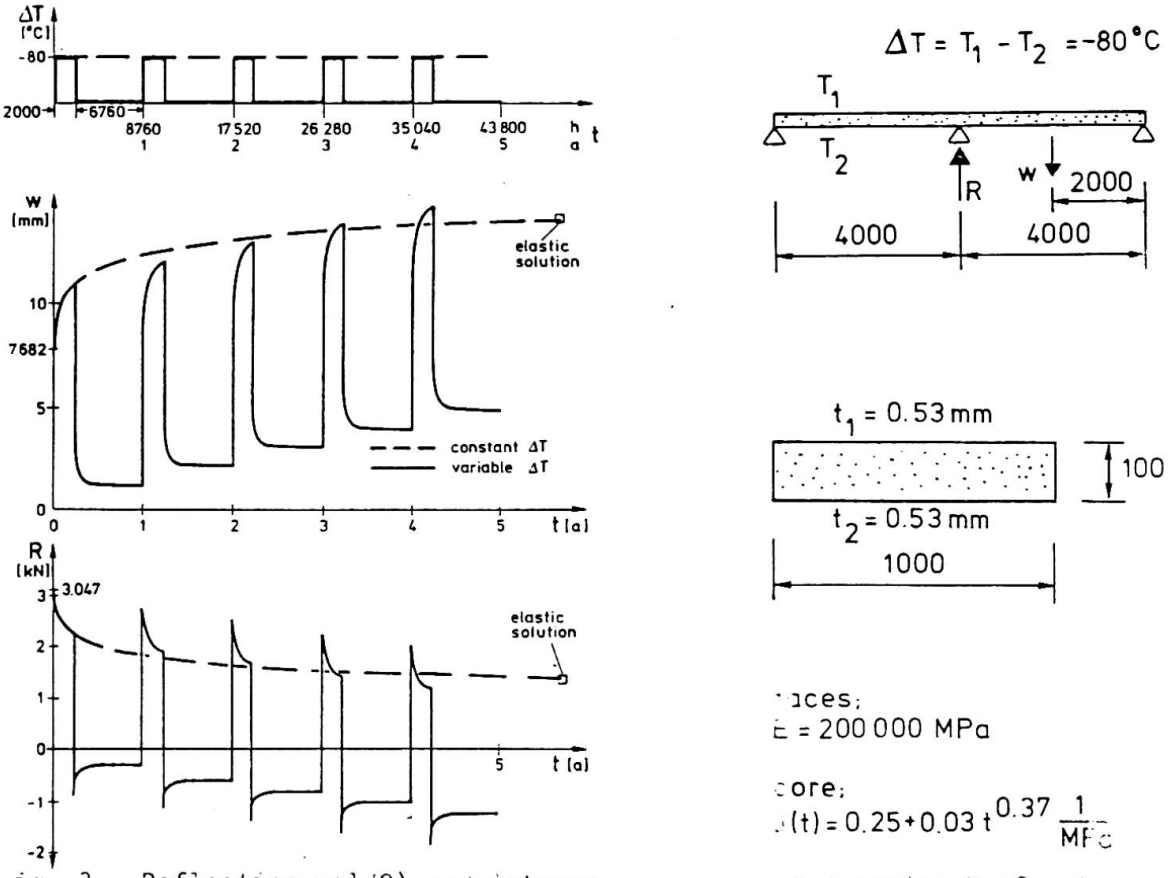

Fig. 3. Deflection w(1/2) and intermediate support reaction R of a sandwich beam caused by a constant temperature difference of -80 °C between the faces.

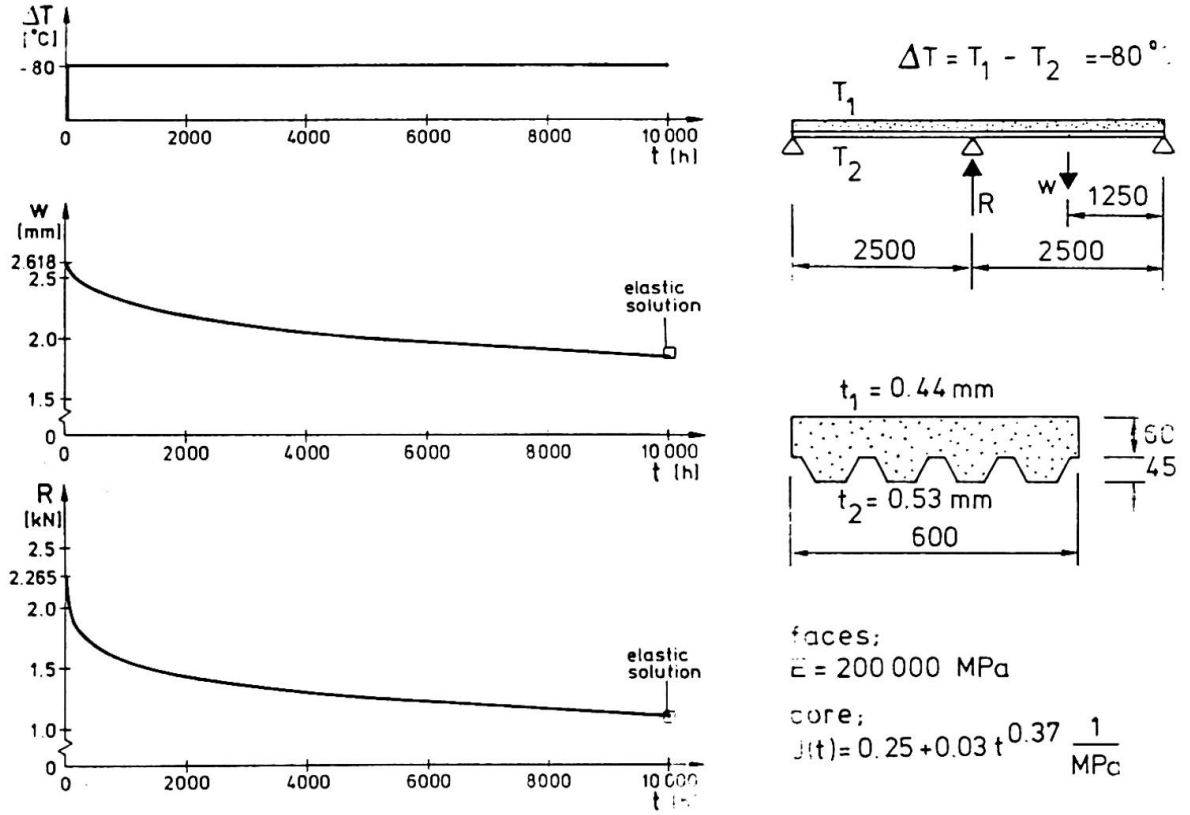

Fig. 4. Deflection w(1/2) and intermediate support reaction R of a profiled faced sandwich beam caused by a constant temperature difference of -80 °C.

is constant over five years and in the second one the thermal load acts 2000 hours in a year (Fig. 3). To the viscoelastic core layer the creep function (1) is used where the shear modulus G and the parameters J_1 and n have the values 4.0 MPa, 0.03 1/MPa and 0.37.

Under a constant temperature gradient the deflections increase and the stresses e.g. support reactions decrease monotonously being delayed. Under the variable thermal load deflections increase faster than in the case of constant load. The stresses get considerable negative values in the unloading phase.

The lower face in the sandwich panel of the second example is profiled. This two span beam is exposed only to a constant temperature difference of -80 ^{o}C. Both the deflections and the stresses of thick faced sandwich beam decrease due to the creep of the core because of the bending stiff face. So the change of the deflections is contrary to those of the thin faced sandwich beam in the first example. The theory of elasticity with reduced shear modulus G(t) = 1/J(t) gives the same results.

4. CONCLUSIONS

The thermal stresses are a significant loading case in the design of sandwich panels. The core material has to be capable to carry the shear stresses and to support the faces against the buckling stresses caused by the own weight, snow and wind loads and further by the temperature difference between the faces over the whole existing temperature. The experiments show, that the most commonly used core materials preserve their mechanical properties up to a temperature of -60 ^{o}C. Nevertheless, the change of strength and modulus values depends on the initial structure of the foam. By many foams a low density indicates also poor strength that is emphasized at low temperatures.

The creep of a viscoelastic core layer diminishes effectively thermal stresses and this is profitable in the design of sandwich structures. However, at low temperatures the creeping proceeds somewhat slower than at room temperature and considerably slower than at high temperatures. Thus the influence of temperature to the reduction of thermal stresses has to be taken into account in foam cored sandwich panels.

5. ACKNOWLEDGEMENTS

The work was financially supported by Technology Development Centre. The companies EKEPANELS, HUURRE OY, ISORA OY, MAKROTALO OY and NESTE OY supplied the material for tests. This support is gratefully acknowledged.

6. REFERENCES

1. Jungbluth, O., Verbund- und Sandwichtragwerke. Springer-Verlag, Berlin 1986.

2. Davies, J.M., Texier, F., Thermal stresses in structural sandwich panels. Proc. Int. Conf. Steel and Aluminium Structures, July 1987.

3. Holmijoki, O., Shear creep of rigid polyurethane foam. Rakenteiden Mekaniikka 17(1984) No. 4 p. 32 - 53. (In Finnish).

Sealants – their Use, Properties and Endurance

Joints d'étanchéité – applications, propriétés et résistance

Dichtungen – Anwendungen, Eigenschaften, Festigkeit

Liisa RAUTIAINEN
Senior Recearch Scientist
Techn. Res. Centre of Finland,
Espoo, Finland

Liisa Rautiainen, born 1950, received her civil engineering degree (M.Sc.) at the Technical University of Helsinki. For 9 years she was involved in durability problems of building materials. Now Liisa Rautiainen is responsible for material studies in the field of building physics.

SUMMARY
The paper discusses briefly the methods for testing the material properties of sealants used in facade joints, a discussion of existing instructions for use, experiences of seals like found lacks and failures and presents the results of 18 years field experiments in Finland.

RÉSUMÉ
L'article traite des méthodes d'essais de joints d'étanchéité utilisés dans les façades. Il passe en revue les directives actuelles pour leurs applications, les expériences réalisées, les faiblesses et les dommages rencontrés et présente les résultats de dix-huit ans d'essais en Finlande.

ZUSAMMENFASSUNG
Dieser Beitrag diskutiert die Prüfmethoden für Dichtungen in Gebäudefassaden, die Gebrauchsanleitungen, die Erfahrungen und Schadenfälle. Die Ergebnisse von Aussenversuchen während 18 Jahren in Finnland werden beschrieben.

1. INTRODUCTION

The strengthening of joints in facade elements has been widely performed with sealants.

In facade joints sealants have to withstand the cyclic stresses due to movements of elements and degradating effects of weathering factors, especially sun radiation and moisture effects, without failure, for several years preferably as long as the facade surfaces.

In practice it has been found that failures with sealants in joints can occur after a relatively short period, 1...5 years after the sealing work.

Because of failures several questions and claims have been made regarding the serviceability of sealant materials in element joints in Nordic climates.

In order to give some references to questions and claims concerning durability of sealants some background information is given, results of field and laboratory experiments and failure examinations collected since the 1970.

2. PERFORMANCE AND MATERIAL REQUIREMENTS OF SEALANTS

The methods generally used for testing the properties of sealants in Nordic Countries are Nordtest Build test methods from 1976 [1]. At present the revision work is going on. According Finnish standards [2] the sealants, their shapes and dimensional requirements must be confirmed (tables 1, 2 and 3, figure 1). It should be noticed that the elongation properties required in each sealant group (table 2) mean elongation or adhesion loss in 100 mm long joint, sealed between concrete/aluminium supports, after heat ageing of 56 days at +70 °C and storage in cold water (+2 °C). The selection of the most suitable sealant dimensions in each case shall be performed according to the evaluated movements of the constructions to be sealed, (e.g. concrete elements), by using the equation 1.

$$d_{min}[mm] = \frac{d\ [mm]}{P\ [\%]} \cdot 100\ [\%] \qquad [1]$$

d_{min} is minimum width of the joint

d is the total movement of the joint width (thermal and moisture movements and drying shrinkage etc.)

P is the maximum allowable movement of the sealants (see table 1)

Table 1. Classification, information on usage and important properties of sealants.

Sealant group	Group 1 Elastic sealants	Group 2 Elastoplastic sealants	Group 3 Film forming, plastic and oil based sealants
Examples of typical binders	polysufides polyurethanes silicones	butyl rubbers polyacrylates	oils (drying nondrying) artificial resins blendproducts
Dimensions of seals: maximum width minimum width	30 mm 6 mm	25 mm 8 mm	25 mm 10 mm
The greatest allowed movement (elongation/compression) of the joint width, P	25 %	15 %	10 %
Typical use arces	Facade sealants	Joints with small movements and protected against weather	

Table 2. Some requirements presented for sealant materials.

Property	Testing method	Sealant group 1	2	3
Elongation with max force, N	NT BUILD 004	≥100 %	≥20 %	≥15 %
Resistance to bases	NT BUILD 011	≥100 %	≥20 %	≥15 %
Shrinkage				
- free	NT BUILD 015	< 20 %	≤20	≤12 %
- restrained	NT BUILD 016	no cracks allowed		
Staining	NT BUILD 014	≤1 mm		
Radiation resistance	NT BUILD 020	no changes in a appearance		

d	Smin
6...12	4... 7
13...20	5... 8
21...30	6... 9

d	Smin
8...12	6...10
13...20	9...12
21...25	11...14

d	Smin
10...12	8...10
13...20	9...12
21...25	11...14

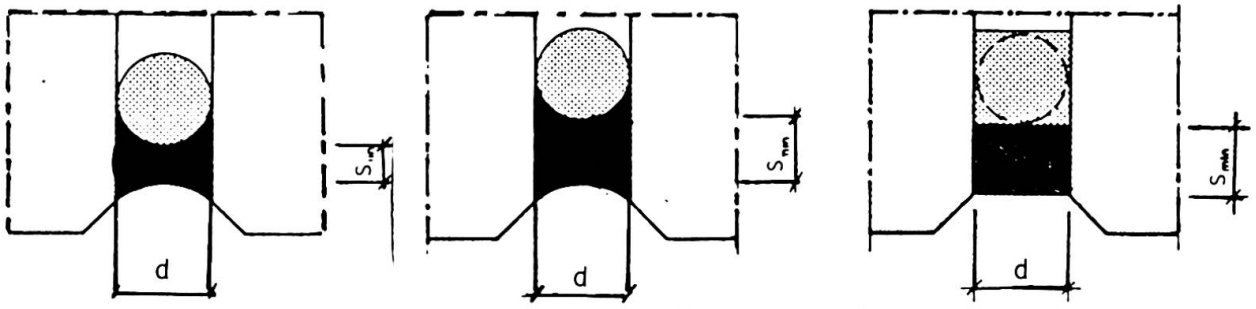

Group 1 sealants Group 2 sealants Group 3 sealants

Figure 1. The shapes of seals made of sealants classified according to groups 1...3.

Table 3. Dimensions of sealants according to sealant group.

Group 1 sealants		Group 2 sealants		Group 3 sealants	
Width, mm d	Thickness, mm S min	Width, mm d	Thickness, mm S min	Width, mm d	Thickness, mm S min
6...12	4...7	8...12	6...10	10...12	8...10
13...20	5...8	13...20	9...12	13...20	9...12
21...30	6...9	21...25	11...14	21...25	11...14

3. FIELD AND LABORATORY EXPERIMENTS

In 1969 field test of eight different sealants were begun (table 4). The test facade, located in Helsinki, (two storeys) consisted of 15 concrete elements, (2400 x 2750 mm), and was directed towards the south, without any protection from sunshine and rain.

Each of the sealants was inserted both into horizontal and vertical joints. The sealing works were performed according to the instructions of the manufacturers of the sealants. Round cellular PE-strips were installed under each sealant.

Table 4. The sealants and joint widths in the field test.

Sealant type	width of vertical joints, mm	width of horizontal joints, mm
1. polysulfide	17	12
2. polyacrylate	16	12
3. polysulfide	20	12
4. polyurethane	18	12
5. oil based product	14	15
6. polysulfide	14	15
7. polysulfide	20	25
8. polysulfide	23	25

The condition of sealants was observed visually up to spring 1987 (18 years) and by hardness measurements up to 1983 (13 years) (table 5). The same sealants, except one polysulfide, were examined in the laboratory. The measured elongation properties are given in table 6.

Table 5. Influences of natural exposure on joints sealed with sealants.

Type of the sealant	Changes in hardness (shore A)		Condition	
	orginal	after 13 years	after 13 years	after 18 years
1. polysulfide	30	45	ADEQUATE [3]	ADEQUATE
2. polyacrylate	30	65...70	vertical joint ADEQUATE horizontal joint GOOD	vertical joint BAD horizontal joint GOOD
3. polysulfide	35...40	45...50	ADEQUATE [2]	BAD
4. polyurethane	45...50	50...65	ADEQUATE	vertical joint ADEQUATE horizontal joint BAD
5. oil based product	40...70	>95	ADEQUATE	BAD
6. polysulfide	30	40	GOOD	vertical joint GOOD horizontal joint BAD [1]
7. polysulfide	40...45	40...45	GOOD	GOOD
8. polysulfide	25...30	15...20	BAD	

1) Level difference of about 15 mm between elements
2) Thickness of the sealant only 1 mm
3) Holes are located in the middle of bubbles

Table 6. Elongation properties of sealants (between Al-concrete substrates)

Sealant type	Elongation at max load after 56 days at +70 °C	
	test temperature +23 °C	test temperature -20 °C
1. polysulfide	200	170
2. polyacrylate blend	~30 (plastic)	<1
3. polysulfide	45	55
4. polyurethane	45	4
5. oil-based sealant	20	2
6. polysulfide	270	200
7. polysulfide	350	550

4. EXPERIENCES ON SEALANT FAILURES

The common failure causes of joints sealed with sealants (due to the) sealants occurring within five years are suumarized in table 7.

Because the sealants used in the example cases were polysulfides the cases should not be generalized to all sealant types. All the cases are under 5 years old.

Table 7. The common failure causes of facade sealants.

Failure type	Cause of the failure
- Cracks in sealant	- Too thin sealant layers (1...2 mm thicknesses)
- Adhesion losses	- Wet joint surfaces during the sealing (salts adhered to sealant)
- Adhesion losses or cohesion brakes in element surfaces	- Too thick sealants compared to width
- Cracks and adhesion losses	- Too small joint and sealant widths compared to element sizes (for example 6 mm joints between 5 m elements)
- Outswelling of the sealants	- Element movements have concentrated and caused narrowing of joints
- Bubbling and perhaps small holes in the bubbles	- In the installation work the surface of the closed cell bottom list has been broken and cellgases have caused bubbling

5. CONCLUSIONS

On the basis of performed field and laboratory experiments and experiences of failure researches the following conclusions can be made:

- The properties of the sealant type influences greatly the durability of the joint. According to the elongation and aging tests (table 6) the best products in the field could also be predicted. An exception was polyacrylate blend sealant which had a better durability in the field than was expected.

- After 18 years exposure there were several sealants which were in good condition without leakage and other failures.
- According to our knowledge, perhaps the most common failure causes are the wrong dimensions of sealants, because of either careless sealing work or careless element installations.

- Taking account of the knowledge gained and also the fact that the sealant materials have been developed during the period 1970.to.1987, it should be quite possible to achieve service lives of 20 years with sealants installed and selected according instructions.

References

1. Register of Nordtest-methods, Nordtest docgen 017, 1986.
2. Joints in external walls, sealing with sealants RT 80-10100 Rakennustietosäätiö, 1980.

Jute Fibre Reinforced Concrete Materials for Building Construction

Beton armé de fibres de jute pour la construction de logements

Mit Jutefasern bewehrter Beton als Baustoff für den Wohnungsbau

M.A. AZIZ
Dr.Eng.
National Univ. of Singapore
Kent Ridge, Singapore

M.A. Aziz obtained his Ph.D. in Civil Engineering from the Univ. of Strathclyde, Glasgow in 1970. He has been actively engaged in teaching, resesarch and consultancy in various disciplines of civil engineering. He is an author of 4 books and 100 over publications.

M.A. MANSUR
Dr.Eng.
National Univ. of Singapore
Kent Ridge, Singapore

M.A. Mansur obtained his Ph.D. in Civil Eng. from the Univ. of New South Wales, Australia in 1979. An author of numerous publications, Dr Mansur is currently a senior lecturer at the Nat. Univ. of Singapore. His research interests include reinforced and prestressed concrete and advanced cementitious composites.

SUMMARY
This paper reports the findings of an experimental investigation conducted on the engineering properties of jute fibre reinforced cement composites. Different lengths of fibres at varying volume fractions were used as reinforcement for cement based matrices to determine the mechanical, thermal and acoustic properties of the composites. The results of this investigation have shown the feasibility of using jute fibres for producing low-cost building materials.

RÉSUMÉ
Cette contribution décrit un projet de recherche sur les caractéristiques d'un béton armé de fibres de jute. L'influence de différentes longueurs des fibres et de différents pourcentages volumétriques sur les caractéristiques mécaniques, thermiques et acoustiques est étudiée. Les résultats ont mis en évidence que le béton armé de fibres de jute peut être utilisé avec succès comme matériau de construction pour de l'habitation bon marché.

ZUSAMMENFASSUNG
Dieser Beitrag beschreibt die Resultate eines Forschungsprojekts über die Eigenschaften von mit Jutefasern bewehrtem Beton. Der Einfluss von verschiedenen Längen der Jutefasern und unterschiedlicher Volumenanteile auf die Zementmatrix wurden untersucht und die mechanischen, thermischen und akustischen Eigenschaften bestimmt. Die Forschungsresultate haben gezeigt, dass der Einsatz von Beton mit Jutefasern als Baustoff für preisgünstige Wohnungen geeignet ist.

1. INTRODUCTION

In developing countries, there has been an acute shortage of cheap but durable building materials for the construction of low-cost housing. The use of jute fibre reinforced cement composites may offer a possible solution in this respect.

Jute is abundantly grown in Bangladesh, China, India, Indonesia and Thailand. It is extracted from a woody type of plant which grows to about 2 m high with a stem diameter ranging from 20 mm to 30 mm. Its bark consists of bundles of fibres running longitudinally down the stem. When harvested, the cut-stems are tied into bundles and kept submerged under water for 20 to 30 days. The tissues of the stems are then decomposed under bacterial action. The resulting soggy mass consisting of strands of overlapping fibres are then stripped off manually, washed in water and dried under the sun.

Jute fibre being cheap, strong and durable, is a prospective reinforcing material for cement-based matrices. Virtually, no studies have been carried out so far to utilize jute fibres for reinforcing concrete materials. This study was initiated to explore the feasibility of utilizing this indigenous fibre for producing fibrous composite in an attempt to solve, to some extent, the acute shortage of low-cost building materials in developing countries.

2. PROPERTIES OF JUTE FIBRES

Typical properties of jute fibres are given in Table 1 [1,2]. The basic requirements of any fibre for producing good quality fibrous concrete are high tensile strength, high elastic modulus, good bond at the fibre-matrix interface, adequate geometric stability, chemical resistance and durability.

Property	Range of values
Fibre length, mm	180 - 800
Fibre diameter, mm	0.10 - 0.20
Specific gravity	1.02 - 1.04
Bulk density, kg/m^3	120 - 140
Ultimate tensile strength, N/mm^2	250 - 350
Modulus of elasticity, kN/mm^2	26 - 32
Elongation at fracture, percent	2 - 3
Water absorption, percent	25 - 40

Table 1 Typical properties of jute fibres

3. PRODUCTION TECHNOLOGY

Uniform dispersion of fibres in a cementitious matrix distributes stresses and improves microcracking. Therefore, the fibres are to be distributed in such a way as to allow them to perform their desired functions and to achieve a composite action between the fibres and the matrix by ensuring adequate interfacial bond. It is well-established [2] that the most exploitable form of fibre-cement composites is to be made by using randomly distributed short discontinous fibres. It is usually possible to incorporate only a small volume of discrete fibres in the matrix, and also economic and other considerations dictate that the use of fibres be optimized. The optimum length and volume fraction of jute fibres are found to 25 mm and 3 percent, respectively [1].

3.1 Matrix Properties

Constituent materials of jute-fibre reinforced concrete (JFRC) are small-diameter discontinuous discrete fibres and a matrix of cement, aggregates, water and admixture (if there is any). The matrix binds the fibres together, protects them from environmental attack and takes part in transfer of stresses to and from fibres. In general, concrete matrices used with jute fibres should have a higher cement content, a lower coarse aggregate content

and a relatively small size aggregates compared to conventional concretes. The dimensional stability of the matrix can be improved by adding various inert fillers and pulverized fuel-ash that modify the flow characteristics and other basic properties of the matrix [2].

3.2 Production Steps

The four major steps in the production of JFRC are fibre preparation, mixing of ingredients, placing and curing. The JFRC construction, unlike other sophisticated engineering constructions, requires a minimum of skilled labour and utilizes the readily available local materials. However, proper attention should be paid to the quality control of materials and construction.

4. FACTORS AFFECTING PROPERTIES

Properties of JFRC are affected by many factors, such as geometry, form and surface characteristics of fibres, properties of matrix, mix design, mixing and placing methods, and casting and curing techniques. In general, the mechanical, thermal and acoustic properties and durability of JFRC are functions of length, volume fraction, and aspect ratio of the fibres, properties of fibres and constituent materials, and casting pressure. Performance of JFRC, like any other material is very much influenced by the production process and quality control. As in conventional fibre reinforced concrete, the jute fibres act as crack-arresters that restrict the growth of flaws in the cement matrix. The uniform dispersion of fibres in the brittle matrix offers improvements in many of the engineering properties such as fracture, tensile and flexural strengths, toughness, fatigue and impact resistance of the composite.

4. EXPERIMENTAL INVESTIGATIONS

A series of tests was conducted to determine the mechanical, thermal and acoustic properties and also to study the durability of JFRC. Figs. 1 and 2 show the stress-strain behaviour in direct tension and load-deflection curves, respectively, of JFRC specimens [1]. Tables 3 and 4 provide quantitative information on the strength properties [1-3]. It can be observed that the inclusion of short randomly distributed fibres increases substantially the tensile, bending and impact strengths.

Mix proportion	Fibre length (mm)	Fibre volume fraction (%)	Tensile strength (N/mm^2)	Modulus of rupture (N/mm^2)	Modulus of elasticity (kN/mm^2)
1 : 0 : 0	25	2	2.36	4.14	10.80
1 : 1 : 0	25	2	2.39	4.50	16.40
1 : 2 : 0	25	2	2.24	3.92	16.00
1 : 1 : 0	38	2	2.30	4.20	17.20

Table 3 Strength properties of JFRC

Concrete type	Impact strength Nm/m^2
Plain concrete	5.80 - 6.30
Jute fibre reinforced concrete	
a. Using 38 mm long fibres	18.80 - 21.40
b. Using 25 mm long fibres	19.40 - 23.20
Mix proportion - 1:2:4, fibre volume fraction = 3 percent fibre length = 25 mm and 38 mm, curing period = 28 days	

Table 4 Impact strength of JFRC

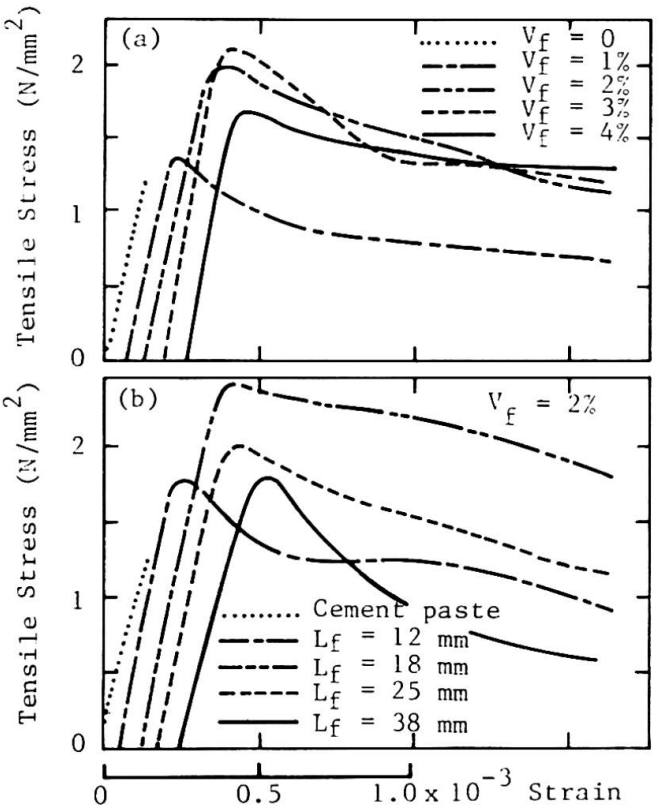

Fig. 1 Stress-strain behaviour of JFRC in direct tension

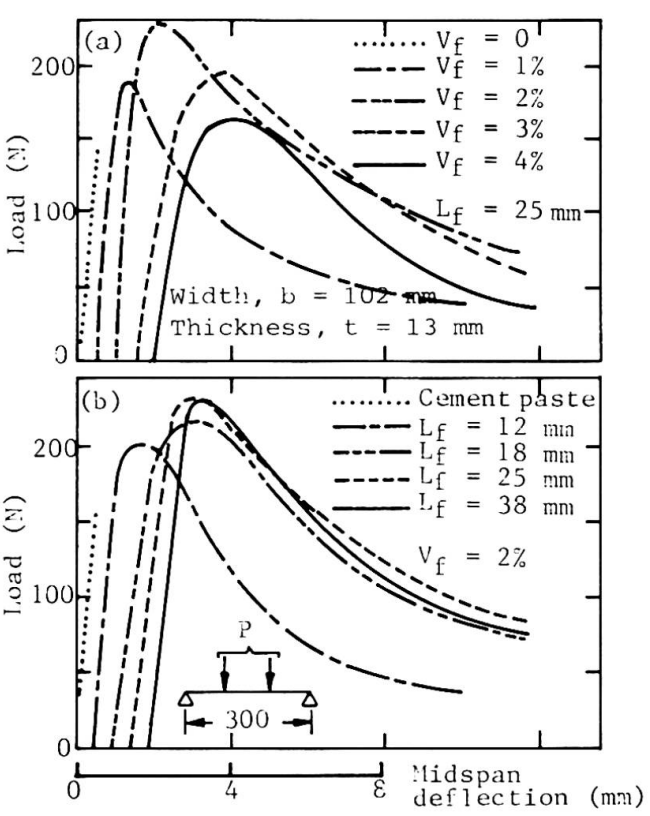

Fig. 2 Load-deflection curves of JFRC

Fibre type	Cement/sand ratio	Fibre volume fraction (%)	Fibre length (mm)	Slab thickness (mm)	Thermal conductivity (W/m^{o}K)
Jute fibre	1 : 0.5	2	25-38	25	0.61
		3	25-38	25	0.68

Table 5 Thermal conductivity of JFRC corrugated slabs

Volume Fraction	Thickness (mm)	Sound absorption coefficient (percent) at a frequency of					
		125 Hz	250 Hz	500 Hz	1000 Hz	2000 Hz	4000 Hz
3%	5	3.4	4.0	5.0	6.0	17.0	29.0
	10	4.5	6.7	5.6	7.0	22.4	42.6
	13	4.5	7.0	5.6	7.2	20.5	32.8
4%	5	5.2	8.5	6.0	9.2	15.2	46.0
	10	4.7	4.2	6.2	11.5	21.3	35.0
	13	4.7	4.5	5.3	7.7	24.6	26.0

Table 6 Sound absorption coefficient of JFRC

Properties	Asbestos cement plain roofing sheets	JFRC plain roofing sheets
1. Flexural strength, N/mm^2 (SFS* = 20)	17.80	18.50
2. Impermeability	excellent	excellent
3. Water adsorption, percent	20.60	16.50
4. Coefficient of thermal conductivity, $W/m^{\circ}K$	0.36	0.34
5. Sound transmission of 833 Hz signal, percent	26 (when dry) 40 (when wet)	24 (when dry) 35 (when wet)
6. Combustibility (BS 476-Part 4)	Non-combustible	Non-combustible
7. Linear expansion, percent	0.24	0.22
8. Density, kg/m^3	1,540	1,780

*SFS = specific surface area = surface area of fibre per unit surface area of sheet 6 mm thickness containing 1 kg cement = 20

Table 7 Comparison between the engineering properties of JFRC and asbestos cement plain roofing sheets [4]

Characteristics and properties	Asbestos cement corrugated roofing sheets	JFRC corrugated roofing sheets
1. Pitch of corrugation, mm	146	146
2. Depth of corrugation, mm	48	48
3. Length of sheets, m	1.5 - 3.0	1.5 - 3
4. Width of sheets, m	1.05	1.00
5. Weight, kg/m^2	13.5	11.8 - 12.57
6. Breaking load for a span of 60 cm, N/m	-	55
7. Breaking load at a span of 100 cm, N/m	50	30
8. Thermal conductivity, $kcal/cm/m^2$	0.24	0.14
9. Water permeability through finished surface in 24 hours	-	almost nil
10. Acid resistance as per I.S.:	9.30×10^3	9.40×10^3

Table 8 Comparison between the engineering properties of JFRC and asbestos cement corrugated roofing sheets

Tables 5 and 6 show the thermal conductivity and sound absorption coefficient of JFRC corrugated slabs, respectively. These values compare very well with those of asbestos cement boards and sheets as shown in Tables 7 and 8.

5. DISCUSSION OF PROPERTIES

JFRC behaves as a homogeneous material within certain limits. The random distribution and high surface-to-volume ratio (specific surface) of the fibres results in a better crack-arresting mechanism. With low fibre contents that are normally used in cement composites (from 2 to 4% by volume), the strain at which the matrix cracks is little different from that of plain concretes. However, once cracking occurs, the fibres act as crack-arresters, and absorb a significant amount of energy as they are pulled out from the matrix without breaking. These properties are useful in precast industry where accidental damage from impact creates large waste. The inclusion of short jute fibres in cement-based matrices, nevertheless, increases the first crack strength and

once the matrix has cracked, the fibres carry a major portion of the tensile stress in the composite material.

Besides its ability to sustain load, JFRC is also required to be sufficiently durable. To ensure durability, care should be taken to select suitable constituent materials in appropriate proportions and good quality jute fibres of specified length and volume fraction for producing a homogeneous and fully compacted mass. Poor dimensional stability of jute fibres due to moisture changes gives rise to durability problems and various protective treatments have been found to improve the situation [4]. The embrittlement of jute-fibre reinforced building materials has been observed in some applications [2,4]. The reason for such embrittlement has been found to be the alkaline pore-water in the composite which dissolves the fibre component. This can be counteracted by replacing 40 to 50% of the cement content by silica fume. The use of high alumina cement also reduces the alkalinity and thus slows down the rate of embrittlement. Sealing the pores with wax or resin, or use of suitable impregnating agents have also been observed to reduce embrittlement to a satisfactory level [4].

The performance properties like permeability, water absorption, thermal expansion, and shrinkage usually vary with fibre concentration [3,4]. These can be significantly reduced by coating the surfaces with suitable paints or by using suitable admixtures.

6. APPLICATIONS

JFRC products like sheets (both plain and corrugated) and boards are light in weight and are ideal for use as roofing and ceiling, and as wall panels for the construction of low-cost housing. Their special usages include applications where energy absorption is the primary requirement or where impact damage is likely to occur such as shatter and earthquake resistant construction. Other conventional applications include rafts and beams for cellular foundation, pavements, slabs and various types of shell structures. All potential applications of JFRC depend, of course, on the ingenuity of the designers and the builders taking advantage of the static and dynamic strength parameters, energy-absorbing characteristics, material performance properties, acoustic and thermal behaviour.

7. CONCLUSIONS

Use of JFRC may help to a great extent in providing low-cost housing in the countries of the Asia-Pacific region like Bangladesh, China, India, Indonesia and Thailand where jute fibres are abundantly available. It requires only a low degree of mechanisation and a small number of trained workers. The use of such building materials is particularly atractive to these countries because of their shortage of capital and skilled manpower. This will also avoid draining of hard-earned foreign exchange and alleviate unemployment problems.

8. REFERENCES

1. MANSUR, M.A. and AZIZ, M.A., A Study of Jute Fibre Reinforced Cement Composites. International Journal of Cement Composites and Lightweight Concrete, England, Vol. 4, No. 2, pp. 75-85, 1982.

2. AZIZ, M.A., PARAMASIVAM, P. and LEE, S.L., Chapter on "Concrete with Natural Fibres" in the book entitled New Reinforced Concretes, edited by R.N. Swamy, Int. Textbook Co., Glasgow, pp. 106-140, 1984.

3. AZIZ, M.A., PARAMASIVAM, P. and LEE, S.L., Natural Fibre Reinforced Concretes in Low-cost Housing Construction. International Journal for Housing Science and Its Applications, Vol. 10, No. 4, pp. 267-278, 1987.

4. GRAM, H.E., Durability of Natural Fibres in Concrete. Swedish Cement and Concrete Research Institute, Report No. 1, Stockholm, 1983.

Use of Fibre Reinforced Plastics in Bridge Structures

Emploi des plastiques renforcés de fibre de verre dans la construction des ponts

Anwendung von Faserverbund-Kunststoff im Brückenbau

Peter HEAD
Director
Maunsell Struct. Plastics Ltd,
London, England

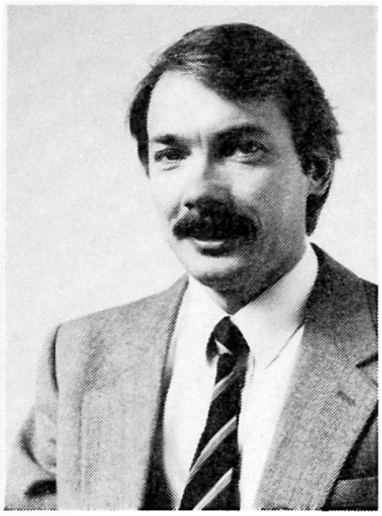

Peter Head, born 1947, graduated from Imperial College, London in 1969. He has been involved in the design and construction of major steel and composite bridges for nearly 20 years, and lectures widely on this subject. He was a founding Director of Maunsell Structural Plastics Ltd, formed by the Maunsell group of civil engineering consultants in 1982, and is responsible for designs of Advanced Composite Structures.

SUMMARY
Fibre reinforced plastics are being increasingly used in bridge construction. The reasons for this are explained and the materials currently available are introduced. Existing applications and research for a wide range of bridge types are described and the potential for future developments are discussed.

RÉSUMÉ
Les plastiques renforcés de fibre de verre sont de plus en plus utilisés dans la construction des ponts. Les raisons en sont expliquées, et les matériaux habituellement disponibles sont présentés. Les applications actuelles et les recherches pour une large gamme de ponts sont exposées, et le potentiel en vue de développements futurs est discuté.

ZUSAMMENFASSUNG
Faserverbundkunststoff kommt im Brückenbau mehr und mehr zur Anwendung. Die Gründe hierfür werden erläutert und die zur Zeit zur Verfügung stehenden Materialen angeführt. Bestehende sowie künftige Anwendungmöglichkeiten auf eine Vielfalt von Brückentypen werden beschrieben sowie die weiteren Entwicklungen in diesem Bereich.

1. INTRODUCTION

The history of bridge engineering is a history of the development of structural materials. Until Ironbridge was built in England in the year 1780, timber and stone had been used almost exclusively in bridge construction. The invention of wrought iron and then the development of steel and reinforced concrete changed bridge engineering completely in the 19th century. The 20th century has so far seen many developments in design and construction methods but relatively few fundamental changes in the materials used. Bridge spans and the number of bridge structures have increased dramatically to meet the demands of the rapid growth of infrastructure, but no new materials have found widespread use in bridges.

Fibre reinforced plastic (FRP) has already been used in prototype bridge structures (Fig.1) but the materials did not have the immediate and obvious advantages that iron and steel offered over timber and stone in the 19th century, except perhaps their potential for the construction of extremely long span bridges. (Although they have very high relative strength to weight ratios they have low stiffness unless expensive high modulus fibres are used. Materials and manufacturing methods for FRP are diverse and design methods are not fully developed.)

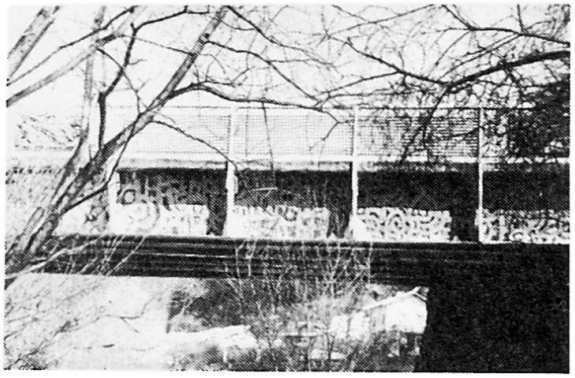

Fig.1 The world's first GRP highway bridge in Ginzi, Bulgaria

As a consequence, FRP had not been seen as a material likely to make an impact on general bridge engineering until the last ten years when the full implications of corrosion of steel in modern bridges was appreciated. FRP was then seen to have major advantages because of its excellent durability particularly in marine and industrial environments, and it is this characteristic which is currently leading to a significant step forward in its use in bridges.

2. WHAT ARE FIBRE REINFORCED PLASTICS?

FRP is a composite material which consists of two discrete phases, a continuous resin matrix surrounding a fibrous reinforcing structure. The reinforcement has high strength and stiffness while the matrix binds the fibres together.

The materials with potential for structural use in bridges are Advanced Composites in which high strength and high modulus fibres are used in relatively high volume fractions and the orientation of the fibres is controlled to enable high stresses to be carried. The reinforcement can be tailored and orientated to follow the stress patterns in the structural members leading to greater design economy than can be achieved with traditional isotropic materials. Varying combinations of flexural, tensile and shear strength and stiffness can be provided either with one reinforcement type or by combining fibres with different moduli.

Different fibre types and resin matrices have been continually developed over the last thirty years and together with many different highly automated manufacturing techniques they offer considerable scope to the designer.

There are three main types of fibre which are currently available for Advanced Composites, glass fibres, aramid fibres and carbon fibres. Resins could be polyester, vinylester or epoxy. Typical properties of composites made from these materials are compared in Table 1 for static load conditions.

Fibre Reinforcement		Glass	Carbon	Aramid	High Tensile Steel Wire
Fibre Fraction	%wt	80	72	67	-
Relative Density	ρ	2.31	1.57	1.36	7.86
Tensile Strength T	GPa	0.95	1.61	1.59	1.82
Tensile Modulus E	GPa	50	136	64.3	200
Specific Strength	T/ρ	44	105	119	24
Specific Modulus	E/ρ	21.6	86.6	47.3	25.4
Materials Cost Ratio* on a weight basis		6	16-20	10-15	1
Materials Cost Ratio* on a strength basis		3	4-5	2-3	1
Materials Cost Ratio* on a stiffness basis		7	5-6	5-8	1

* Materials cost ratio here is the 1987 cost relative to steel wire for use in cables or ropes.
Cost ratios for other applications will be different.

Table 1 Properties of composites with high proportions of unidirectional fibre reinforcement

3. APPLICATIONS OF FIBRE REINFORCED PLASTIC IN BRIDGES

3.1 Reinforced Concrete Bridges and Columns

One of the first uses of glass reinforced plastics (GRP) in bridges was in permanent formwork for concrete. The GRP was often manufactured using hand lay-up techniques with poor quality control and many engineers' early experiences with these materials has given GRP a bad reputation. However, recently developed manufacturing techniques now enable high quality economic structural GRP members to be produced.

Since GRP has high tensile strength and excellent durability it is logical to consider whether Advanced Composite GRP panels could be economically used not only as permanent formwork, but also as part of the structure to resist external loads and to protect against corrosion. These possibilities have been the subject of research work [1] and as a result helically wound GRP tubes have now been used in column construction for marine structures as a replacement for steel tubes filled with concrete. A GRP tube, having a high proportion of helical reinforcement, is an ideal material for encasing concrete because the concrete takes the entire axial load, the Poisson expansion in the circumferential direction is smaller than the concrete and the tensile strength in the circumferential direction is very high. Thus the GRP casing counteracts lateral expansion of the concrete under load and when used in a short column the axial strength of the concrete core increases over its uniaxial value and can reach a triaxial failure strength of up to four times the uniaxial value. It has been proposed that fibre reinforced plastic casings could be used in 'T' and 'I' bridge beams to improve the strength and ductility of the concrete in the compression zone in addition to providing formwork and corrosion protection. Tests on rectangular concrete beams with GRP casings and unidirectional GRP reinforcement have showed encouraging results and further research is being undertaken [1].

3.2 Prestressed Concrete Bridges

Severe corrosion of bridge prestressing strands in structures built only 20 years ago has been discovered and failures have occurred. Research into alternative non-corrosive materials has increased considerably as a consequence and the most advanced developments have been in the use of glass fibre reinforced plastic strands called Polystal.

A considerable research and development programme has been undertaken in West Germany on the use of Polystal strands for post tensioning concrete bridges. The first highway bridge to be constructed using these materials was a continuous two-span structure Die Brücke Ulenbergstrasse, also in Düsseldorf, which was completed in 1986 [2]. This 15 metre wide bridge has spans of 21.3 and 25.6 metres and consists of a 1.57 metre deep slab which was cast insitu with steel reinforcement. The slab was post-tensioned with 59 Polystal prestressing tendons, each made up from 19 glass reinforced plastic rods (nominal diameter 7.5mm) anchored in a specially designed block, and each tensioned to a working load of 600kN. 1300m^3 of concrete was used in the bridge, with 125 tonnes of steel reinforcement and 4 tonnes of glass reinforced plastic prestressing tendons. The bridge was built as part of a research project undertaken jointly by Strabag Bau-AG and Bayern AG.

3.3 Bridge Enclosure and Aerodynamic Fairings

The concept of 'Bridge Enclosure' was a prizewinner in the 1981 Civil Engineering Innovation Competition organised in the United Kingdom [3]. The proposal was to suspend a floor beneath the girders of steel composite bridges to provide inspection and maintenance access and to enclose the steelwork to protect it from further corrosion (Fig.2) [4]. A cellular GRP floor is being used in the world's first major bridge enclosure currently being installed on the A19 Tees Viaduct in the United Kingdom (Fig.3). The floor area is 16,000m^2 and contains 250 tonne of Advanced Composite materials.

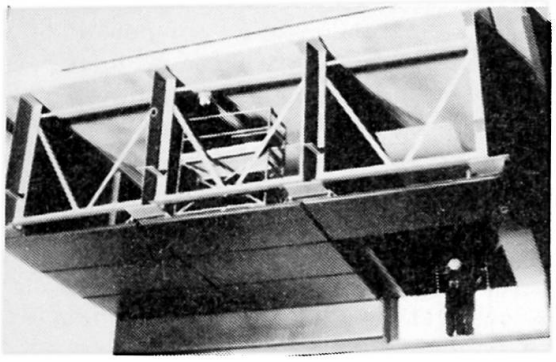

Fig.2 Model of a bridge with a GRP enclosure fitted

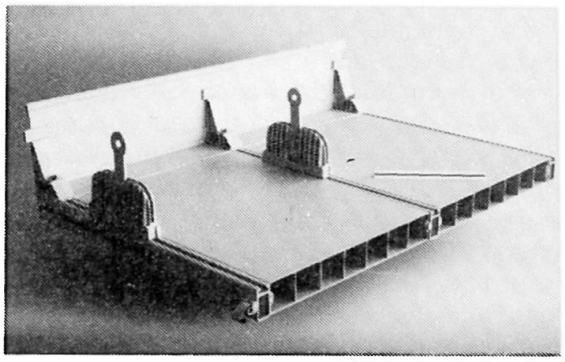

Fig.3 Model of the GRP enclosure floor for the A19 Tees Viaduct

The concept of bridge enclosure may have even more important implications for the future design of long span bridges. Currently steel box girders are often used for the deck girders of such bridges in order to provide an aerodynamic shape, to minimise exposed steel areas and to give good torsional stiffness.

However the development of cable-stayed bridges has resulted in a recent increase in the use of plate girders for long span bridges. The addition of fibre reinforced plastic enclosures around such structures would not only enable maintenance costs to be greatly reduced, but would also enable the shape of the cross section to be optimised by extending the enclosure into a fairing to give minimum drag consistent with aerodynamic stability (Fig.4a). The concept could be further extended to complete enclosure of the deck and traffic for extremely long span bridges in which the design for lateral wind is likely to dominate the structural form (Fig.4b).

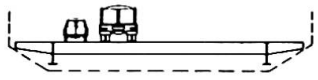

a) ENCLOSURE AND FAIRINGS

b) COMPLETE ENCLOSURE

Fig.4 Enclosures around long span bridge decks

3.4 Glass Reinforced Plastic Bridges

The development of bridges constructed entirely out of fibre reinforced plastic started with the construction of prototype footbridges in Europe and North America in the late 1970s. The first GRP highway bridge is believed to be a 10 metre span bridge constructed in Bulgaria in 1981/82 using hand lay-up techniques (Fig.1). The second all GRP bridge is the 20-metre span Miyun Bridge in Beijing, China which is a prototype structure completed in October 1982 [5]. This bridge is the culmination of 25 years of Chinese research into the structural use of plastics.

Although the materials for GRP bridges are always likely to be more expensive than steel or concrete, the savings in fabrication cost may be considerable if highly automated production of large advanced composite members is developed. It is possible that complete box girder structures may be pultruded in the future, with a manufacturing facility being set up on site for large projects. The pultrusion process is shown schematically in Fig.5. Speed of construction, savings in erection costs and savings in foundations will also contribute to economy. However the biggest attraction is likely to be the low maintenance costs of such structures.

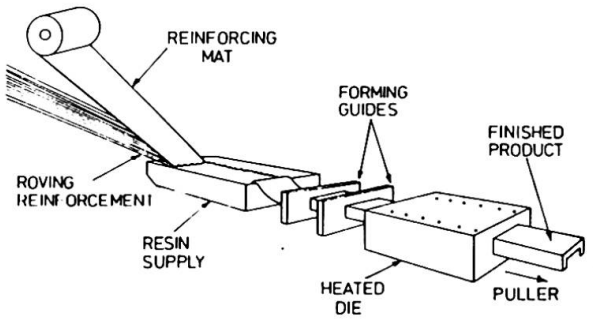

Fig.5 Diagram showing the pultrusion process

3.5 Cable Supports for Long Span Bridges

The advantages of the high strength to weight ratio of FRP are most important in very long span structures and are best illustrated by their potential for forming the main cables of suspension bridges. The theoretical limit of suspension bridge spans constructed from currently available high strength

steel wire is around 5000 metres because the cables can only just support their own weight. If the full properties of Kevlar or carbon fibre reinforced plastic cables were able to be exploited the theoretical limiting span would increase to over 10,000 metres. Recent investigations indicate that the economic span for use of FRP cables in suspension bridges may be about 4000 metres [6]. However the lateral loading effects of wind and aerodynamic stability may be difficult to design for in bridges with such long spans.

4. CONCLUSIONS

Fibre reinforced plastics have many potential uses in bridges, either on their own, or compositely with steel or concrete and their use is certain to grow rapidly in the future. New forms of bridge structure are likely to develop and eventually the materials may enable the frontiers of long span bridge technology to be pushed further than current steel materials permit.

Many of the possible developments described are a long way in the future and first it will be necessary to continue research and development into the long term behaviour of FRP materials through the construction of more prototype structures in addition to laboratory work. It will also be necessary to develop design codes of practice and materials standards and specifications which will enable reliable and economic use to be made of FRP. Advances are now being made in these areas in the United Kingdom [7] and this may contribute to a wider understanding and use of fibre reinforced plastics in bridges of the future.

REFERENCES

1. FARDIS M.N., FRP-encased Concrete as a Structural Material. Magazine of Concrete Research, December 1982.

2. WEISER M., Erste mit Glasfaser-Spanngliedern vorgespannte Betonbrücke, Beton- und Stahlbetonbau, 1983.

3. HEAD P.R., GRP Walkway Membranes for Bridge Access and Protection, British Plastics Federation, 13th Reinforced Plastics Congress, 1982.

4. BISHOP, R.R., Transport and Road Research Laboratory Report 83.

5. SHU YAO, Chinese Crossing first for Plastics Pioneers, New Civil Engineer, 14th April 1983.

6. RICHMOND B., HEAD P.R., Alternative Materials in Long Span Bridge Structures, Kerensky Memorial Conference, June 1988.

7. HEAD P.R., TEMPLEMAN R.B., The Application of Limit State Design Principles to FRP, BPF 15th RP Congress, 1986.

Turmartige Bauwerke aus glasfaserverstärkten ungesättigten Polyesterharzen

Construction of chimneys and towers with polyester resin and glass fibre products

Construction de tours et cheminées en résine polyester armée de fibres de verre

Günther ACKERMANN
Doz. Dr. sc. techn.
Hochschule für Architektur
Weimar, GDR

Günther Ackermann, geboren 1929, promovierte 1962 an der Hochschule für Bauwesen Cottbus. Von 1964 arbeitete er vierzehn Jahre an der Bauakademie der DDR auf dem Gebiet der ingenieurtheoretischen Grundlagen von Flächentragwerken und Plastkonstruktionen. Seit 1978 ist er Dozent für Stahlbeton- und Plastkonstruktionen.

Eberhardt RICHTER
Dipl.-Ing.
Bauakademie der DDR
IHLGB

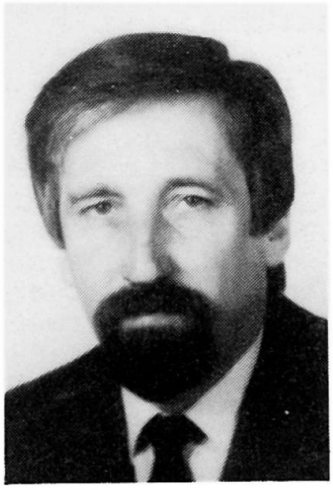

Eberhardt Richter, geboren 1935, studierte an der TH Dresden bis 1961. Er arbeitete neun Jahre im Stahlbrückenbau. Seit 1970 ist er als Gruppenleiter für Tragwerksentwicklung im Institut für Heizung, Lüftung und Grundlagen für Bautechnik tätig und bearbeitet Entwicklungsaufgaben zum Leichtbau; Flächen-, Sandwich- und Stahlleichtkonstruktionen.

ZUSAMMENFASSUNG
Auf der Grundlage einer umfangreichen Produktion von Polyesterharzen und Glasseidenerzeugnissen wurden eine Reihe von Konstruktionen aus glasfaserverstärkten ungesättigten Polyesterharzen entwickelt und gebaut. Im Beitrag wird ein Überblick gegeben zu der Bauweise von Abgasschornsteinen sowie über die Konstruktions- und Bemessungsprinzipien unter den spezifischen Produktionsbedingungen.

SUMMARY
With the development of an extensive production capacity of polyester resin products, a series of fibre glass resin structures was constructed. This paper gives as outline of the principles of design and construction of waste gas chimneys under specific production conditions.

RÉSUMÉ
Une série de constructions a été exécutée sur la base d'une production étendue de résines de polyester et de soies de verre. Cet article donne un aperçu de la méthode de construction de cheminées ainsi que des principes de construction et de dimensionnement dans des conditions de production spécifiques.

1. ENTWICKLUNGSTENDENZEN

Durch die schnelle Entwicklung im Bau von Industrieanlagen mit ständig steigenden Anforderungen an die Bauwerke erlangt die Optimierung des Bauaufwandes durch die richtige Auswahl der Baustoffe eine große Bedeutung. Die Verbundbaustoffe mit einer Matrix aus Kunststoffen und Verstärkungsmaterialien aus Glasfasern, die gegenüber vielen traditionellen Baustoffen ein günstigeres Verhältnis von Gewicht/Traglast/Langzeitverhalten haben, sind besonders vorteilhaft, wenn hohe Beanspruchungen durch ein einwirkendes Medium vorliegen. Die Voraussetzungen für das konstruktive und technologische Konzept der Anwendung von GUP sind

- Angebot von Polyesterharzen mit speziellen Eigenschaften und Glasseidenerzeugnisse, wie Matten, Gewebe und Rovings
- Herstellung von Zylinderschalen auf Wickelanlagen mit Durchmessern bis 5000 mm und Längen bis 6000 mm, mit innerer und äußerer Chemieschutzschicht sowie mit optimalen Aufbau der Verstärkungsmaterialien in Längs- und Ringrichtung
- Laminiertechnik für Montagestöße, Zu- und Abgänge, Abdeckhauben, Störkanten und Rippen.

Unter diesen Bedingungen wurden turmartige Bauwerke für folgende Anwendungen entwickelt:

- Abgasschornsteine (Temperatur $\leq +60^{\circ}C$)
- Luftansaugschlote für Produktionsbauten der Chemie
- Antennenmaste und Eisschutzzylinder
- Rauchgas- und Chlorwaschtürme.

2. EXPERIMENTALBAUTEN ALS ANWENDUNGSBEISPIELE

Nachfolgend werden die in Bild 1 dargestellten, gebauten turmartigen Bauwerke betrachtet. Die tragende Konstruktion ist das in ein Blockfundament eingespannte, auskragende Rohr. Bei der Festlegung der Wanddicke wurde davon ausgegangen, daß ein optimales Tragverhalten durch eine Zylinderschale mit größerer Wanddicke bei der kontinuierlichen Wickeltechnologie besser und ökonomischer zu erreichen ist als bei Verwendung von Rippen, Spanten oder eines Sandwichaufbaues. Die Wanddicken betragen 25 bis 7 mm für die in Bild 1 gezeigten Türme. Die Schornsteine sind komplett aus GUP, lediglich die Verankerungsteile wurden in Chromnickelstahl ausgeführt.

Der Hauptlastfall für die genannten Bauwerke ist der Lastfall Wind. Infolge der Böigkeit und des aerodynamischen Verhaltens des Windes werden die Schornsteine in Ausströmrichtung statisch und dynamisch auf Biegung beansprucht und quer zur Ausströmrichtung bei den kritischen Windgeschwindigkeiten in Schwingung versetzt. Nachfolgend werden in Tabelle 1 die Eigenfrequenzen ν und die kritischen Windgeschwindigkeiten v_{krit} für die GUP-Schornsteine angegeben /1, 2/.

Aus dem Vergleich mit der Normgeschwindigkeit v = 34,6 m/s zur Bestimmung des Staudruckes bis zu einer Höhe von 20 m erkennt man die Empfindlichkeit der GUP-Schornsteine gegenüber den Querschwingungen. Als Maßnahmen gegen diese Querschwingungen wurden entsprechend den technologischen Möglichkeiten der Ausführungsbetriebe die SCRUTON-Wendel und die gelochte zylindrische Röhre eingesetzt /2/. Die Wirkung dieser Dämpfungsbauteile ist in den

Vergleichen der Tabelle 2 veranschaulicht. Die Zahlen geben an, die Verhältnisse der Biegebeanspruchung aus Wind am Einspannquerschnitt aus der statischen und dynamischen Last und der Ersatzlast aus dem Querschwingverhalten ohne und mit Dämpfungsbauteilen zu der statischen Last ohne Dämpfungsbauteile.

Tabelle 1:

Nr.	ν /$\frac{1}{s}$/	ν_{krit} /$\frac{m}{s}$/
1	1,883	15,1
2	1,292	10,3
3	1,350	17,7
4	1,176	15,4

Tabelle 2:

Nr.	Bauwerk ohne Dämpfungsbauteile			Bauwerk mit Dämpfungsbauteile		
	stat. Last	stat.+dyn. Last	Ersatzlast Querschw.	stat. Last	stat.+dyn. Last	Ersatzlast Querschw.
1	1	1,42	3,97	-	-	-
2	1	2,14	9,63	1,63	3,58	3,97
3	1	1,69	8,99	1,77	2,70	2,79
4	1	1,50	8,30	1,91	2,96	3,07

Aus diesen Vergleichen ergeben sich einige wesentliche Schlußfolgerungen. Bei einem GUP-Schornstein ohne Dämpfungsbauteile werden die Biegebeanspruchungen aus der Ersatzlast der Querschwingungen bedeutend größer als die aus der statischen und dynamischen Last. Die Querschwingungen sind daher maßgebend für die Nachweise der Trag- und Nutzungsfähigkeit.

Bei einem GUP-Schornstein mit Dämpfungsbauteile werden die Biegebeanspruchungen aus der Ersatzlast der Querschwingungen und der statischen und dynamischen Last etwa gleich groß.

Bei Anwendung von Dämpfungsbauteilen ergeben sich also erhebliche Materialeinsparungen, auch wenn die Dämpfungsbauteile zusätzlichen Aufwand erfordern.

3. TRAGVERHALTEN

Die turmartigen Bauwerke sind orthotrope, dünnwandige Kreiszylinderschalen mit Öffnungen im unteren Bereich sowie mit ring- und spiralförmigen Verstärkungen in unterschiedlichen Bereichen. Die Berechnung des Schnittgrößen-, Spannungs- und Verformungszustandes kann mit der Methode der finiten Elemente durchgeführt werden. Für die praktische Berechnung ist es aufgrund der vorliegenden geometrischen Verhältnisse vertretbar, das reale statische System durch folgende Ersatzsysteme anzunähern /3/.

- Frei auskragender, unten eingespannter Stab zur Berechnung der Stabschnittgrößen M, N, Q, der Längs- und Schubspannungen und der horizontalen Verschiebungen;
- Kreisförmiger, geschlossener Stab zur Berechnung der Ringschnittgrößen M_φ, N_φ, Q_φ und der Ringspannungen /3/.

Als Belastungen wurden betrachtet Eigenmasse, Wind, Temperatur, Sonnenanstrahlung und Schiefstellung. Weiterhin sind die maßge-

Bild 1
Dynamisch beanspruchte Bauwerke
Freitragende Schornsteine aus GUP

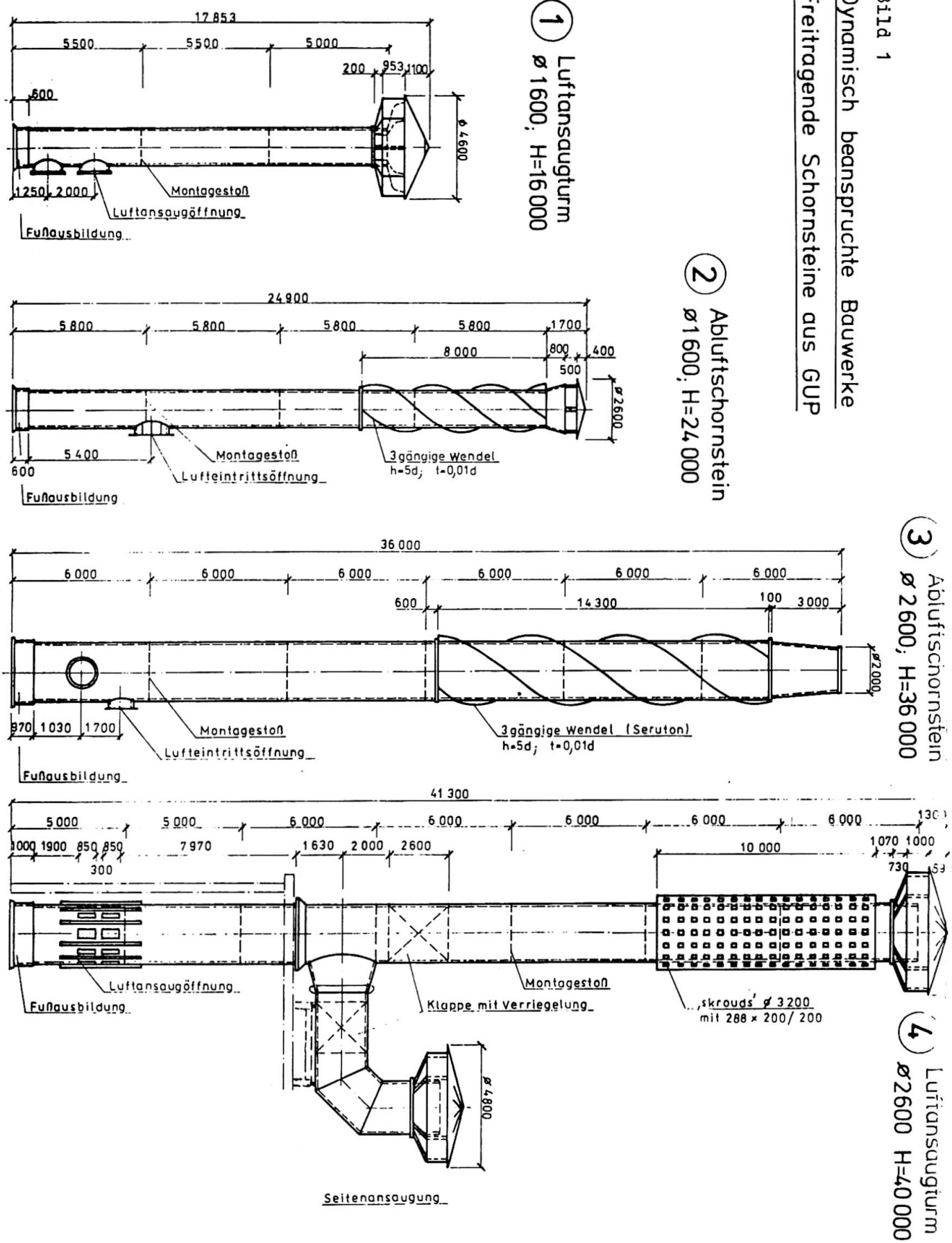

benden Montagelastfälle untersucht worden.
Die Nachweise der Trag- und Nutzungsfähigkeit erfolgten nach der Methode der Grenzzustände unter Erfassung der zeitabhängigen Einwirkungen und des Medieneinflusses /4/. Dabei fanden Berücksichtigung die Grenzzustände für die Tragfähigkeit

- Bruch beliebiger Art
- Stabilitätsverlust

und die Grenzzustände für die Nutzungsfähigkeit

- horizontale Verschiebungen
- Dehnung (Rißbildung).

Dabei wurden vorausgesetzt

für die zulässige Verschiebung $f_{zul} = \frac{H}{80} \cdots \frac{H}{50}$

für die zulässige Dehnung $\varepsilon_{zul} = 0{,}6$ o/oo

Die Entwicklung dieser Konstruktionen aus GUP wurde in der Bauakademie der DDR, IHLGB, durchgeführt.

Literatur

/1/ TRÄTNER, A.: Windwirkungen auf schwingungsgefährdete Bauwerke. Bauforschung - Baupraxis Heft 48, Bauakademie der DDR, Bauinformation DDR, Berlin, 1980

/2/ RUSCHEWEYH, H.: Dynamische Windwirkungen an Bauwerken Praktische Anwendungen. Bauverlag GmbH, Wiesbaden und Berlin

/3/ ACKERMANN, G.: Turmartige Bauwerke aus glasfaserverstärkten Plasten. Plaste und Kautschuk 30 (1983), 12, 693-697

/4/ ACKERMANN, G.; BEUTNER, M.: Dünnwandige einschichtige Konstruktionen aus Plastwerkstoffen - Empfehlungen zur Berechnung. Bauforschung - Baupraxis Heft 104, Bauinformation DDR, Berlin, 1982

Leere Seite
Blank page
Page vide